A PERFORMANCE STUDY AND CHARACTERIZATION OF A SINGLE USE PHARMACEUTICAL VIBRATIONAL MIXER USING COMPUTATIONAL FLUID DYNAMICS

A Thesis

presented to

the Faculty of California Polytechnic State University,

San Luis Obispo

In Partial Fulfillment

of the Requirements for the Degree

Master of Science in Mechanical Engineering

by

Michael Christian Eichermueller

December 2014

COMMITTEE MEMBERSHIP

TITLE:	A performance study and characterization of a single use pharmaceutical vibrational mixer using Computational Fluid Dynamics
AUTHOR:	Michael Christian Eichermueller
DATE SUBMITTED:	December 2014
COMMITTEE CHAIR:	Dr. Kim Shollenberger, Mechanical Engineering Professor at California Polytechnic State University
COMMITTEE MEMBER:	Dr. Patrick Lemieux, Mechanical Engineering Associate Professor at California Polytechnic State University
COMMITTEE MEMBER:	Max Blomberg, Operations at Meissner Filtration Products, Inc.

ABSTRACT

A performance study and characterization of a single use pharmaceutical vibrational mixer using Computational Fluid Dynamics

Michael Christian Eichermueller

A single use pharmaceutical mixer was analyzed for performance with various system configurations using Computational Fluid Dynamics. The analysis was conducted across a range of oscillation frequencies and liquid fill levels within a fully sealed mixing tank to determine the rate of fluid homogenization, liquid shear, velocity profiles and force application utilizing a single and dual mixer flat plate head configuration. These characteristics are useful for predicting the expected mixing time of a fluid and how much fluid shear is acting on protein cultures that are intended to be grown in the mixing vessel. General trends show that larger fill volumes take longer to homogenize, though as the volume increases the time for homogenization increases by a smaller factor, showing increased mixing efficiency at larger volumes. Furthermore, higher frequency oscillations yield little benefit for homogenization time with only 20% gains when increasing the frequency from 6 Hz to 12 Hz. The shear analysis shows that higher oscillation frequencies increase the wall shear acting on the fluid by an exponential amount, indicating that the higher frequencies are counterproductive toward protein production. Velocity analysis shows that zones of stagnation exist within the mixing system that slow fluid homogenization and exist at the same locations regardless of mixer oscillation frequency. Force application on the mixer head was analyzed to compare to analytical hand calculations to provide a basis of model validation, ultimately showing congruency and that the fluid flow is primarily pressure driven.

Keywords: CFD, vibrational mixing system, performance study, mixing analysis

ACKNOWLEDGMENTS

The author would like to thank Meissner Filtration Products, specifically Max Blomberg and Michael Priestman, for sponsoring this thesis and supplying the necessary equipment for the purpose of data validation as well as a high performance server blade for calculating the 3D model. The author would like to thank Dr. John Ridgely for his support and guidance in using Linux operating system and the use of his Linux lab for the summer to run several parallel computations, reducing the total computation time by 30 weeks. The author would like thank Professor Hans Mayer for his support in refurbishing and testing with the PIV system, which will be useful for further model validation. Most importantly, the author would like to thank Dr. Kim Shollenberger for her advice and mentorship throughout this project.

TABLE OF CONTENTS

Page

LIST OF TABLES

LIST OF FIGURES

I. INTRODUCTION

Saltus M200

The Saltus M200 is the flagship model of the new single use vibrational mixing systems developed by Meissner Filtration products, Inc, a company specializing in pharmaceutical filtration and manufacturing equipment. The product line features a simple design that involves fully sealed interchangeable containment bags with thermally bonded integrated mixer components of two different configurations within the bag. By using vibrational mixing instead of rotational mixing, concerns regarding leakage and foreign matter intrusion are reduced due to the lack of a bearing, allowing for a more controlled sterile environment. The secondary goal of vibrational mixing is to use short stroke lengths and low frequency oscillations to drive high flow rate mixing with low fluid velocity and fluid shearing. Low fluid shear is a key quality for a pharmaceutical mixing system to reduce the destruction of materials such as fragile proteins.

Figure 1 is a picture of the Saltus M200. Meissner Filtration Products, Inc.

Practical applications of the Saltus M200 mixing system are in the pharmaceutical industry for the hydration of cell culture media, buffer preparation, product reconstitution from concentrated solutions, homogenization of solutions, and chemical inactivation to affect viral clearance [1]. The overall effect is a fully automated system that is rapidly deployable and can quickly produce the required fluids in batches.

Mixing Parameters

The Saltus system comes with a 250 L open top stainless steel vessel that acts as the structural component of the fully sealed containment bag where the mixing occurs. The vessel is built from a 22 inch NPS Schedule 10 pipe with an internal diameter of 0.546 m and a height of 1.2 m. The containment bag is able to fill the entire volume of the vessel, though the system is designed to run with an air gap at the top and a nominal fill of 200L.

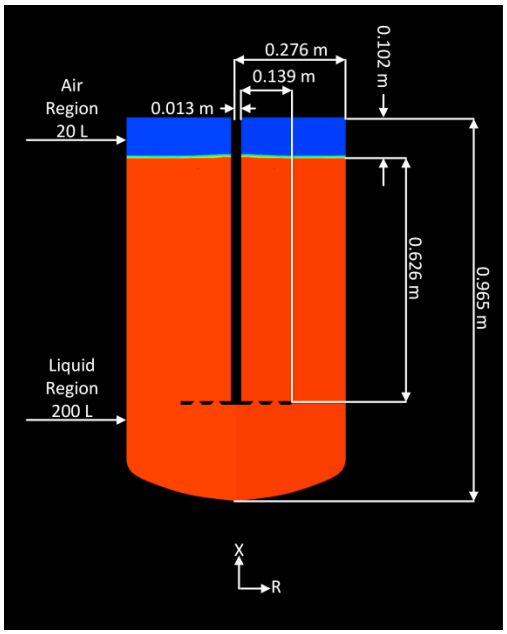

Figure 2 shows a two dimensional axisymmetric representation of the mixer vessel in the single mixer configuration.

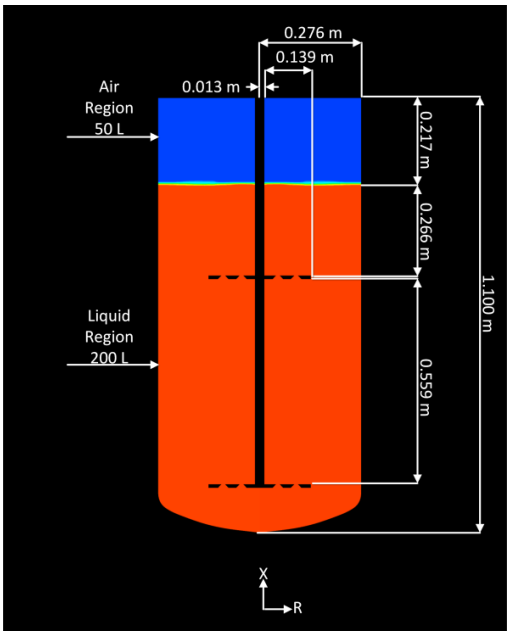

Figure 3 shows a two dimensional axisymmetric representation of the mixer vessel in the dual disk configuration.

Down the centerline of the tank is a polypropylene mixer head and shaft that is controlled by a PLC controller and motor for the ability to oscillate vertically at speeds between 6 Hz and 12 Hz with a peak to peak amplitude of 6.35 mm. The shaft supporting the mixer disk is between 0.70 and 1.00 m long for the single and dual mixer configuration, respectively. The single disk configuration has the mixer head at the bottom of the shaft, whereas the dual mixer configuration has one mixer head at the bottom and a second mixer head 0.56 m up from the bottom. Both configurations use the same mixer head, which is 0.279 m in outer diameter, 6.35 mm thick with 72 large jets that have an entry diameter of 12.7mm, an outlet diameter of 6.35 mm, and 12 smaller jets that have an entry diameter of 4.78 mm and the same outlet diameter of 6.35 mm. In both cases the change in jet diameter is accompanied by a 45 degree chamfer.

Figure 4 shows a three dimensional solid model visualization of the mixer head and single mixer head shaft.

The goal of the project is to determine how efficiently the two different mixer configurations perform the task of mixing two fluids and how mixer head frequency

affects the overall performance. Key points of interest are in the time it takes for the mixture to achieve a predetermined composition, long term steady state composition, and the amount of shear stress the fluid encounters, which can negatively affect the mixing effectiveness. Basic assumptions will be made for this analysis to simplify the problem scope in order to achieve results in a reasonable amount of time and with available resources. The mixer head and shaft were assumed to be rigid with no twist, torsion or bending. The region of interest in the tank was comprised of an incompressible water phase and ideal gas air phase. Finally, the mixer head had to oscillate vertically in the tank with smooth sinusoidal motion.

List of Terms

$\boldsymbol{A}$ = Area (m^2)

$\boldsymbol{a_{pp}}$ = Peak to peak mixer amplitude (m)

$\boldsymbol{f}$ = Frequency (Hz)

$\boldsymbol{\dot{m}}$ = Mass flow rate (kg/sec)

$\boldsymbol{\rho}$ = Fluid density (kg/m^3)

$\boldsymbol{\pi}$ = Pi constant (≈3.14)

$\boldsymbol{P}$ = Pressure (Pa or N/m^2)

$\boldsymbol{r}$ = Radial Location (m)

$\boldsymbol{R}$ = Radius

$\boldsymbol{F_A}$ = Reaction force (N)

$\boldsymbol{t}$ = time (sec)

$\boldsymbol{v}$ = Fluid Velocity (m/sec)

II. BACKGROUND

Conservation of Mass Analysis

Hand calculations were initially performed to determine characteristic behaviors around the mixer head, particularly the fluid velocity through the jets. This information aided in model selection and meshing requirements. Following this, a momentum analysis was conducted to check the steady state results around the mixer head.

The control volume for the calculations focuses on the region below the mixer head with the lower boundary at a steady region of flow, the top boundary at the upper surface of the mixer head, and the left and right boundaries to be walls with zero surface shear, representing both the axis and an inner wall of the tank. The control volume was created to be axisymmetric with the inner tank wall being of the same diameter as the outer diameter of the mixer head. It is particularly difficult to estimate what the velocity field would look like beyond the mixer head, so a simplifying assumption is made that all the flow passes through the mixer head.

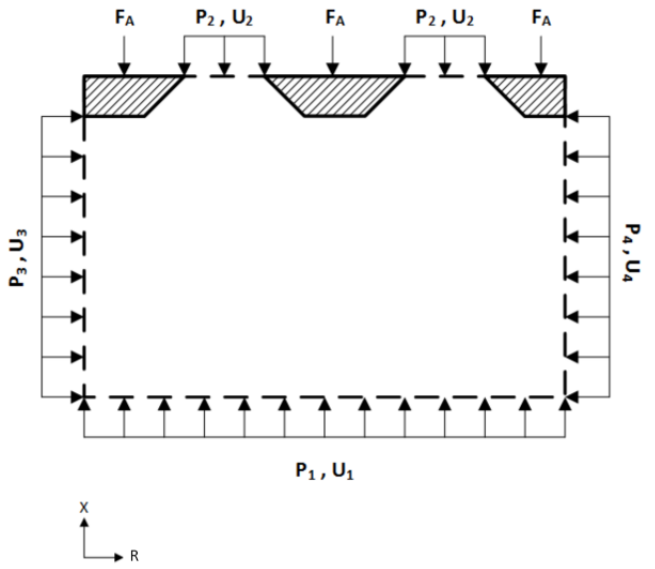

Figure 5 shows the control volume diagram for the momentum analysis. Each surface of the control volume has a pressure (P_i), velocity (U_i), and reaction force from material surfaces (F_i) acting on it. The analysis is one dimensional and only requires the variables in the x direction.

It is not directly important what the geometry of the mixer head is or how many jets are represented in the control volume, but rather how much outlet flow area is available through the mixer head. For a two dimensional axisymmetric analysis, a cross sectional slice of the mixer head was taken from the sponsor provided solid model drawings which are used to calculate the amount of outlet area created by the mixer head. Outlet flow areas are calculated for the cross sectional planes that include both the largest outlet flow area (four jets) and smallest out flow area (two jets), as well as for the complete three dimensional model.

Conservation of mass dictates that mass flow entering the control volume, as shown in Figure 5, has to equal that leaving the control volume, shown in Equation 1 [2]. For an incompressible flow with constant density, inlet flow velocity and area are directly related to the outlet flow velocity and area as shown in Equation 2.

$$\boldsymbol{\dot{m}_1 = \dot{m}_2} \qquad \textbf{Equation 1}$$

$$\rho_1 v_1 A_1 = \rho_2 v_2 A_2$$

$$\boldsymbol{v_2 = \frac{v_1 A_1}{A_2}} \qquad \textbf{Equation 2}$$

The inlet velocity is assumed to be sinusoidal with amplitude of 6.39 mm and a frequency of 12 Hz. For the initial analysis, only the peak velocity of 0.490 m/sec was used. Conservation of mass shows that the flow velocity passing through the jets should be between 1.64 and 4.41 m/sec, as shown in Table 1 below.

Table 1 contains the calculated data for jet velocity analysis for the maximum head velocity at 12 Hz oscillation speed.

Configuration	Inlet Flow Area (m^2)	Outlet Flow Area (m^2)	Inlet Flow Velocity (m/sec)	Outlet Flow Velocity (m/sec)
Two Jet Cross-section	0.0613	0.0096	0.490	3.14
Four Jet Cross-section	0.0613	0.0183	0.490	1.64
Three Dimensional Model	0.0613	0.0068	0.490	4.41

Conservation of Momentum Analysis

The next step in the process was to determine the force acting on the mixer head based on fluid momentum analysis [2]. The only force of interest is the reaction force F_A that the mixer exerts against the fluid flow; therefore, the force is only calculated in the X-direction as shown in Figure 5 above. Two assumptions are made, the first is that there is a negligible amount of gravitational effect on the fluid and the second is that the fluid is inviscid. Introducing viscous effects makes the calculation much more complex than necessary for comparing with CFD results. Forces in the X-direction then become:

$$\Sigma F_x:\ P_1A_1 - P_2A_2 + \rho v_1^2 A_1 - \rho v_2^2 A_2 - F_A = 0 \qquad \textbf{Equation 3}$$

Using Bernoulli's equation to solve for P_2 and using V_2 from Equation 2, Equation 3 can be arranged to get:

$$F_A = P_1(A_1 - A_2) + \rho v_1^2 \left(A_1^2\left(1 - \frac{1}{2A_2}\right) - \frac{A_2}{2}\right) \qquad \textbf{Equation 4}$$

The full derivation of the above equation can be found in Appendix D. The same values for inlet and outlet areas are used in the momentum analysis as in the conservation of mass analysis; though the inlet velocity differs. The maximum flow that the mixer head encounters is when the flow around it is at steady state during mixing and the mixer head is moving counter to that flow at maximum velocity. In this case, it is assumed that the flow surrounding the mixer is moving no faster than the mixer head itself at peak velocity. Therefore, the inlet velocity superimposes the sinusoidal velocity profile of the mixer head with a constant velocity of maximum mixer head speed. The mixer head speed is shown in the equation below:

$$v_{mixer} = a_{pp}\pi f \cos(2\pi f t) \qquad \textbf{Equation 5}$$

The maximum speed of the mixer head occurs when the cosine term is equal to one, leaving behind the amplitude, pi and oscillation frequency. Therefore, with the control volume moving with the mixer head, the relative velocity encountered is:

$$v_{mixer} = a_{pp}\pi f(\cos(2\pi f t) + 1) \qquad \textbf{Equation 6}$$

Substituting Equation 6 into Equation 4 as v_1 to form Equation 7 and assuming that P_1 is at zero gauge pressure, F_A can then be solved with the four modeled oscillation speeds with the solution as shown in Figure 6.

$$F_A = P_1(A_1 - A_2) + \rho\left(a_{pp}\pi f(\cos(2\pi f t) + 1)\right)^2 \left(A_1^2\left(1 - \frac{1}{2A_2}\right) - \frac{A_2}{2}\right) \qquad \textbf{Equation 7}$$

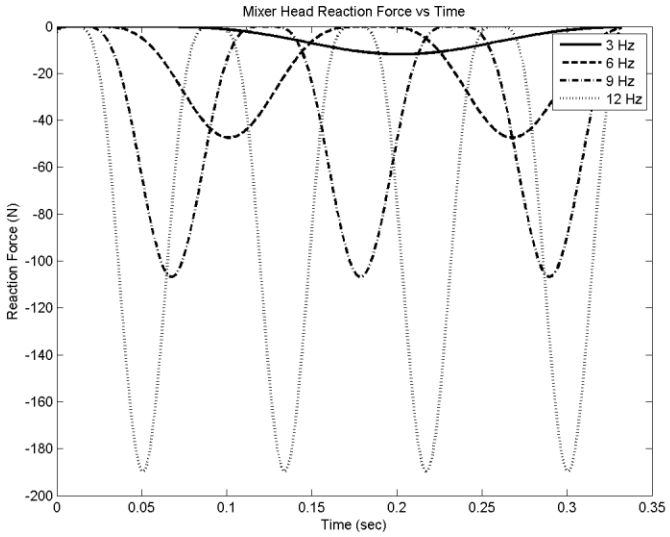

Figure 6 shows the calculated reaction force (F_A) encountered by the mixer head with four cases of mixer oscillation frequencies.

The results from the momentum analysis show an apparent flat-topping that occurs as the relative velocity of the fluid flow approaches zero. This effect of flat-topping comes from the velocity term being squared in Equation 7. Once the velocity is below 1 m/sec the reaction force rapidly approaches zero and stays there over a long span of time. The desired information from this analysis is the peak to peak reaction force that occurs on the head which is strictly dependent on the relative flow velocity acting on the mixer head. The difference in the minimum and maximum reaction force is an overestimation since the flow is idealized but can be used for comparison to the CFD results later in Chapter 4.

III. COMPUTATIONAL FLUID DYNAMICS

Three programs from the ANSYS workbench version 15.0 were used to produce, simulate, and post-process all models. More specifically, ICEM CFD 15.0 was used to produce both the two dimensional and three dimensional meshes. The models were further generated and simulated using Fluent 15.0. Initial post processing for images and data output were conducted with CFD-Post and further followed up with MATLAB.

ANSYS Fluent is an advanced simulation software used for modeling fluid flow, heat transfer, and chemical reactions in complex geometries [3]. Fluent has two numerical methods for solving flows: pressure based solvers and density based solvers. Pressure based has been developed for incompressible low speed flows whereas the density based solver is for high speed compressible flows. For either method the software will solve the governing integral equations for conservation of mass and momentum. This analysis will require the pressure based solvers as the flow is far below compressible speeds [3]. The pressure based solver will extract the pressure field by solving for pressure or pressure correction equations obtained by manipulating the continuity and momentum equations. The software can utilize additional models to solve for multiphase models such as gas-liquid flows utilizing the Volume-Of-Fluid (VOF) model and liquid-liquid mixing utilizing the Species model [3]. Advanced meshing tools are provided in the software that enable boundaries and cell zones to move and remesh based on input data provided by the user [3].

This chapter will discuss the Fluent mesh design, case setup and refinement studies required for proper viscous flow analysis. Background research was conducted to develop an initial approach to setting up the CFD model. More specifically, the use of dynamic meshing [4], species mixing [5], mesh generation and VOF method [6].

Mesh Development – Two Dimensional Axisymmetric

The two dimensional axisymmetric mesh was developed progressively in four main stages. The first stage constructed a crude mesh with excess refinement to test various viscous models for stability, the second stage created a mesh to test mesh refinement, the third stage created a mesh to test the required model conditions of the VOF method, Species and Dynamic Mesh, and the fourth stage created a final mesh for the complete CFD study. In addition, after the completion of the third stage, a three dimensional mesh was created based on the results of the axisymmetric mesh development.

For the first stage, a planar cut was taken from the sponsor provided three dimensional solid model that extended from the central axis outward in order to capture the maximum amount of mixer head jets. The region of interest is the length of the mixer tank and the radius of the mixer head. This has been chosen because it contains the control volume of the mass conservation calculation performed in Chapter 2 shown by Figure 5. A fully dimensioned drawing of the mesh can be found in Appendix A. An element seed size of 0.1 mm was chosen for the region 150 mm up and downstream of the mixer head. The element seed size was allowed to expand up to 10 mm for the remainder of the model. This method limits the total amount of nodes in the system yet still captures the fine detail of flow around the mixer head.

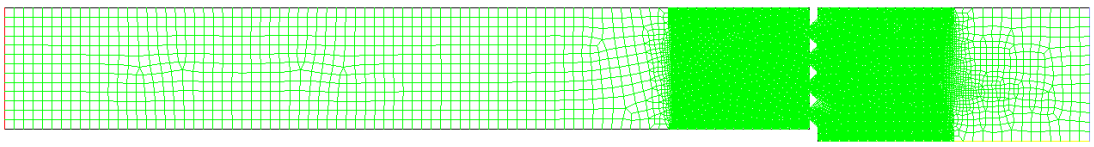

Figure 7 shows the diagram of the mesh configuration for the first stage in analysis. The flow is modeled as a pipe flow for comparison to the conservation of mass hand calculations.

The mesh includes a mixed set of boundary conditions. In Figure 7 above, the blue boundary at the right is a constant velocity inlet, the red left boundary is a constant pressure outlet, the yellow boundary at the bottom is the axis, and the remaining boundaries are no slip walls. The no slip condition in the model will analyze a viscous flow, which will be used for the final homogenization analysis, but will differ from the inviscid hand calculations performed earlier. The inviscid analysis will suffice in determining a viscous model within an order magnitude of accuracy. The above depicted mesh has a total of 40613 nodes.

The second stage in the analysis required multiple meshes to test variations in mesh refinements and effects on the solution. Meshes with wall seed sizes of 10 mm, 5 mm, 2 mm and 1 mm were tested on the same geometric configuration as shown in Figure 7. Smaller element seed sizes produce models with larger quantities of elements as show in Table 2.

Table 2 shows the total number of elements for various element seed sizes as applied to the initial validation mesh.

Element Seed Size (mm)	Total Elements
10	5774
5	14414
2	77258
1	295478

The third stage in the analysis requires a mesh that accurately represents the tank and mixer assembly for the purpose of implementing dynamic meshing, VOF method, and species calculations. The tank walls were further improved in the meshing software using the spline feature in order to capture the curvature of the bottom of the tank and convert what was the constant velocity inlet in the stage one mesh to a wall boundary condition. The constant pressure outlet from the stage one mesh was also

converted to a no slip wall boundary condition, fully enclosing the mixer system as it is in the actual system. Closing the system with walls allows the flow to circulate causing a mixing action, rather than having an inflow and outflow as in the stage one mesh. The first iteration of this second mesh showed that using four jets was ineffective at producing the flow required for mixing for axisymmetric modeling purposes because it did not produce the required pressure below the mixer head. At this point, the model was altered to use a cutting plane in the three dimensional solid model that utilizes only two mixer jets.

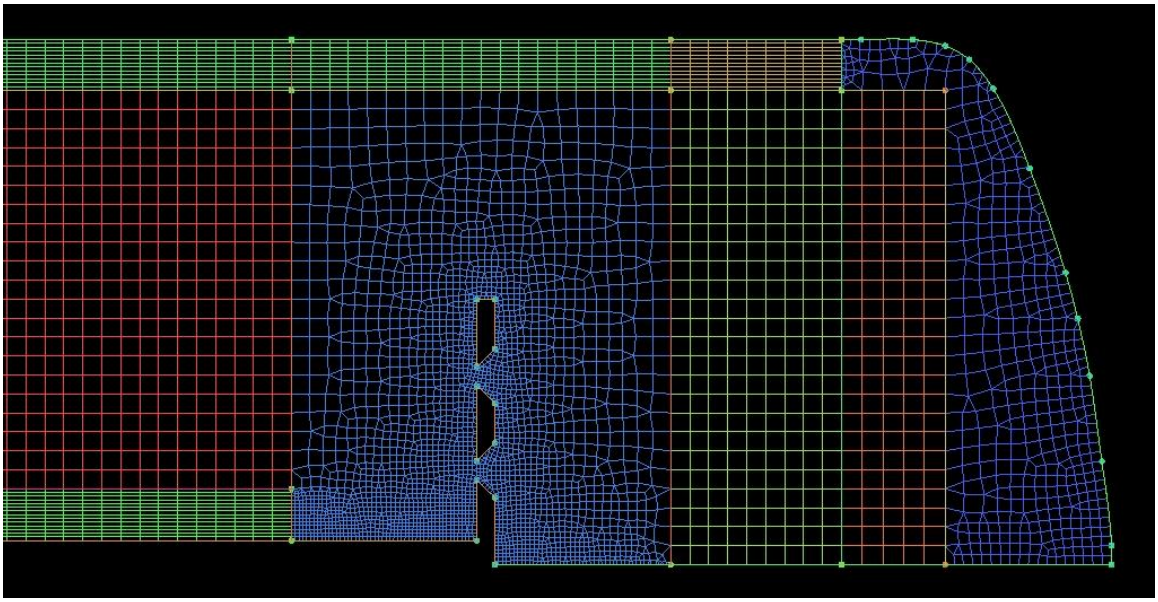

Figure 8 shows the second stage mesh, focusing on the region close to the mixer head.

The mesh was then subdivided into multiple regions in order to finely control the number of nodes and maintain orthogonality for a higher quality mesh. Within 2 cm of all the wall boundaries the mesh size is limited to a maximum of 2 mm to accurately determine the boundary layer. Between the wall regions where the bulk of the flow occurs, the mesh size is set to a maximum of 10 mm. As shown above in Figure 8, the purple region surrounding the mixer head is allowed to grow its elements as necessary

to maintain the 2 mm seed size around the head and conform to the 10 mm size in the general flow region. This same purple region and the green region above it that connects to the tank inner wall are also defined as the dynamically meshing region which oscillates at a prescribed rate of 6 and 12 Hz.

The final stage of the two dimensional analysis is to finely refine the mesh with knowledge gained from the model development in the second stage. A highly orthogonal mesh was produce with minimal skew with the result of improved computation time despite having more nodes than the previous versions.

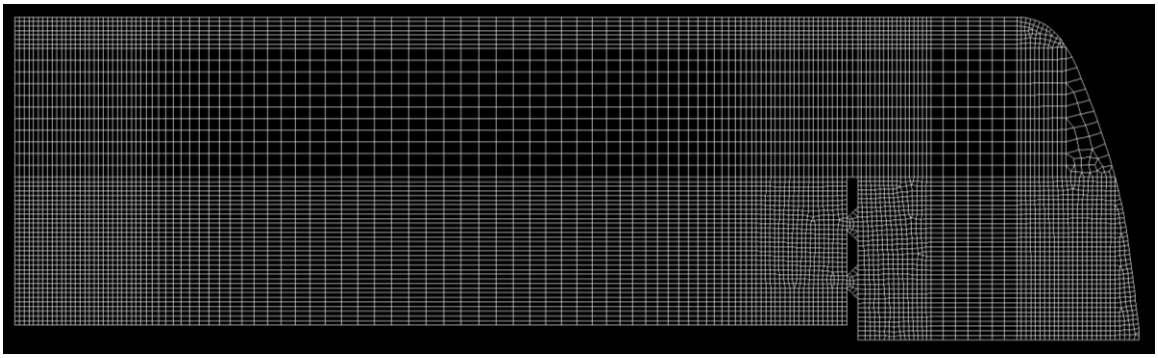

Figure 9 shows the highly refined mesh for the single mixer configuration that was used for the main modeling that was performed.

The dynamic region in this mesh was reduced to only include the top and bottom boundary of the mixer head and the regions above it extending radially to the wall. Radially extending the dynamic mesh to the walls prevents skewing of elements as the mixer head is oscillating and the potential of producing a negative volume element which would cause divergence in the model. The reduction in the dynamic mesh region reduces the time spent calculating the next position of moving nodes, and therefore the overall time spent on transient calculations. The final location where meshing was improved is the region where the gas/liquid boundary resides. It was noticed that the interpolation of the VOF method in regions of coarse meshes caused the liquid phase to transition into the gas phase over long duration models. The real system maintains

discrete phases when using water as the liquid and air as the gas; therefore having the liquid phase transition into the gas region is a significant problem. For this reason the mesh was refined in the gas region and 10 mm below where the gas/liquid boundary exists. Further mesh refinement would be necessary to produce more accurate results in regions around the mixer shaft so as to not overstate the size of the boundary layer. Though, with the computational availability at the university, the complete mesh refinement would be limited to the current state so that the analysis can be finished in a reasonable amount of time. This final mesh was then also extended to the dimensions of the dual mixer configuration with the same settings for the region surrounding the second mixer head.

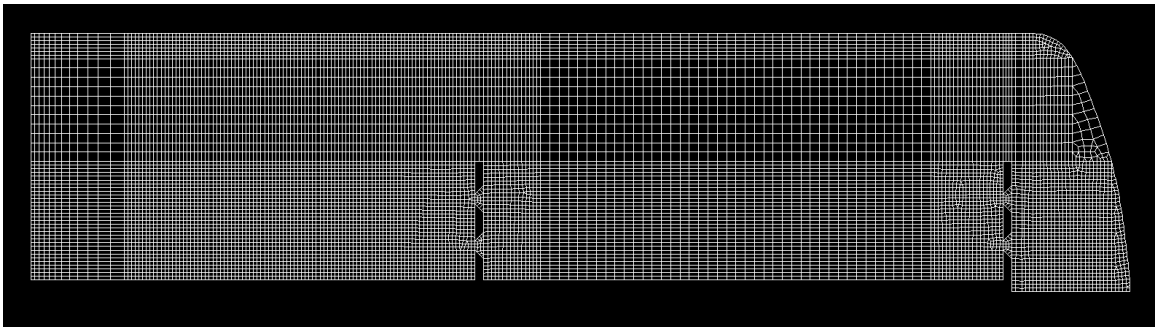

Figure 10 shows the final mesh that was used for the dual mixer configuration of the analysis.

Mesh Development – Three Dimensional Periodic

The final mesh that was developed was the three dimensional mesh, which was also an extension of the axisymmetric meshes. Producing this mesh was much more labor intensive than the previous meshes requiring significant manual reworking. Utilizing the existing symmetry of the mixer head, the solid model was cut into a 60 degree wedge with the wedge faces bisecting the mixer head directly through the set of 3 mixer jets. The solid model was then imported and adjusted to match the setup of the

actual system. Blocking was then used to establish the region of interest within the tank and surrounding the mixer components. The blocks that contain the mixer plate were cut and fitted to conform to the shape of the mixer head. During this, the seed sizes for the mesh were also selected to match similar sizing to the two dimensional axisymmetric cases. The front and rear face of the wedge are set to periodic faces, which in this case will match up the nodes on the two faces and allow the modeled flow to induce swirl. The regions are then otherwise left much the same as in the two dimensional case. The walls of the tank, shaft and mixer head are set to no slip conditions. The entire region 200 mm above and below the mixer head are set to move in the dynamic mesh due to the high skewness of the elements around the mixer head that are produced by the blocking algorithm. The final mesh produced is shown in Figure 11.

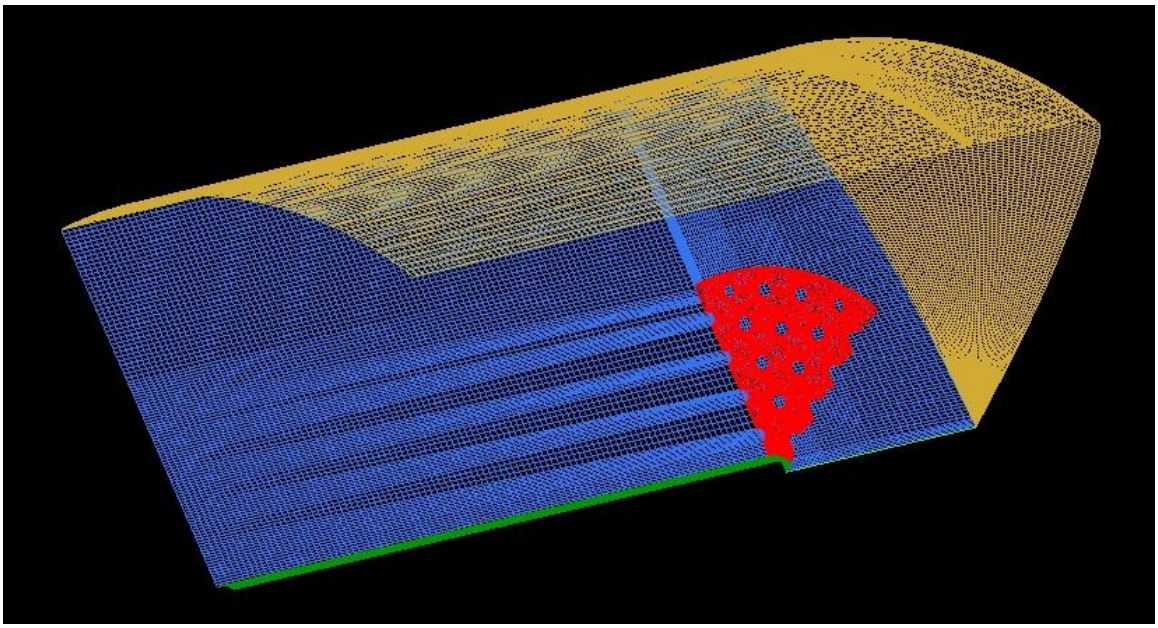

Figure 11 shows a three dimensional representation of the single mixer configuration mesh with only the edge shells showing.

Model Development – Viscous Model Selection

The first step in the analysis is to select the proper viscous model and test it with the first stage mesh, comparing the results to the conservation of mass analysis performed in Chapter 2. Similar to the hand calculations, the inlet velocity on the CFD model was set to the maximum velocity that the mixer head encounters at 12 Hz, the highest mixer oscillation rate. Then, six different viscous models (laminar, K-Epsilon, K-Omega, K-Omega Shear Stress Transport, K-Kl-Omega, and Reynolds stress) were run for up to 500 iterations to test for convergence and solution. Each viscous model has advantages over the other based on the type of flow being analyzed. The laminar model is the least computationally intensive but lacks the ability to model turbulent flows and can be immediately removed as a modeling option. The K-Epsilon model is designed for fully turbulent flows though, not effective for calculating adverse pressure gradients and boundary layer separation, and also requires good y+ wall treatment [7]. The K-Omega model is able to overcome the shortfalls with the K-Epsilon model and is insensitive to y+ enhanced wall treatment though is sensitive to the free stream K and Omega values [7]. In other words, the K-Epsilon model is able to model the free stream flow very well, whereas the K-Omega model is effective at modeling flow near the wall; both require two coupled equations which are equally computationally intensive. K-Omega Shear Stress Transport overcomes the free stream issues in K-Omega by combining the K-Omega model with the K-Epsilon model [7]. The advantage of this model is countered with more computing requirements since three coupled equations are required for solving. The K-Kl-Omega Transition model is able to more accurately model the transition from laminar to turbulent flow and further overcome issues of the above mentioned viscous models but is also more computationally intensive by requiring four coupled equations [7]. The final model tested is the Reynolds Stress Model that is the most computationally intensive model but most accurate for very complex flows [7]. Qualitative and

quantitative results are shown below regarding the viscous model selection in Figures 12-17 for peak velocity.

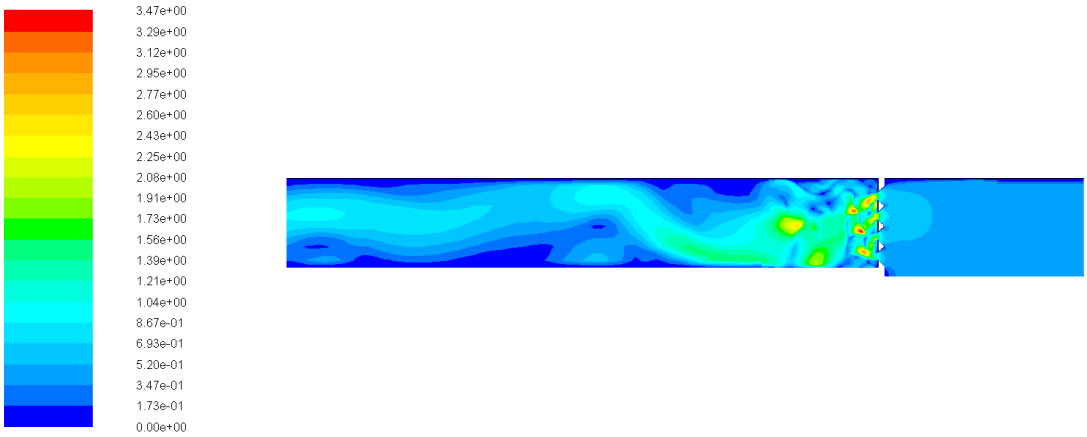

Figure 12 shows the results of the laminar viscous model. This model shows chaotic motion after the mixer jets as well as a peak velocity far beyond the calculated value of 1.64 m/sec.

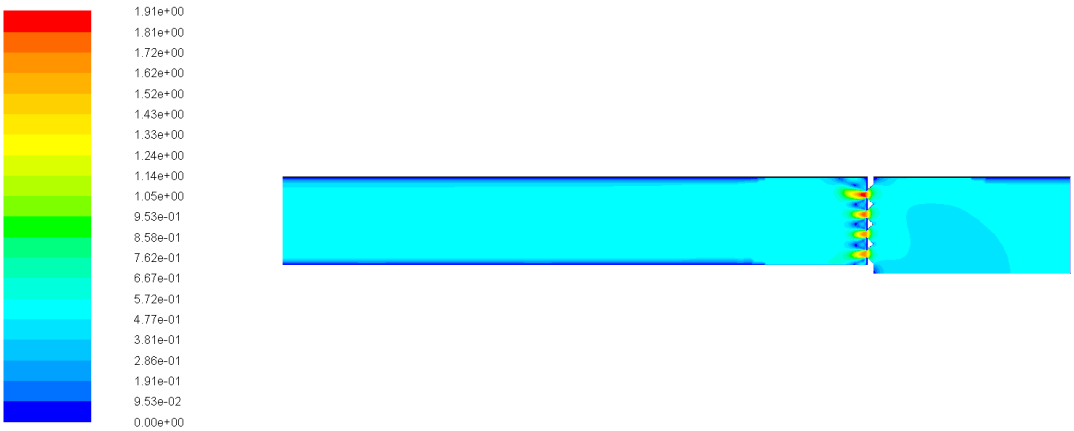

Figure 13 shows the results of the k-epsilon model. These results show steady results and a peak velocity that has approximately 16.5% difference from the hand calculated value.

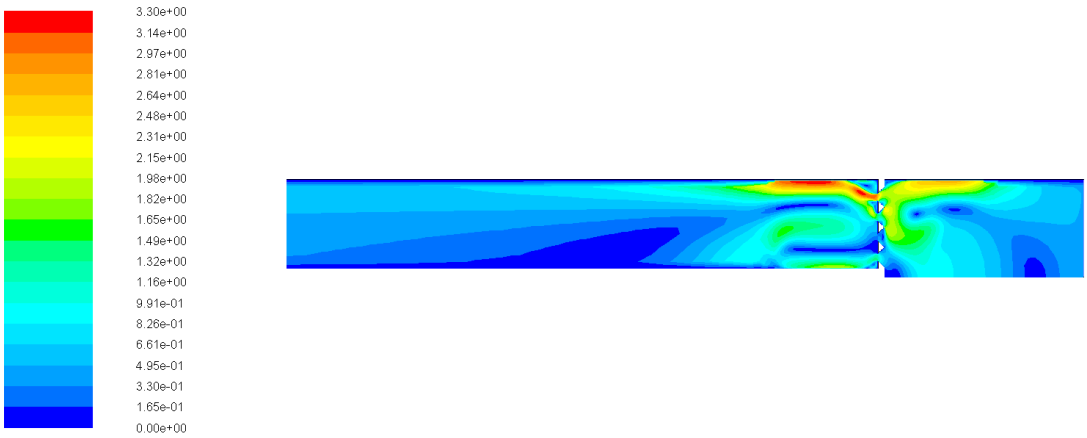

Figure 14 shows the results of the k-omega model. These results show unsteady flow downstream of the mixer head and has approximately 101% difference for the peak flow velocity from the hand calculation.

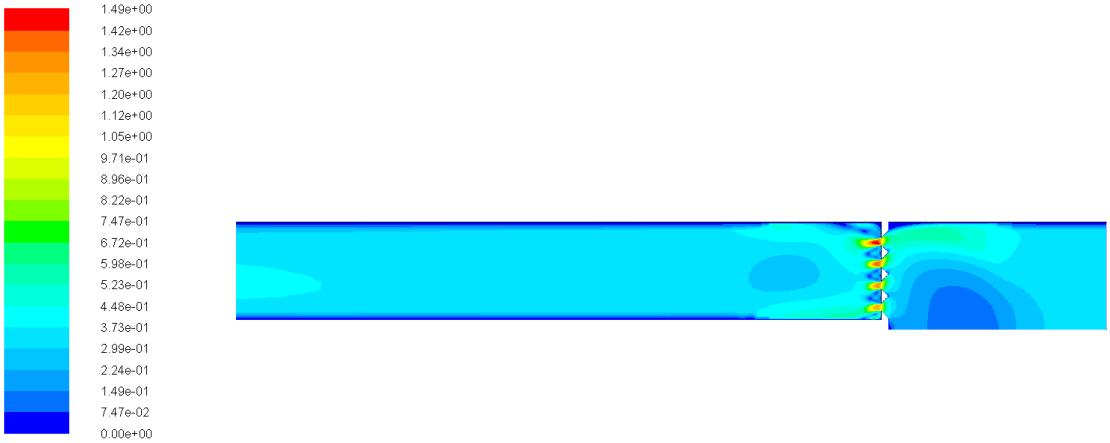

Figure 15 shows the results of the k-kl-omega viscous model. This result shows steady flow after the mixer head and the maximum velocity has a difference of approximately 9.1% from the hand calculation.

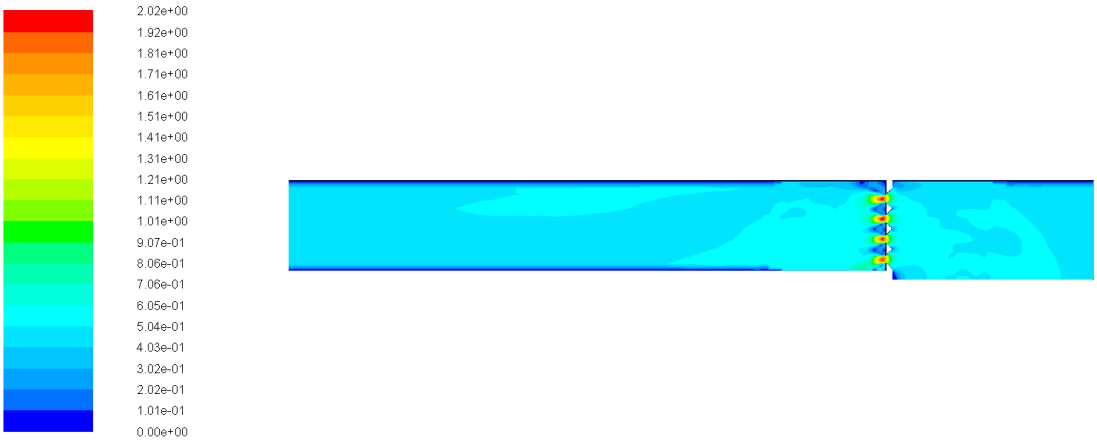

Figure 16 shows the results of the Reynolds stress viscous model. The results show steady flow after the mixer head and the maximum velocity has a difference of approximately 23.7% from the hand calculation.

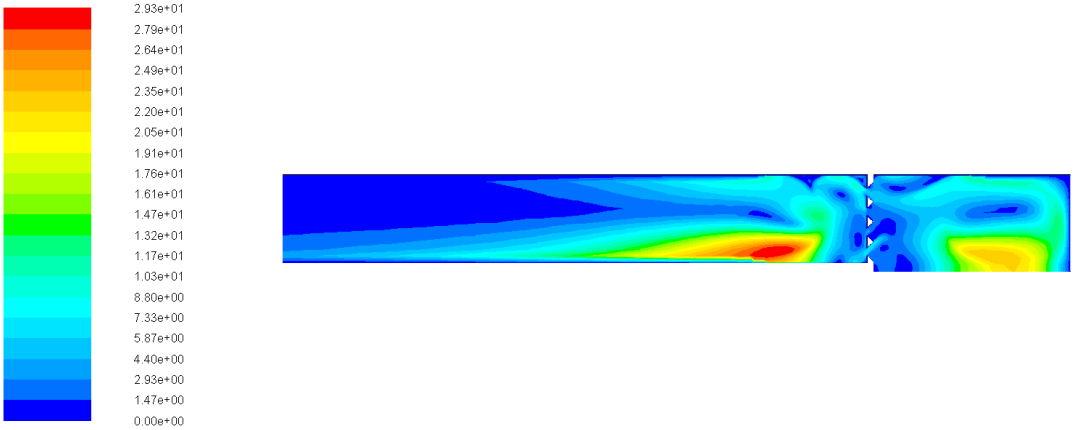

Figure 17 shows the results of the SST viscous model. The results show unsteady flow and has a difference of 78.7% for the peak velocity from the hand calculation.

Qualitatively analyzing the results show that the laminar, K-Omega and K-Omega SST models produce unsteady flows as seen by pockets of high velocity flow downstream of the mixer face. The remaining three viscous models were then quantitatively analyzed and compared to the inviscid hand calculation. The higher complexity of estimating the velocity profile and peak velocity within the jet is not a trivial subject with viscous flow and is not required for the scope of this project. For this thesis, it was decided that the inviscid hand calculation will suffice for comparing different viscous flow models. The

quantitative comparisons show that the K-Kl-Omega viscous model had the lowest percent difference from the hand calculated values and therefore was used for the remainder of the analysis. Table 3 below shows the results from the model analysis.

Table 3 shows the results from the viscous model testing with percent difference calculated from the mass conservation hand calculation.

Viscous Model	Peak Velocity (m/sec)	Percent Difference from Hand Calculation
Hand Calculation	1.64	0%
Laminar	3.47	112%
K-Epsilon	1.91	16.5%
K-Omega	3.30	101%
K-Omega SST	2.93	78.7%
K-Kl-Omega	1.49	9.1%
Reynolds Stress	2.02	23.7%

The final configuration constants for the viscous model are left at the default values since modification of these values would require validation that is beyond the scope of this project. Viscous model configurations are shown on the next page in Table 4 and can also be found with the complete case configurations in Appendix E.

Table 4 shows the settings for the viscous model when representing the flow past the mixer head.

Viscous Model Configuration	
Solution Methods	
Model	Transition K-Kl-Omega
Scheme	SIMPLE
Gradient	Least Squares Cell Based
Pressure	PRESTO!
Momentum	Second Order Upwind
Turbulent Kinetic Energy	Second Order Upwind
Laminar Kinetic Energy	Second Order Upwind
Transient Formulation	First Order Implicit
Solution Controls - Under-Relaxation Factors	
Pressure	0.3
Density	1.0
Body Forces	1.0
Momentum	0.7
Turbulent Kinetic Energy	0.8
Laminar Kinetic Energy	0.8

Model Development – Transient Considerations

This analysis requires multiple case studies for different fill volumes and mixer speeds. With limited analysis time and computing power, research into the size of time steps became critical. Four similar models were tested based on the second stage mesh development to test for required element size and computation times. Figure 19 below shows the velocity profile at a location 0.25 m upstream of the pressure outlet as shown in Figure 18.

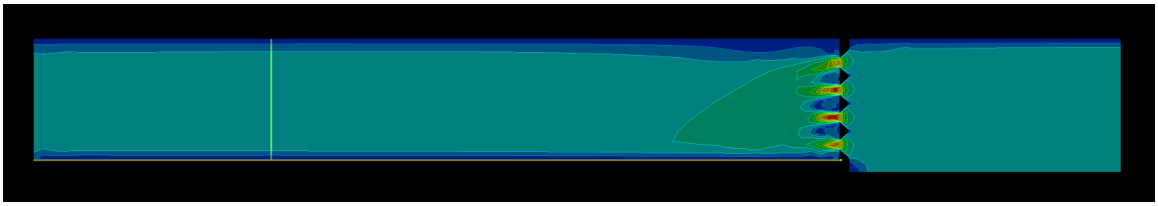

Figure 18 shows velocity contour results for the stage two mesh with a seed size of 1 mm. The line for the velocity profile for Figure 19 is shown as the vertical yellow line at 0.25 m. The line for the wall shear profile in Figure 20 is shown as the yellow line along the mixer shaft.

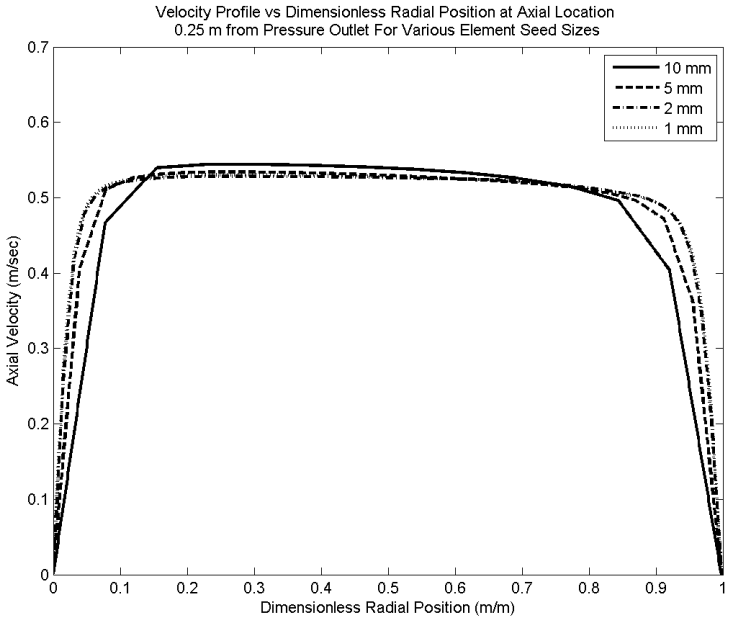

Figure 19 shows the velocity profile 25 cm upstream of the pressure outlet of the initial model.

It is noticed that at an element size of 2 mm, there is very little gain when further reducing the element size by a factor of 50%. Data extracted from the velocity profile shows that 2 mm is effective for modeling near wall flow whereas 5 mm is good for modeling flow between the walls. The percent error along the centerline of the flow (radial position x/L = 0.5) is 0.35% between the 1 mm seed size and the 5 mm seed size. The percent error close to the wall at location x/L of 0.02 is 5.4% between the 2 mm and 1 mm seed size, which is a significant improvement compared to the 63% error between the 10 mm seed size and 2 mm seed size.

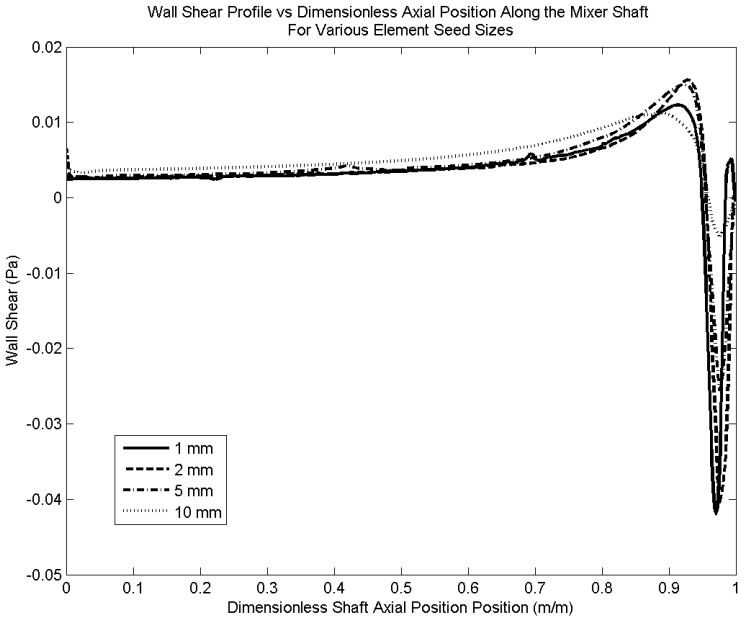

Figure 20 shows the mixer shaft wall shear stress in the second stage mesh with varying element sizes.

Similar to the velocity profile, the wall shear along the shaft was determined with the four different element seed sizes. At the location x = 0.25 m, the percent difference between the 1 mm and 2 mm seed size is 0.8% showing that the 2 mm seed size is sufficiently refined for the near wall region.

Table 5 contains the data from the initial mesh element seed analysis.

Element Seed Size (mm)	Total Elements	Time Per Iteration (sec)
10	5774	0.011
5	14414	0.020
2	77258	0.100
1	295478	0.679

While testing the various levels of refinement, the time per iteration was calculated with results shown in Table 5 above. The time per iterations was tested on a computer using an Intel i7-2670 QM processor with a capacity of 70.4 GFLOPS. The actual final analyses were performed on computers with an Intel E-6600 processor with only 19.2

GFLOPS of computing capacity, so actual iteration times would be increased by a factor of 3.7. Based on vendor provided data, it takes approximately 20 second for the physical mixer system to achieve periodic steady state and approximately 3 minutes for a mixture to be fully homogenized. To accurately track the flow generated by the sinusoidal motion of the mixer head, the full cycle of the oscillating motion was divided into 20 parts, 10 parts for the upstroke and 10 parts for the downstroke. This means that the time steps are sized to approximately 4 ms for the 12 Hz oscillation frequency and up to 16 ms for the 3 Hz frequency. Since multiple attempts for analysis were expected to fine tune the model and check for errors, it was decided that no more than two weeks be spent on a single model. Multiple simulations were conducted to test for an acceptable residual for the model which was determined to be at 10^{-6} for all model terms. To limit the amount of calculation time required, the transient simulation was limited to 50 iterations per time step. Table 6 shows the results of the calculations required for the total model time in real time based on 200 seconds of simulation reference time at 4 ms time steps and 50 iterations per time step which consists of a total of 2,500,000 iterations. As shown by Table 6 it is reasonable to have a model that is similarly sized to the 2 mm seed element size with approximately 77,000 elements for the analysis to finish within two weeks.

Table 6 shows the computer performance data from the initial mesh seeding analysis, which is used to approximate the total solution time required for the full sized model using available compute sources.

Element Seed Size (mm)	Total Elements	Time per Iteration (sec) for Q-2670 Processor	Expected Time per Iteration (sec) for E-6600 Processor	Total Model Time (hrs)
10	5774	0.011	0.041	28.3
5	14414	0.020	0.074	51.4
2	77258	0.100	0.370	257.0
1	295478	0.679	2.510	1744.7

Model Development – Dynamic Meshing, Species, and VOF

The analysis requires three tertiary models in order to fully model the system as required: 1. Dynamic Meshing, 2. Species, and 3. Volume of Fluid. Each model has its own settings and nuances that require specific attention as described below.

For the mixer head to oscillate, the mesh has to move in regions the same way it would in real life. To start, a C file was written that models the motion of the mixer head velocity as shown below.

```
/************************************************************
* 1-degree of freedom equation of motion (x-direction)
* compiled UDF
************************************************************/

#include "udf.h"

DEFINE_CG_MOTION(object_mov, dt, vel, omega, time, dtime)
{
real a, w, pi;
pi = 3.1415;

/* define motion variables */
a = 0.013/2; /* 0.013m movement amplitude */
w = 12 * pi * 2; /* 12Hz frequency calculated in radians*/

/* define object movement law */
vel[0] = a * w * cos(w*time-pi/2);
vel[1] = 0;
vel[2] = 0;
}
```

The velocity of the moving components is modeled one dimensionally as the mixer head only moves vertically in the mixing tank. The orientation of the meshes in both the axisymmetric and three dimensional cases are such that the mixer head moves only in the x-component as indicated by vel[0] in the code excerpt above. This C file was then compiled and added into a library of User Defined Functions (UDF) in Fluent. The compiled UDF is then applied to specifically chosen regions of the mesh as shown below in Figure 21.

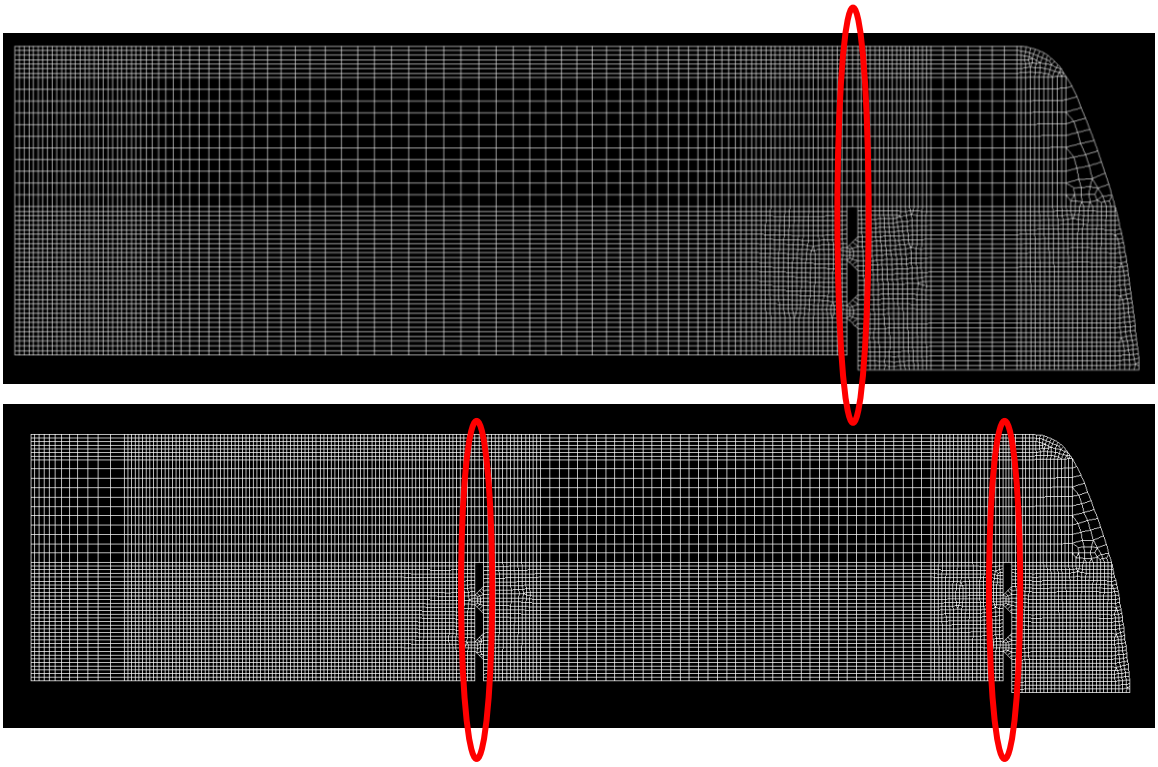

Figure 21 shows the dynamic mesh regions of the single and dual mixer configuration meshes circled in red for the final analysis.

Fluent has three methods to dynamically mesh: Layering, Spring, and Remeshing. As the name describes, Spring will shrink or extend mesh elements in the same way that a spring deforms. A drawback with this is that for the linear motion that the mixer head undergoes, the elements around the mixer head will become more or less skewed at different stages of the sinusoidal stroke. Remeshing, also as the name describes, will re-mesh the dynamic mesh portion of the model with the drawback that the mesh cannot be finely controlled. Layering is a dynamic mesh method that will split and merge elements as a form of adjusting a mesh. A target element size is picked and then as the elements of a mesh around a moving boundary becomes either smaller or larger than a prescribed volume ratio, either multiple elements will combine into a single element or split into multiple elements in order to conform with the target size. For the two dimensional models, a target element size of 4 mm was chosen with a split ratio of 0.6 and a merge ratio of 0.4. The three dimensional model uses a 4 mm target element

size and the same split and merge ratios as in the two dimensional models. A key advantage of the layering method is that the elements along the mixer boundary remain orthogonal and that the skewness is limited by the split and merge ratio.

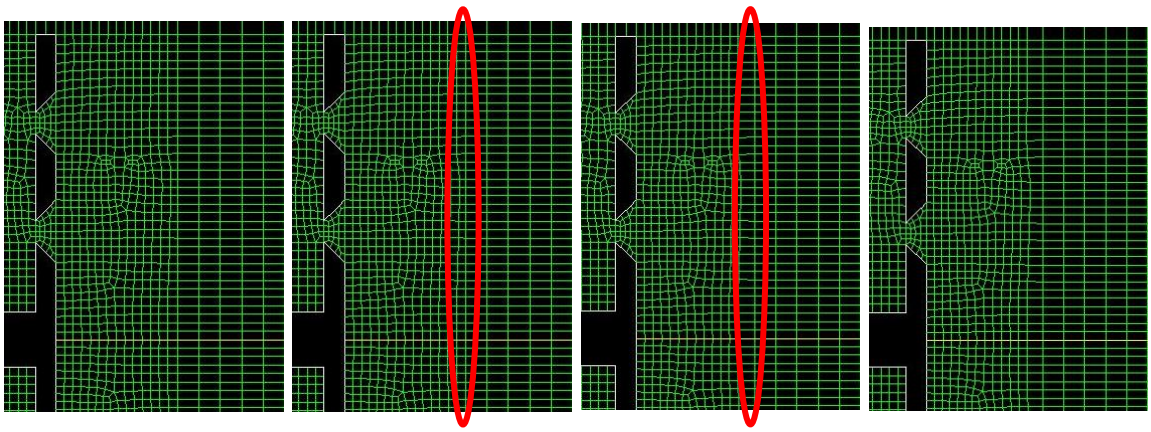

Figure 22 shows the progression of the mixer head along the x-axis (right direction) and the merging of two lines of elements between the finely meshed region around the mixer head and the coarse region using the layering dynamic mesh method in Fluent. Notice the disappearance of the element edges within the circled region as the elements combine.

The last step in dynamic meshing was to ensure that the time step was accurately sized such that the dynamic boundary does not move more than one element length between two time steps in order to prevent negative cell volume errors. With the 2 mm target element size, a 0.6 merge ratio and the peak velocity at each oscillation frequency, the largest time step that each case can utilize is 2 ms, 3 ms, 4 ms, and 8 ms for the 12 Hz, 9 Hz, 6 Hz, and 3 Hz respectively.

The species model was used to calculate and track the concentrations of two miscible fluids. For this study, water was used for both species A and B but still treated as two separate fluids. Initially the viscous model will be run until the flow in the mixer system reaches a steady state velocity in the fluid region sufficiently far enough from the mixer head to not be affected directly by mixer oscillations. Once steady state was achieved, the liquid was divided into two regions, species A and species B. At this point

the model was allowed to run until the liquid achieved a homogenized state. To ensure that the primary mode of mixing was pressure and viscously driven, the diffusion rate between the two species was reduced to 1 x 10^{-6} s^{-1}. The settings for the species model are otherwise set to default settings.

The VOF is the last model that needed to be utilized for this study. An air phase needed to be created and set as the primary phase by recommendation of the Fluent user manual [3]. Fluid regions in the mesh are then defined as either phase 1 (air) or phase 2 (water mixture) as shown in the diagrams below.

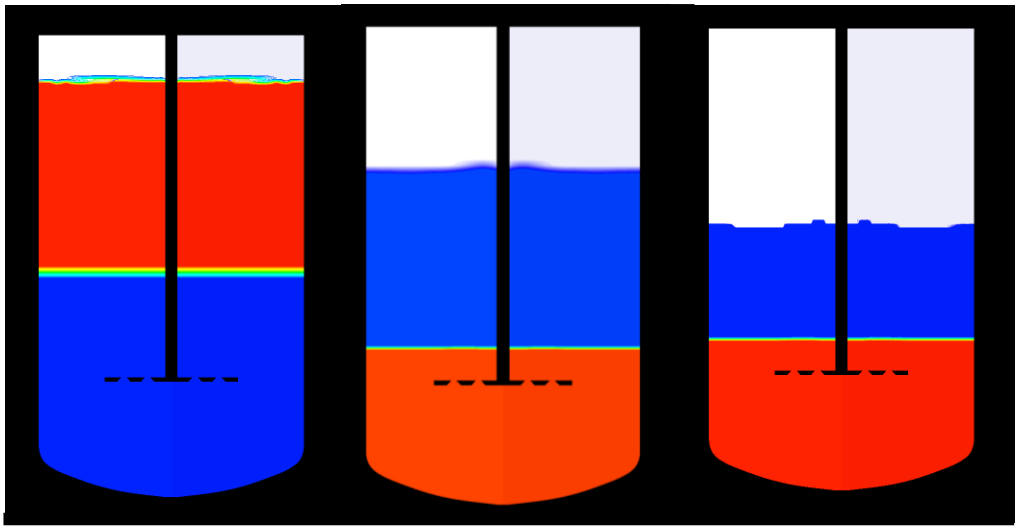

Figure 23 shows the three fill levels used for the two dimensional axisymmetric single mixer analysis: 200L, 150L, and 100L from left to right. The blue and red regions indicate the two discrete liquid species at the start of the mixing portion of the analysis. The white region represents the air region above the fluid.

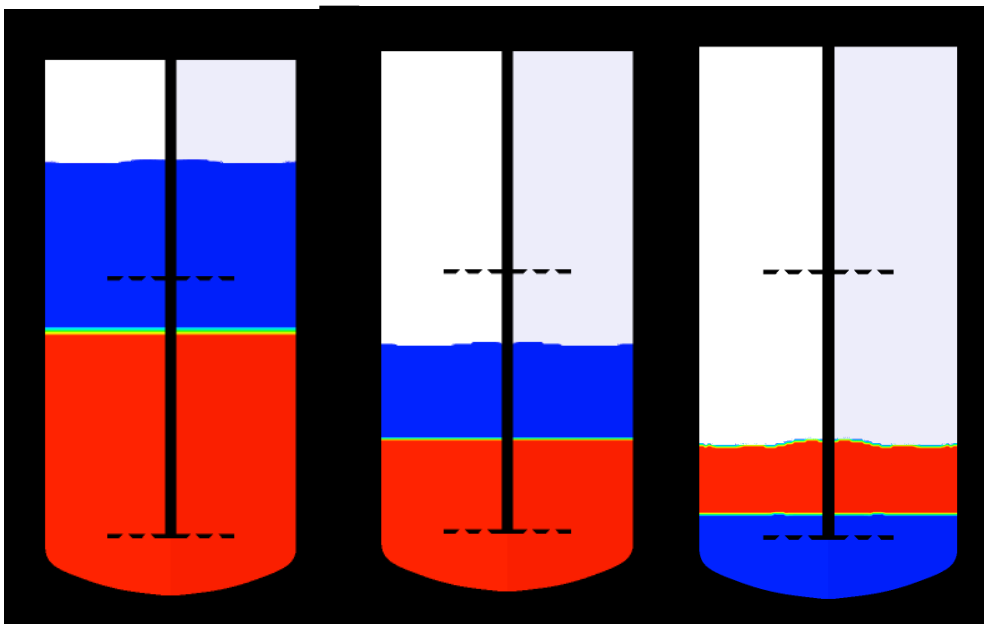

Figure 24 shows the three fill levels for the two dimensional axisymmetric dual mixer analysis: 218 L, 118 L, and 68 L from left to right. The blue and red regions indicate the two discrete liquid species at the start of mixing. The white region represents the air region above the fluid. Notice that the mixing for the 118 L and 68 L is only agitated by the bottom mixer.

For the VOF method to run on two dimensional axisymmetric cases utilizing more than a single processing core, the mesh cannot be partitioned with the default METIS method but rather, with evenly spaced radial partitions. Not doing so results in VOF divergence issues that causes air phase to randomly show up at locations in the liquid phase.

With the three additional modeling methods of VOF, dynamic meshing, and species, it was important to revisit the transient calculations. The final single and dual mixer meshes consisted of 7273 and 10675 elements, respectively. The solve time per iteration with all the modeling methods active was approximately 0.104 sec and 0.155 sec for the single and dual mixer case, respectively, on the E-6600 processor. Since the dynamic meshing requires 2 ms time step size instead of the originally calculated 4 ms, the total calculation time was recalculated with 5 million iterations instead of 2.5 million

for a fully homogenized mixture, resulting in a total computation time of approximately 215 hours for the dual mixer case. The added complexity in the added equations increases the computing requirement enough that the mesh needed to be coarsened in order to collect data in a reasonable amount of time. While the mesh in the single mixer configuration could be further refined to match the same total number of elements as the dual mixer, it was left as is to maintain similarity in the mesh surrounding the mixer head between the two different configurations for post processing.

IV. POST PROCESSING

Mixing Effectiveness

The homogenization time for several operating configurations were analyzed and compared. The criteria for perfect homogenization is the average volumetric concentration at time = 0 s for each case based on the initial quantities of arbitrary fluids A and B. In order to achieve perfect mixture, the models would need to run indefinitely, so it is more realistic to establish a tolerance. For this analysis ±2.5% of perfect mixture was selected to call fully homogenized as depicted below in Figure 25.

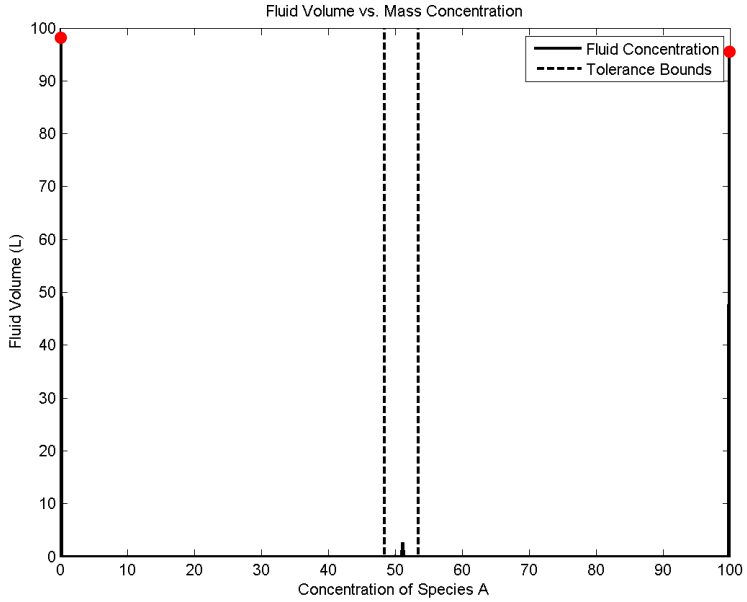

Figure 25 shows the concentration of liquid A and B at the initial mixing time step for the 200 L single mixer configuration analysis. The dotted lines show the upper and lower bounds of the fully homogenized state based on the average concentration from the initial quantities of the two liquids. Red dots are used to indicate the initial quantities of A and B.

In order to limit the total computation time further, the mixture needed 95% of the volume to be considered fully homogenized as a point of diminishing returns is reached when approaching optimal concentration. This progression is depicted below in Figure 26 and Figure 27 as the volume within the tolerance bounds increases with mixing time while

the change in the maximum and minimum concentration levels within the tank decrease with time.

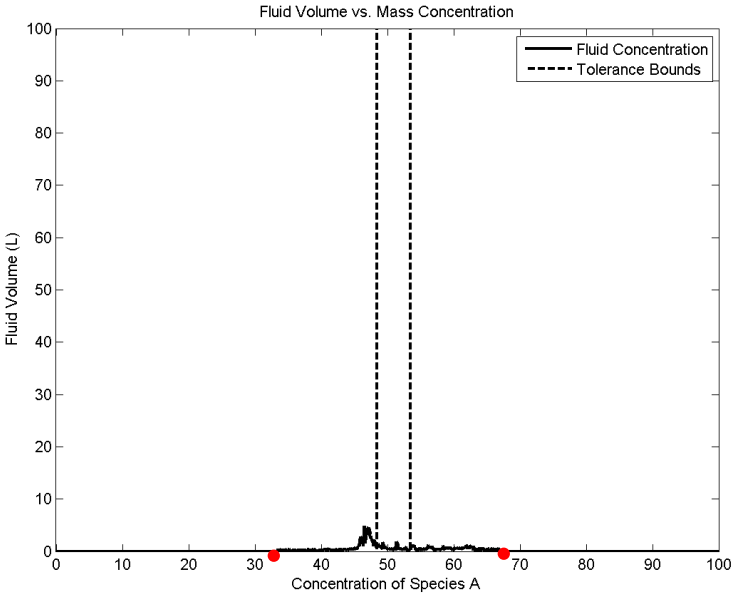

Figure 26 shows the total volume across the range of concentrations at t = 90 sec after mixing initiation. The maximum and minimum concentration of the fluid are indicated with red dots.

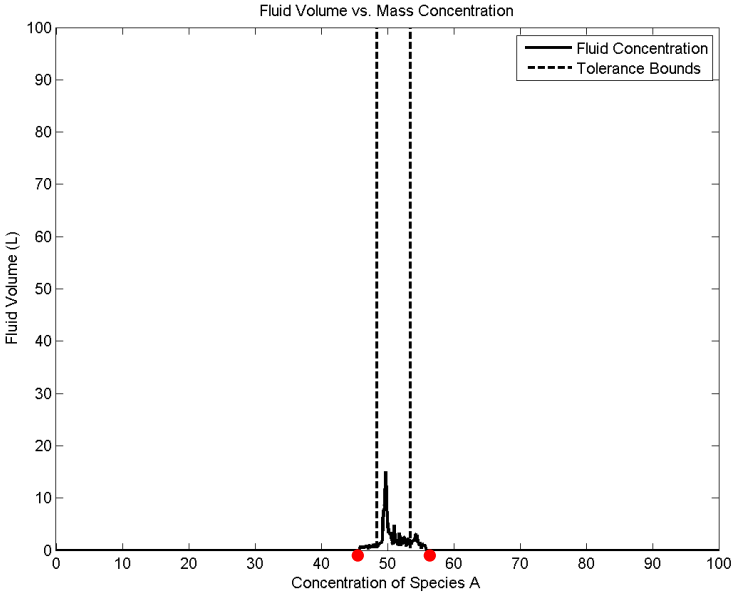

Figure 27 shows the total volume across the range of concentrations at t = 190 sec after mixing initiation. The maximum and minimum concentration of the fluid are indicated with red dots. At this time step, approximately 95% of the fluid is within the tolerance bounds.

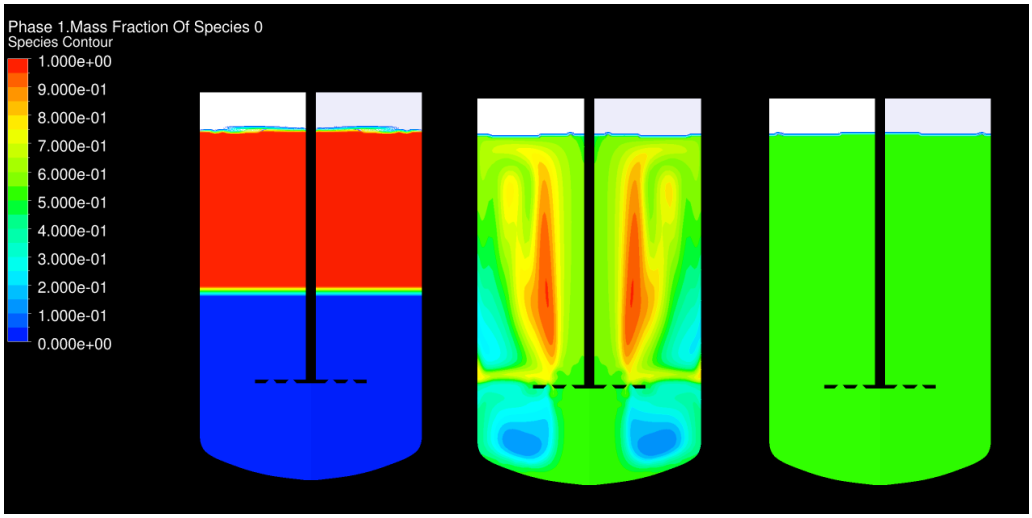

Figure 28 shows the single mixer configuration being mixed at a frequency of 12 Hz for t = 0, 30, and 190 seconds of mixing. The starting volume of fluid A (red) is 97 L and B (blue) is 100 L at t = 0 s. The expected result is a fluid with 49% concentration of fluid A and 51% concentration of fluid B which is achieved after 194 seconds of mixing.

After achieving a fully homogenized state, data is then exported for further post processing in MATLAB using code provided in Appendix C that outputs results as shown in Appendix A. Table 7 below shows the time required for full homogenization and improvements over the two tested oscillation speeds, as well as Figure 29 that visually depicts the results.

Table 7 shows the results from the homogenization analysis conducted on the two mixer configurations over varying tank fill volumes at 6 and 12 Hz.

	Oscillation Speed (Hz)	Tank Liquid Fill (L)	Homogenization Time (sec)	Improvement from 6 Hz to 12 Hz
Dual Mixer	6	68	119	-
	6	118	182	-
	6	217	276	-
	12	68	82	31%
	12	118	165	9%
	12	217	225	18%
Single Mixer	6	101	174	-
	6	148	224	-
	6	197	230	-
	12	101	152	13%
	12	148	201	10%
	12	197	203	12%

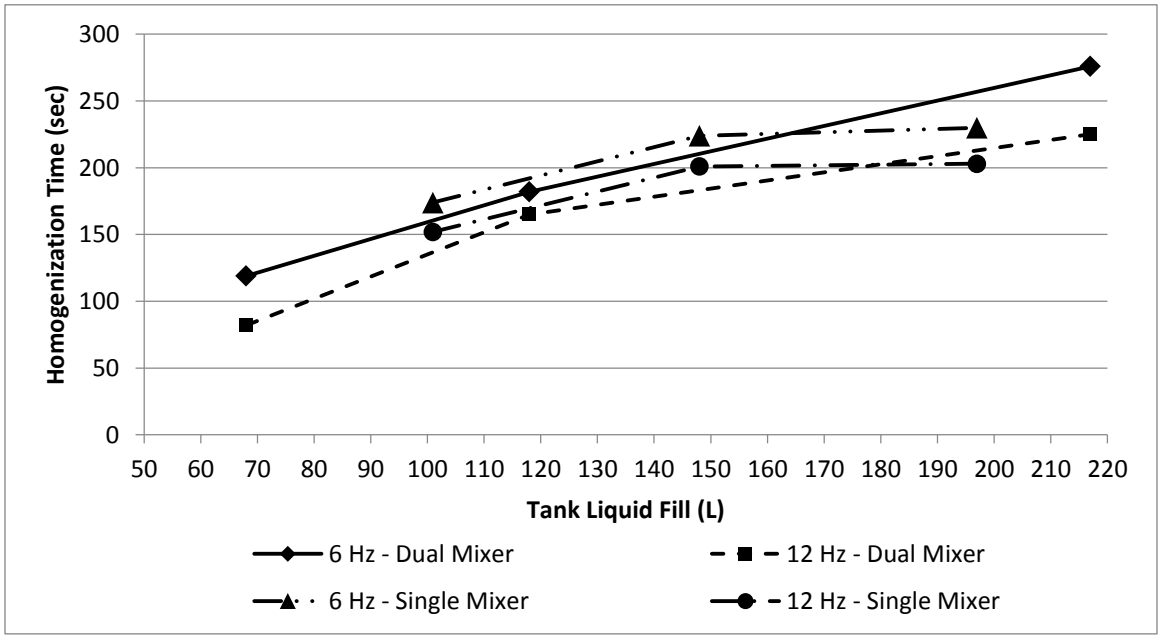

Figure 29 graphically depicts the results shown in Table 7. The results show the longer homogenization time required for higher quantities of tank liquid fill. Notice that at 100 L the time required to fully homogenize is similar for both single and dual mixer configurations, which is expected due to both cases only using a single mixer head for agitation.

The results show the expected upward trend in homogenization time as the fill volume increases. As expected, higher oscillation rates of the mixer yield shorter homogenization times, though the benefit of twice the frequency improves homogenization time only by an average of 20%. Finally, it is noticed that higher tank fill quantities do benefit from the amount of fluid that is homogenized since an increase of 100% of fluid only requires an average of 40% more time for complete homogenization.

An important result to note from this analysis is that using the dual mixer configuration provides little benefit in homogenization time over the single mixer configuration. At the 68 L and 118 L fill quantity only one mixer head was used in the dual mixer configuration, at which point the single mixer system could be used instead. When comparing the 118 L fill volume of the dual mixer configuration with the 100 L fill

volume of the single mixer configuration, the total homogenization time only increases by 3% for each respective oscillation frequency despite 20% more fill. Since both configurations use only one mixer for agitation, this shows that the closer proximity of the mixer head to the bottom wall has a positive effect on homogenization time. The time required for homogenization at the 200 L fill level indicates that the single mixer configuration homogenizes faster than the dual mixer configuration. This is highlighted in Figure 30 by the streamlines of the single and dual mixer configuration which surround each mixer head with a circular region of flow. The single mixer configuration produces two larger regions of flow circulation throughout the tank. Alternatively, the dual mixer configuration produces three smaller regions of circulation, which ultimately hinders the flow from circulating throughout the entire tank. The circulating flow in both cases produce a region at the center of the circulation where fluid becomes trapped and takes longer to homogenize with the rest of the tank.

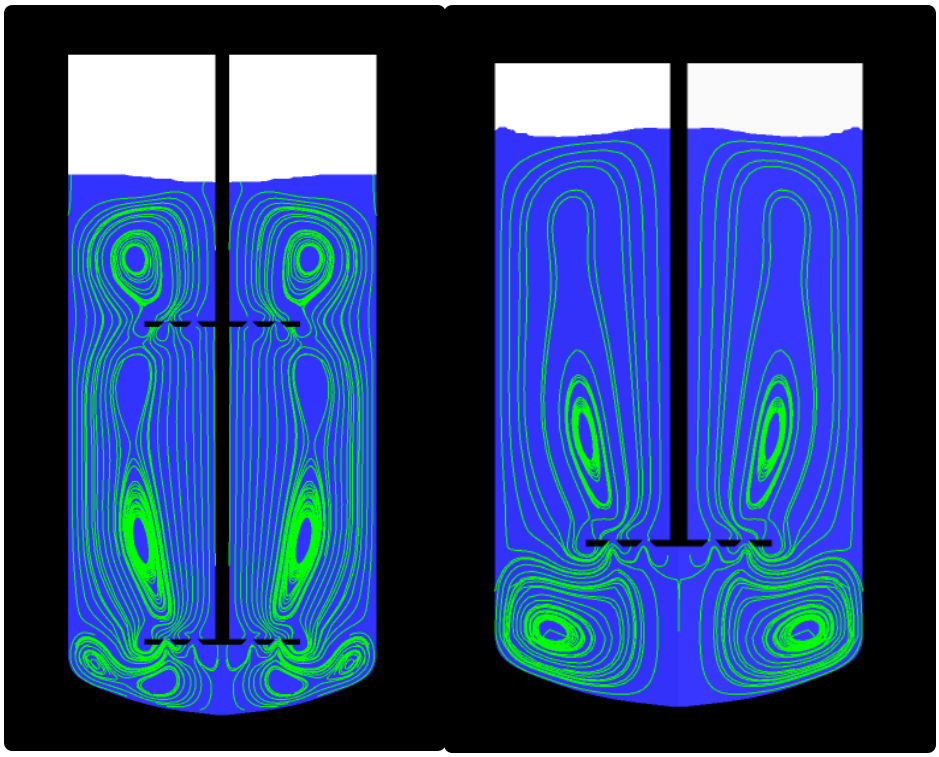

Figure 30 shows the streamlines for the dual mixer and the single mixer configuration. Notice that each mixer head generates its own region of circular flow with a dead zone in the center of it.

Momentum Analysis

Similar to the hand calculated forces that act on the bottom surface of the mixer head as shown in Chapter 2, CFD-POST was used to determine the forces acting on the bottom edges of the mixer head. The data was then extracted again and further analyzed in MATLAB using code included in Appendix C with results shown in Figure 31 through Figure 34. The hand calculations (Equation 7) show that the force data can be offset in magnitude by increases or decreases in the surrounding ambient pressure; therefore, values for surrounding pressure were selected in order to get the simulation data to overlap with the hand calculated data. The hand calculations tend to overshoot the CFD model due to the assumptions that are made to produce Equation 4. The

assumptions from the hand calculations state that the entire flow passes through the mixer head with none bypassing the side of the mixer and that the ambient flow around the mixer head is moving at the same rate as the peak mixer speed. Based on a peak to peak comparison between the two data sets, the difference between the hand calculation and CFD model are less than 12.1%. With the assumptions of an idealized, inviscid flow that were made in the hand calculations, such similarities in data show that the movement of the liquid around the head is primarily pressure driven.

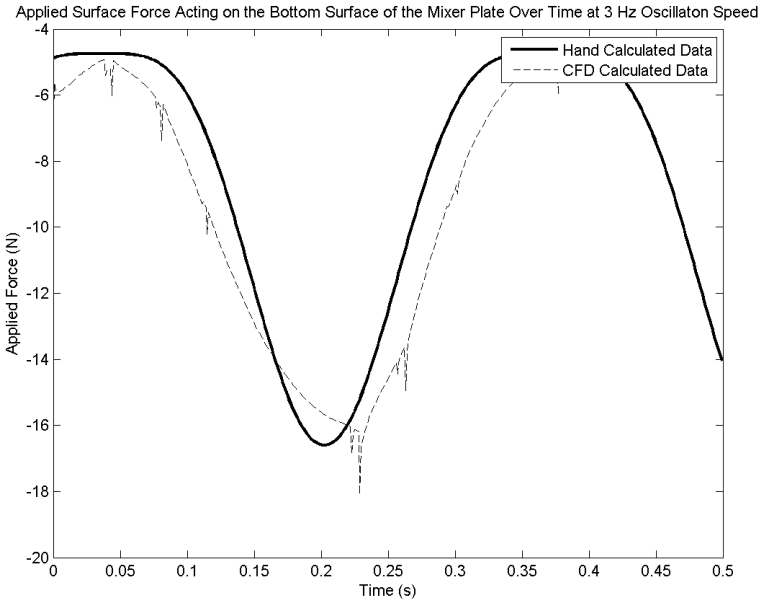

Figure 31 depicts the force applied over time on the bottom of the mixer head at 3 Hz oscillation rate. Hand calculated data is offset in magnitude in order to overlap with the simulation data.

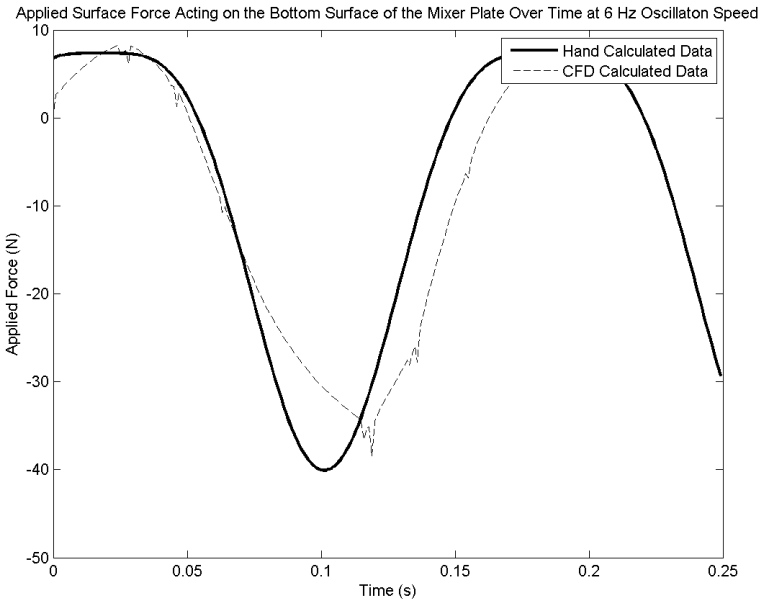

Figure 32 depicts the force applied over time on the bottom of the mixer head at 6 Hz oscillation rate.

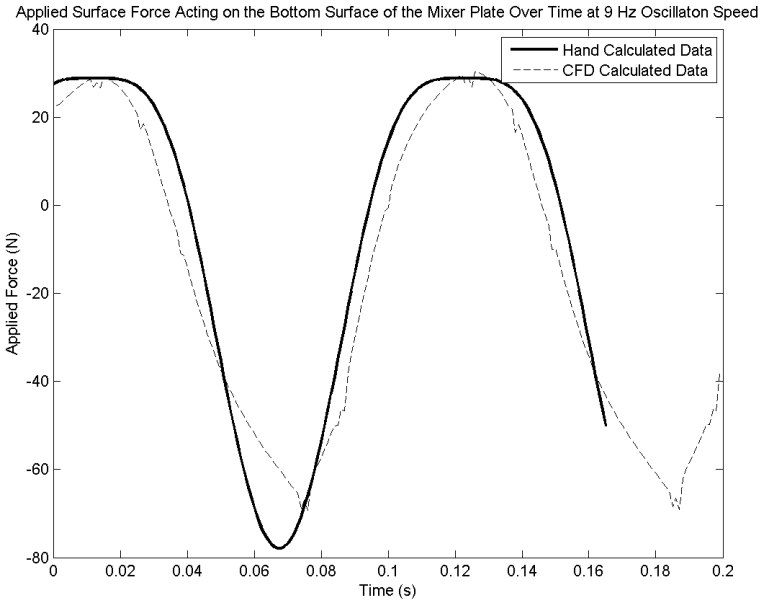

Figure 33 depicts the force applied over time on the bottom of the mixer head at 9 Hz oscillation rate.

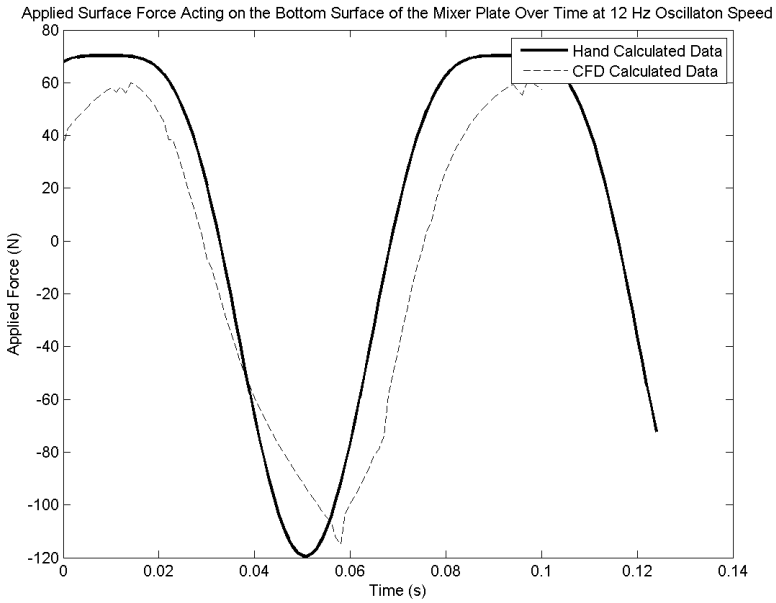

Figure 34 depicts the force applied over time on the bottom of the mixer head at 12 Hz oscillation rate.

Table 8 compares the results of the reaction force acting on the mixer head between the analytical hand calculations and the CFD model output.

Mixer head oscillation frequency	Peak to Peak force amplitude from Equation 4 (N)	Peak to Peak force amplitude from CFD Model (N)	Percent Difference from Equation 4
3 Hz	11.86	11.33	4.47%
6 Hz	47.44	42.55	10.3%
9 Hz	106.7	94.44	11.5%
12 Hz	189.8	166.9	12.1%

Wall Shear Stress Analysis

Using CFD-POST, data regarding the wall shear stress was extracted from the individual two dimensional axisymmetric models and compared for each configuration.

The extracted data was normalized along the length of the shaft from the top of the mixer head to the gas/liquid boundary. Shear stresses acting on the shaft in the air region are insignificant to those within the liquid region and are therefore neglected. Data was collected at varying mixer speeds for both the single and dual mixer configuration at the same relative stroke location in order to provide consistent results. Using transient data with time steps of 1 ms, each data set was extracted at the moment of peak wall shear stress.

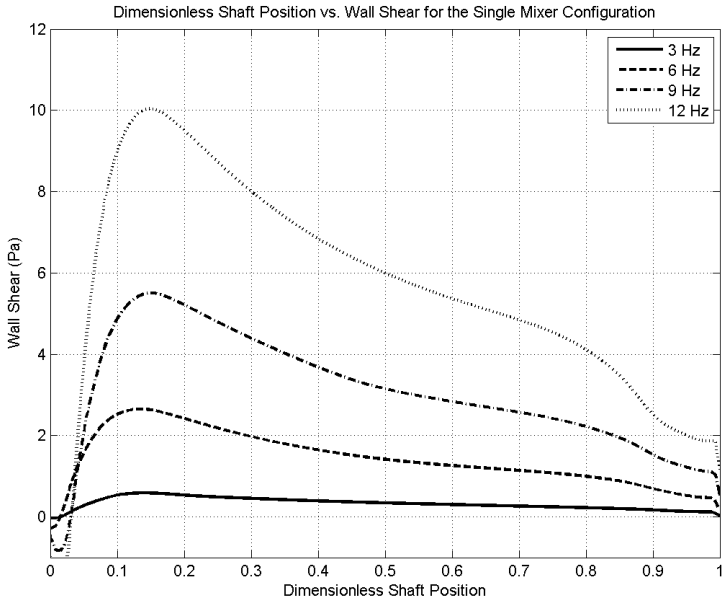

Figure 35 shows the single mixer configuration shaft wall shear stress for the four analyzed mixer speeds, 3, 6, 9, and 12 Hz.

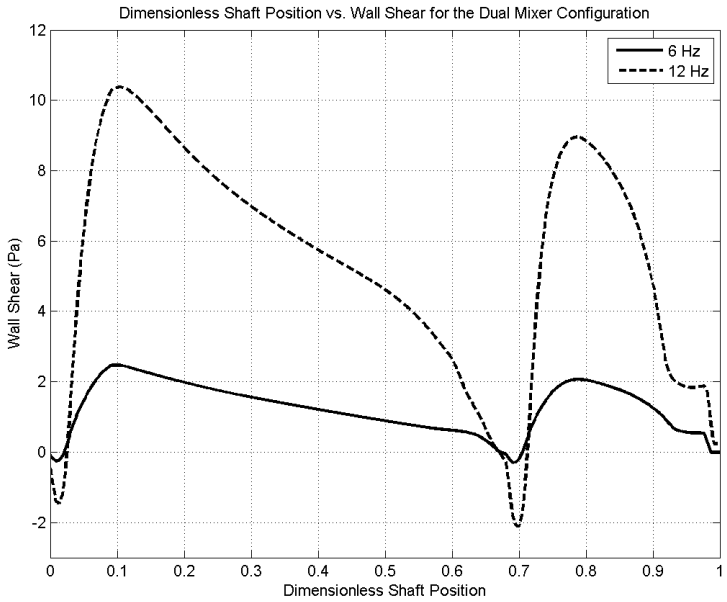

Figure 36 shows the dual mixer configuration shaft wall shear stress for the two analyzed speeds, 6 and 12 Hz.

The extracted results show that increases in mixer oscillation speed cause a square increase in maximum wall shear stress. The shear stress data is then normalized by the maximum shear for each case to check for consistency with the varying oscillation speeds. As seen in Figure 37 and Figure 38 below, both sets of data show very consistent results with the exception of the region close to the mixer heads (as x/L approaches 0.00 for both configurations and x/L approaches 0.68 on the dual mixer configuration as well), where the effects of turbulent eddies can produce varying results dependent on the flow past the corner that adjoins the shaft to the mixer head. This indicates that peak wall shear can be reasonably predicted for other operating speeds between 3 Hz and 12 Hz that were not analyzed.

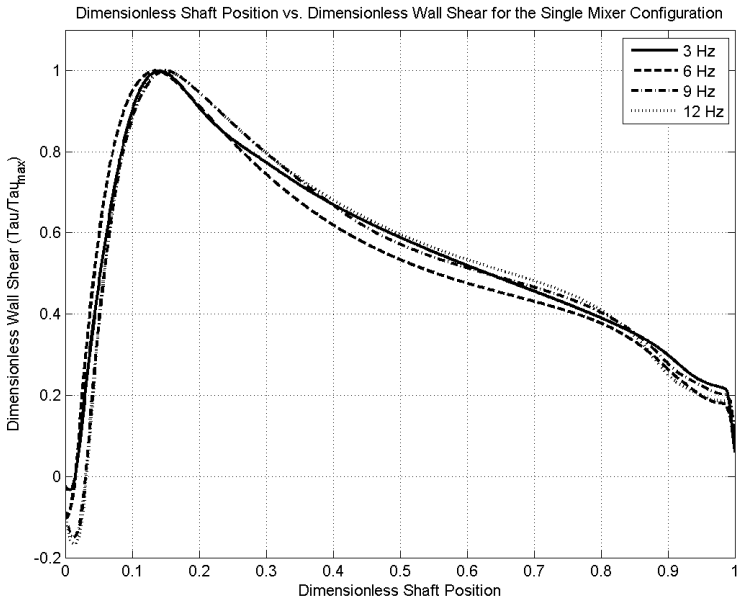

Figure 37 shows the wall shear along the shaft for the single mixer configuration non-dimensionalized by the maximum shear for each oscillation speed.

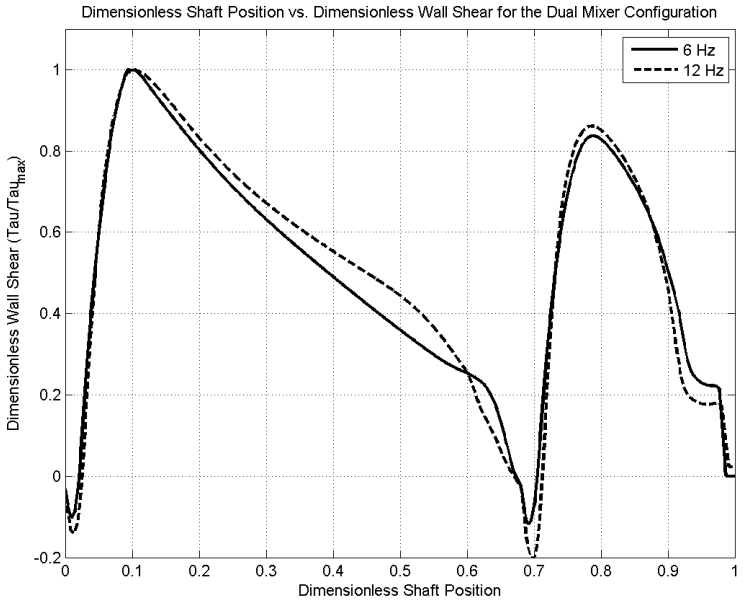

Figure 38 shows the wall shear along the shaft of the dual mixer configuration non-dimensionalized by the maximum shear for each oscillation speed.

A final wall shear comparison was made between the two dimensional axisymmetric case and the three dimensional case, both of which were set to oscillate

with a head frequency of 12 Hz and a tank fill of 200 L. The two models show the same trends in the wall shear stress along the mixer shaft, though at different magnitudes. Velocity data shows that the three dimensional model has a much slower flow velocity than the two dimensional axisymmetric cases, which also translates to the lower wall shear stress along the shaft. Due to constraints in computing power, further analysis into the three dimensional model could not be completed that may indicate the reason for lower velocity beyond differences in mixer head geometry.

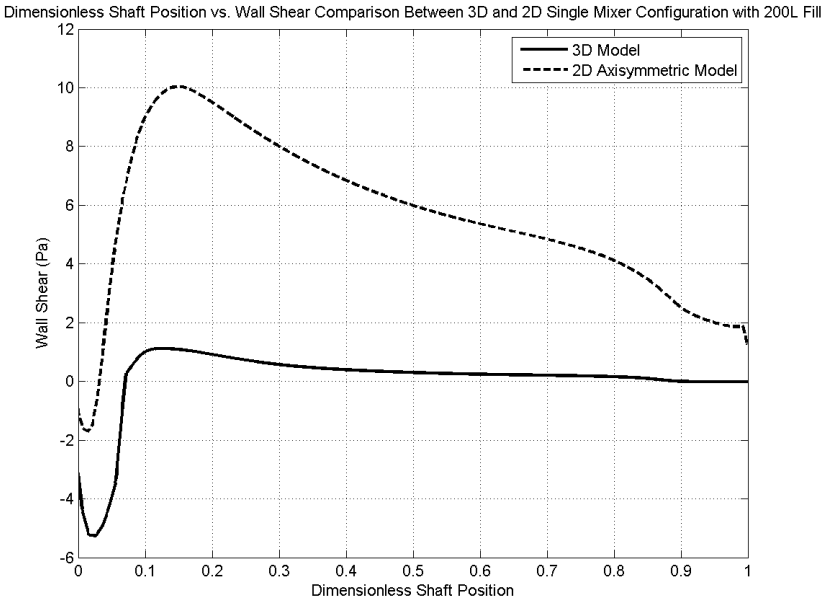

Figure 39 shows the comparison of shaft wall shear stress for the single mixer configuration at 200 L volume fill and a mixer oscillation rate of 12 Hz for the three dimensional and two dimensional axisymmetric model.

It is key to note that the two dimensional model assumes that the mixer head jets produce a ring of flow through the mixer head at two radial positions on the mixer head, whereas the three dimensional model produces multiple individual circular jets of flow. By integrating the open area on the mixer head for the radial position between the axis and the outer edge of the mixer head, it was found that the two dimensional mixer not only has more total flow area, but also has more flow area closer to the mixer shaft.

While the three dimensional mixer analysis increases flow area gradually along the radius of the mixer head, it does begin passing the flow through the mixer closer to the axis. The closer location to the axis for the flow-through area can cause a higher intensity eddy that produces the larger magnitude negative wall shear as seen in Figure 39 between x/L = 0 and x/L = 0.08. As shown below in Figure 40, when plotting the dimensionless area along dimensionless radial position, 33% of the total area for the two dimensional mixer is achieved at a radial location of 0.35, where-as the same ratio of total area is not achieved until 0.5 for the three dimensional case. This indicates that the two dimensional mixer is able to flow more fluid closer to the mixer shaft than the three dimensional case which explains the fact that the two dimensional case has larger wall shear than the three dimensional case.

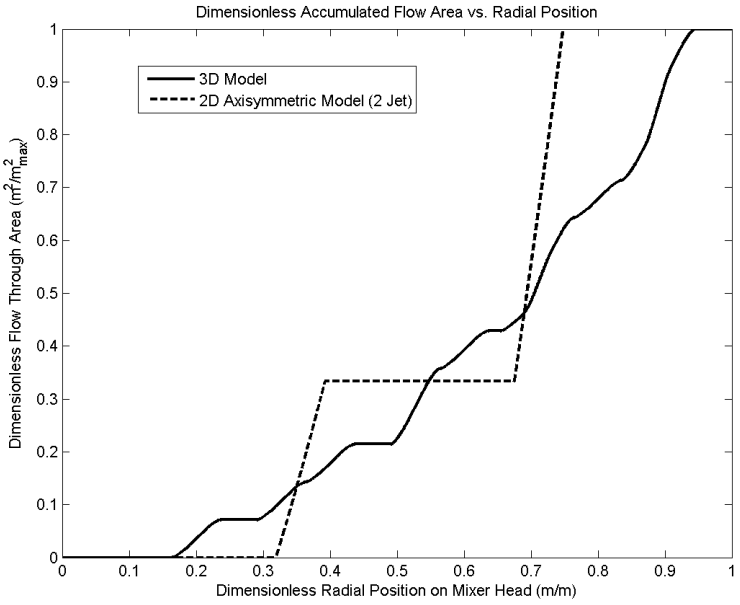

Figure 40 shows the growth of the total flow area on the mixer plate along the dimensionless radial location.

Velocity Trend Analysis

Further analysis was conducted using velocity profiles at arbitrary axial locations along the mixer shaft that start at the shaft surface and extend radially outward to the inner tank surface. For the single head mixer, locations 25%, 50% and 75% of the submerged shaft length above the mixer were chosen, as shown below in Figure 41. Similarly, 25%, 50% and 75% of the shaft length between the bottom and top mixer and 50% between the top mixer and the liquid/gas boundary were selected for the dual mixer case as shown below in Figure 42.

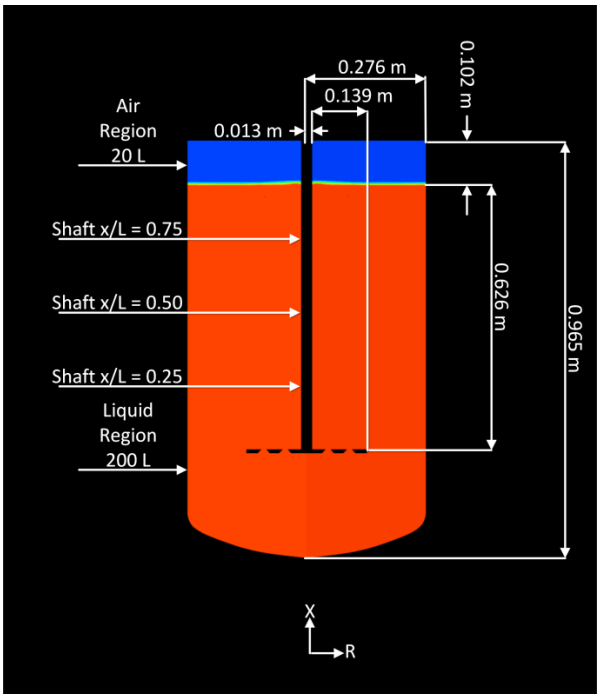

Figure 41 shows the single mixer configuration with the location of the fluid boundary as well as the velocity profile axial locations.

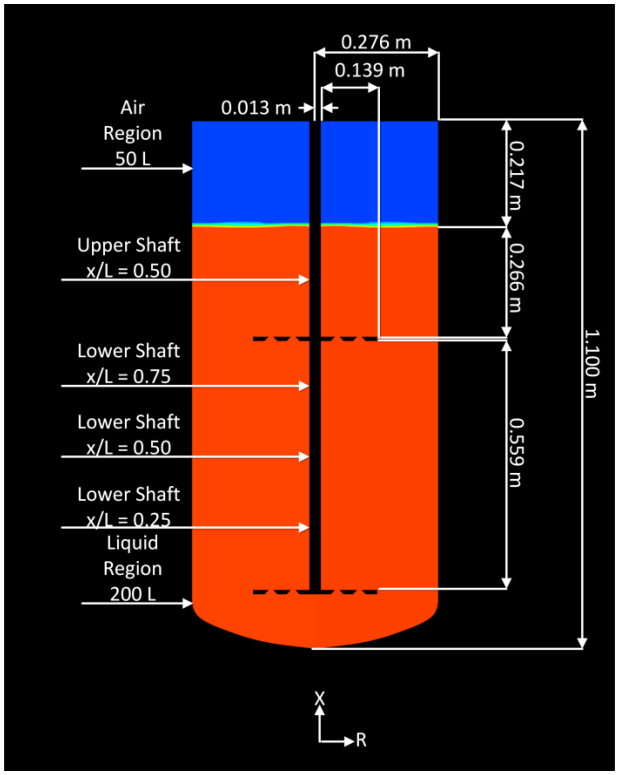

Figure 42 shows the dual mixer configuration with the locations of the fluid boundary as well as the velocity profile axial locations.

Using the same method as above in the shear stress data, the same stroke positions at which shear stress are maximum were analyzed for all oscillation speeds. Data for each axial location mentioned can be found in Appendix B. Below in Figure 43 and Figure 44, the velocity profile half way between the mixer head and liquid/gas surface for the single mixer configuration and halfway between the two mixer heads in the dual mixer configuration are depicted. The remaining data that is not shown follows the same trend and is not included in this portion of the report, but can be found in Appendix B.

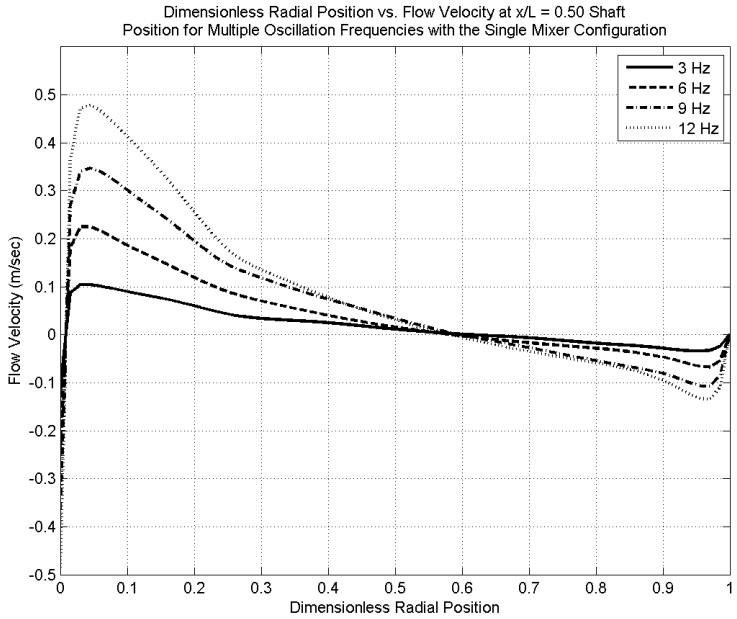

Figure 43 shows the velocity profile extending radially outward from the mixer shaft surface to the inner wall of the tank at the axial location half way between the mixer head surface and liquid/gas boundary for the two dimensional single mixer configuration.

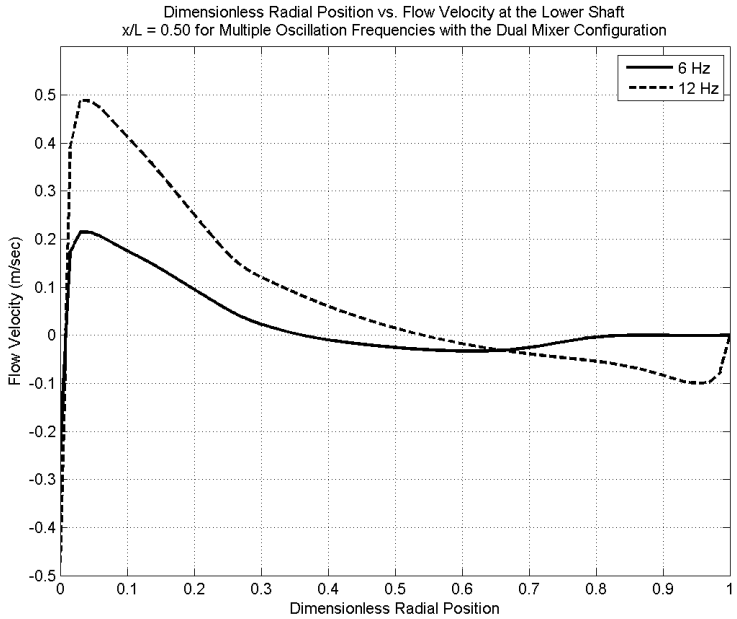

Figure 44 shows the velocity profile extending radially from the mixer shaft surface to the inner wall of the mixing tank at the axial location half way between the two mixer heads of the dual mixer configuration.

As expected, the velocity profile changes proportionally with changes in mixer oscillation speed. An interesting note seen in the velocity profile data for the single mixer configuration is that all four of the simulated mixer oscillation speeds cross at the same dimensionless radial location, indicating that the structure of the flow is unaffected by changes in mixer oscillation speeds. This shows that changes in mixer speed will not affect the flow pattern in the system and therefore the same stagnation points will exist when running the system at speeds between 3 Hz and 12 Hz. It also depicts that some flow does bypass around the mixer head as shown in Figure 43 and Figure 44 by the positive flow velocity beyond the dimensionless radial position r/R = 0.5. The bypassing that occurs agrees with the result that the hand calculated results for mixer head reaction force are higher than those of the CFD model.

Similar to the shear stress analysis, a comparison was made between the three dimensional and two dimensional axisymmetric cases with the oscillation frequency of 12 Hz and 200 L fill volume. The three dimensional model shows a similar shape of the flow velocity curve compared to the two dimensional case, though with a reduction in velocity by a factor of about 2.5 as shown in Figure 45 on the next page. The location at which the flow is zero is the same for both cases, showing that the circulation in the flow remains the same for either model.

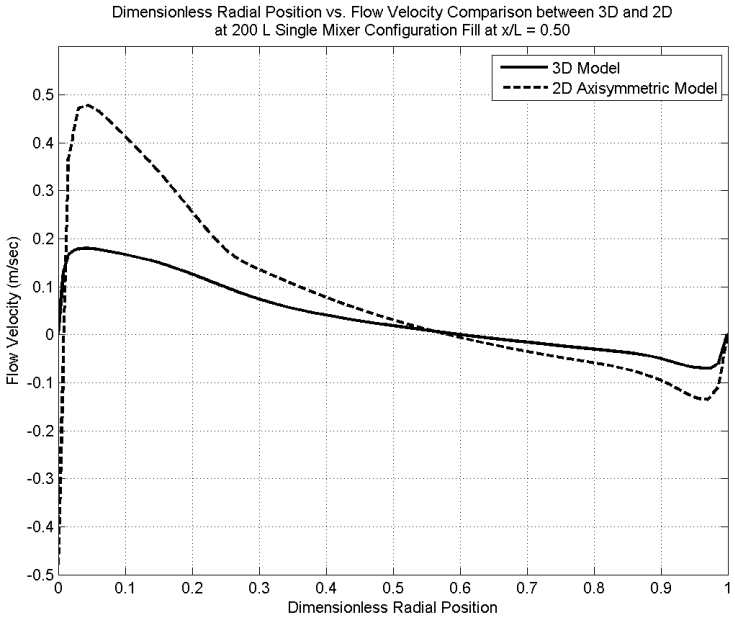

Figure 45 shows the radial velocity profile comparison between the two and three dimensional models at the dimensionless shaft position x/L = 0.50.

V. CONCLUSION

The analysis of the Meissner Saltus Mixing system characterized the mixing effectiveness of the system and shaft wall shear stress. In addition, force application on the mixer head from fluid momentum and velocity profiles at multiple locations in the mixer system were characterized for validation purposes.

The mixing effectiveness was analyzed and three key points were found to be important for homogenization: 1.) the use of the dual mixer configuration, 2.) the location of the lower mixer head from the tank surface, and 3.) the presence of deadzones in the circulating flow. The simulation of the system shows that the existing dual mixer configuration provides little advantage in homogenization time over the single mixer configuration. The advantage that the dual mixer configuration has is when only the lower mixer head is used for agitation due to the closer proximity to the lower tank wall as opposed to the single mixer configuration that showed only a 3% increase in homogenization time for an extra 20% of liquid fill. When both mixer heads are used in the dual mixer configuration, the homogenization time continually increases to a higher value up to 218 L, unlike the single mixer configuration that asymptotes after 150 L of fill volume. The increasing mixing time for the dual mixer configuration comes from the three regions of flow that occur surrounding each mixer which interact poorly. With the current design, it is recommended to use only the single mixer configuration. Further design research can be conducted to determine better geometry and independent designs for each mixer head of the dual mixer configuration to potentially increase the mixing performance to a rate that is significantly better than the single mixer configuration. A separate study can be performed to determine the optimum axial location for the lower mixer to achieve the shortest homogenization time. The analyses performed did not account for swirl around the center axis, which is another useful topic

of further research. By adding swirl, the fluid can gain centrifugal motion that can draw fluid out of the deadzones at the center of the circulating regions of the flow as observed by the axisymmetric and three dimensional models.

Wall shear analysis showed that the fluid encounters two maximum shear values, one positive along the shaft with the fluid motion and one negative flowing with the eddy just after the mixer head. The maximum shear encountered was 10.0 Pa and 10.4 Pa for the single and dual mixer configuration, respectively. This indicates that the single mixer configuration will produce less destructive flow for the fluid being mixed and that having two mixer heads with longer mixing time is counterproductive towards protein production.

The force applied on the mixer head showed congruency with the hand calculations, which shows that the model is sufficiently validated. The peak difference between the hand calculation and CFD simulation was 12.1% at the 12 Hz oscillation frequency. The difference is attributed to the assumptions made during the hand calculations which force the fluid to flow entirely through the mixer jets as opposed to some short circuiting that occurs around the mixer plate and that the assumed relative fluid flow is higher than the actual observed flow. The assumptions in the hand calculations therefore add more force to the mixer head, generating a conservative estimate to the force applied to the fluid.

The velocity analysis shows both the trend in fluid velocity versus the mixer head oscillation frequency and the presence of dead zones in the flow. The fluid velocity at various locations in the tank was shown to scale directly with the mixer oscillation frequency. Knowing the correlation between the mixer oscillation frequency and fluid velocity allows for the flow velocity to be controlled. The velocity analysis also shows that the location of stagnation points in the flow is independent of oscillation frequency;

stagnation points are always occurring at the same location. Therefore, the flow pattern within the tank can be predicted at any mixer head speed however, dead zones in the circulating flow always exist, thereby hindering homogenization.

The next stage in analysis, would be to collect PIV data from the system to further validate the three-dimensional model. Once the model has been validated, the geometry of the mixing system can be modified and re-simulated with the CFD code until an improved design is created, at which point, the system can be retested with the new design. An OpenFOAM version of the two dimensional axisymmetric model has been created though it has not been used for a simulation due to time constraints. This model can be used as a low cost simulation by the sponsor to use at their own facility without the need to purchase any software licenses as would be required by ANSYS Fluent.

BIBLIOGRAPHY

[1] Meissner Filtration Products, Inc., "Saltus M200 Single-Use Mixing System," 29 October 2014. [Online]. Available: https://www.meissner.com/products/onetouch/saltus.asp.

[2] F. M. White, "Control Volume Formulations," in *Viscous Fllow*, McGraw Hill Education, 2013, pp. 98-99.

[3] ANSYS, Inc, "Introduction to ANSYS Fluent," in *ANSYS Fluent User's Guide, 15.0*, Pennsylvania, 2014.

[4] K. M. D. a. S. L. Mahan, "Vibromixers - Take the Plunge," *FLUENT News,* p. 1, Fall 2002.

[5] Z. Fang, "BioPharm International: Applying Computational Fluid Dynamics Technology in Bioprocesses-Part 2," 1 May 2010. [Online]. Available: http://license.icopyright.net/user/viewFreeUse.act?fuid=MTMwMzAwMzE%3D. [Accessed 1 June 2011].

[6] M. N. E. M.H. Vakili, "CFD analysis of turbulence in a baffled stirred tank, a three-compartment model," *Chemical Engineering Science,* vol. 64, pp. 351-362, 2009.

[7] ANSYS, Inc, "Theory Guide: Turbulence," in *ANSYS Fluent User's Guide*, Pennsylvania, 2014.

APPENDIX A – OUTPUT DATA

Single Mixer Configuration Mixing Results

12 Hz – 200 L Fill

Analysis Settings

Time steps analyzed:	23
Time step size (sec):	10
Tank Volume (L):	250
Number of Histogram bins:	1000
Mixture tolerance (+-%):	2.5

Calculated Data

Air Volume (L):	53
Liquid Volume (L):	197
Liquid A Starting Volume (L):	97
Liquid B Starting Volume (L):	100
Maximum Head Velocity (m/sec):	0.490
Minimum Head Velocity (m/sec):	-0.490
Maximum Head Force Encountered (N):	60.414
Minimum Head Force Encoutnered (N):	-115.051
Time for 95% volume to achieve mixing tolerance (sec):	203

Analysis Data

Time	Mixture Quality
0	1%
10	5%
20	6%
30	5%
40	7%
50	9%
60	11%
70	12%
80	15%
90	17%
100	22%
110	30%
120	43%
130	52%
140	58%
150	64%
160	67%
170	72%
180	77%
190	85%
200	94%
210	98%
220	99%
230	99%

12 Hz – 150 L Fill

Analysis Settings

Time steps analyzed:	22
Time step size (sec):	10
Tank Volume (L):	250
Number of Histogram bins:	1000
Mixture tolerance (+-%):	2.5

Calculated Data

Air Volume (L):	102
Liquid Volume (L):	148
Liquid A Starting Volume (L):	82
Liquid B Starting Volume (L):	66
Time for 95% volume to achieve mixing tolerance (sec):	201

Analysis Data

Time	Mixture Quality
0	0%
10	6%
20	8%
30	10%
40	14%
50	18%
60	27%
70	39%
80	42%
90	48%
100	52%
110	56%
120	59%
130	65%
140	69%
150	74%
160	80%
170	85%
180	88%
190	91%
200	95%
210	98%
220	100%

12 Hz – 100 L Fill

Analysis Settings

Time steps analyzed:	16
Time step size (sec):	10
Tank Volume (L):	250
Number of Histogram bins:	1000
Mixture tolerance (+-%):	2.5

Calculated Data

Air Volume (L):	149
Liquid Volume (L):	101
Liquid A Starting Volume (L):	42
Liquid B Starting Volume (L):	59
Time for 95% volume to achieve mixing tolerance (sec):	152

Analysis Data

Time	Mixture Quality
0	6%
10	6%
20	21%
30	27%
40	32%
50	37%
60	40%
70	44%
80	48%
90	53%
100	58%
110	64%
120	70%
130	77%
140	85%
150	94%
160	100%

6 Hz – 200 L Fill

Analysis Settings

Time steps analyzed:	24
Time step size (sec):	10
Tank Volume (L):	250
Number of Histogram bins:	1000
Mixture tolerance (+-%):	2.5

Calculated Data

Air Volume (L):	53
Liquid Volume (L):	197
Liquid A Starting Volume (L):	107
Liquid B Starting Volume (L):	90
Maximum Head Velocity (m/sec):	0.245
Minimum Head Velocity (m/sec):	-0.245
Maximum Head Force Encountered (N):	8.747
Minimum Head Force Encoutnered (N):	-38.452
Time for 95% volume to achieve mixing tolerance (sec):	230

Analysis Data

Time	Mixture Quality
0	0%
10	2%
20	10%
30	4%
40	11%
50	15%
60	14%
70	15%
80	19%
90	23%
100	28%
110	33%
120	38%
130	43%
140	49%
150	55%
160	59%
170	63%
180	68%
190	72%
200	78%
210	85%
220	90%
230	95%
240	98%

6 Hz – 150 L Fill

Analysis Settings

Time steps analyzed:	24
Time step size (sec):	10
Tank Volume (L):	250
Number of Histogram bins:	1000
Mixture tolerance (+-%):	2.5

Calculated Data

Air Volume (L):	102
Liquid Volume (L):	148
Liquid A Starting Volume (L):	84
Liquid B Starting Volume (L):	65
Time for 95% volume to achieve mixing tolerance (sec):	224

Analysis Data

Time	Mixture Quality
0	0%
10	5%
20	4%
30	8%
40	9%
50	15%
60	16%
70	15%
80	21%
90	25%
100	29%
110	33%
120	37%
130	43%
140	49%
150	56%
160	60%
170	65%
180	70%
190	75%
200	80%
210	86%
220	93%
230	99%
240	100%

6 Hz – 100 L Fill

Analysis Settings

Time steps analyzed:	18
Time step size (sec):	10
Tank Volume (L):	250
Number of Histogram bins:	1000
Mixture tolerance (+-%):	2.5

Calculated Data

Air Volume (L):	138
Liquid Volume (L):	112
Liquid A Starting Volume (L):	67
Liquid B Starting Volume (L):	45
Time for 95% volume to achieve mixing tolerance (sec):	174

Analysis Data

Time	Mixture Quality
0	6%
10	6%
20	12%
30	10%
40	10%
50	13%
60	20%
70	24%
80	34%
90	42%
100	53%
110	59%
120	64%
130	69%
140	74%
150	80%
160	86%
170	93%
180	98%

Dual Mixer Configuration Mixing Results

12 Hz – 200 L Fill

Analysis Settings

Time steps analyzed:	23
Time step size (sec):	10
Tank Volume (L):	250
Number of Histogram bins:	1000
Mixture tolerance (+-%):	2.5

Calculated Data

Air Volume (L):	33
Liquid Volume (L):	217
Liquid A Starting Volume (L):	101
Liquid B Starting Volume (L):	117
Time for 95% volume to achieve mixing tolerance (sec):	225

Analysis Data

Time	Mixture Quality
0	11%
10	11%
20	22%
30	23%
40	26%
50	29%
60	30%
70	32%
80	34%
90	37%
100	40%
110	43%
120	48%
130	54%
140	61%
150	65%
160	69%
170	72%
180	76%
190	80%
200	84%
210	89%
220	93%
230	97%

12 Hz – 100 L Fill

Analysis Settings

Time steps analyzed:	18
Time step size (sec):	10
Tank Volume (L):	250
Number of Histogram bins:	1000
Mixture tolerance (+-%):	2.5

Calculated Data

Air Volume (L):	132
Liquid Volume (L):	118
Liquid A Starting Volume (L):	47
Liquid B Starting Volume (L):	70
Time for 95% volume to achieve mixing tolerance (sec):	165

Analysis Data

Time	Mixture Quality
0	0%
10	6%
20	6%
30	6%
40	7%
50	9%
60	11%
70	14%
80	21%
90	46%
100	73%
110	76%
120	79%
130	82%
140	85%
150	88%
160	93%
170	97%
180	98%

12 Hz – 50 L Fill

Analysis Settings

Time steps analyzed:	11
Time step size (sec):	10
Tank Volume (L):	250
Number of Histogram bins:	1000
Mixture tolerance (+-%):	2.5

Calculated Data

Air Volume (L):	182
Liquid Volume (L):	68
Liquid A Starting Volume (L):	34
Liquid B Starting Volume (L):	34
Time for 95% volume to achieve mixing tolerance (sec):	82

Analysis Data

Time	Mixture Quality
0	0%
10	4%
20	9%
30	25%
40	72%
50	79%
60	84%
70	89%
80	94%
90	99%
100	103%
110	103%

6 Hz – 200 L Fill

Analysis Settings

Time steps analyzed:	28
Time step size (sec):	10
Tank Volume (L):	250
Number of Histogram bins:	1000
Mixture tolerance (+-%):	2.5

Calculated Data

Air Volume (L):	33
Liquid Volume (L):	217
Liquid A Starting Volume (L):	87
Liquid B Starting Volume (L):	130
Time for 95% volume to achieve mixing tolerance (sec):	276

Analysis Data

Time	Mixture Quality
0	0%
10	1%
20	10%
30	6%
40	17%
50	14%
60	12%
70	26%
80	20%
90	21%
100	22%
110	23%
120	26%
130	30%
140	33%
150	36%
160	42%
170	54%
180	69%
190	76%
200	80%
210	86%
220	88%
230	89%
240	89%
250	91%
260	92%
270	94%
280	96%

6 Hz – 100 L Fill

Analysis Settings

Time steps analyzed:	21
Time step size (sec):	10
Tank Volume (L):	250
Number of Histogram bins:	1000
Mixture tolerance (+-%):	2.5

Calculated Data

Air Volume (L):	132
Liquid Volume (L):	118
Liquid A Starting Volume (L):	47
Liquid B Starting Volume (L):	70
Time for 95% volume to achieve mixing tolerance (sec):	182

Analysis Data

Time	Mixture Quality
0	0%
10	5%
20	6%
30	9%
40	9%
50	9%
60	11%
70	16%
80	19%
90	23%
100	31%
110	45%
120	66%
130	78%
140	81%
150	83%
160	87%
170	90%
180	94%
190	98%
200	100%
210	100%

6 Hz – 50 L Fill

Analysis Settings

Time steps analyzed:	12
Time step size (sec):	10
Tank Volume (L):	250
Number of Histogram bins:	1000
Mixture tolerance (+-%):	2.5

Calculated Data

Air Volume (L):	182
Liquid Volume (L):	68
Liquid A Starting Volume (L):	34
Liquid B Starting Volume (L):	34
Time for 95% volume to achieve mixing tolerance (sec):	119

Analysis Data

Time	Mixture Quality
0	1%
10	4%
20	6%
30	8%
40	12%
50	18%
60	31%
70	61%
80	78%
90	81%
100	85%
110	90%
120	96%

APPENDIX B – FIGURES

Velocity Profiles – Single Mixer Axisymmetric

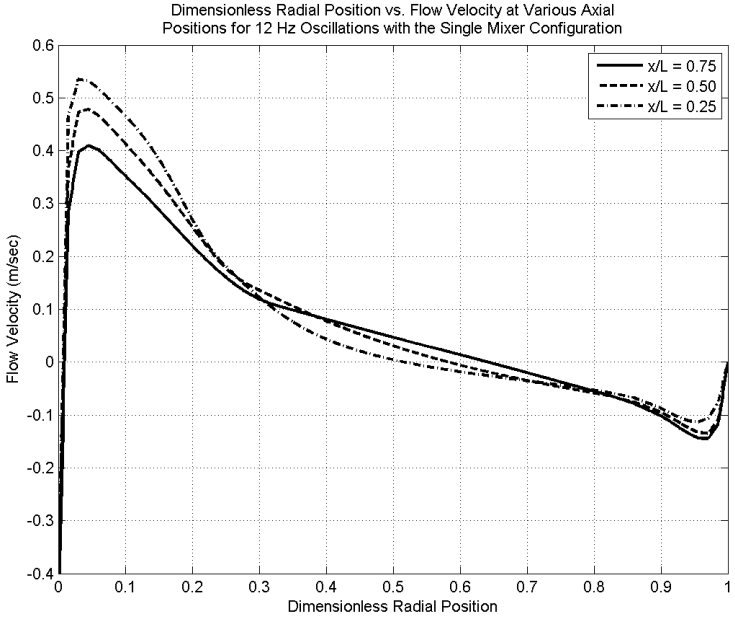

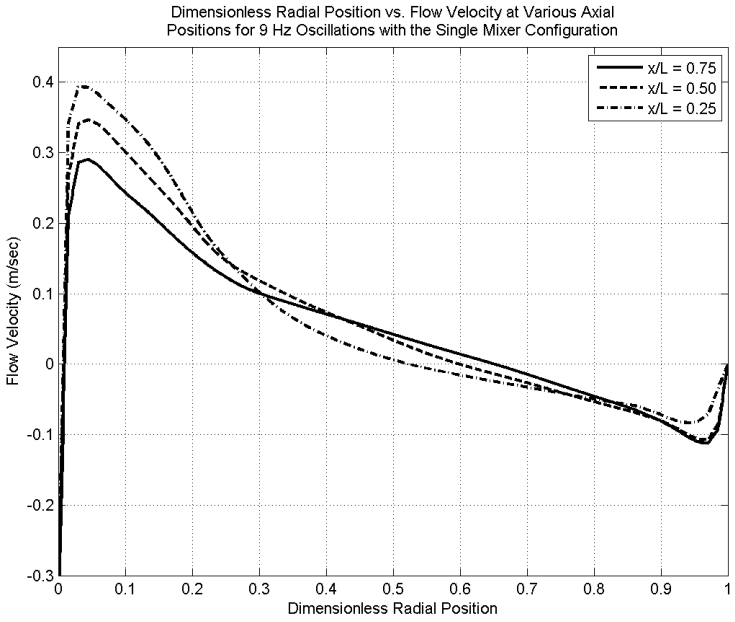

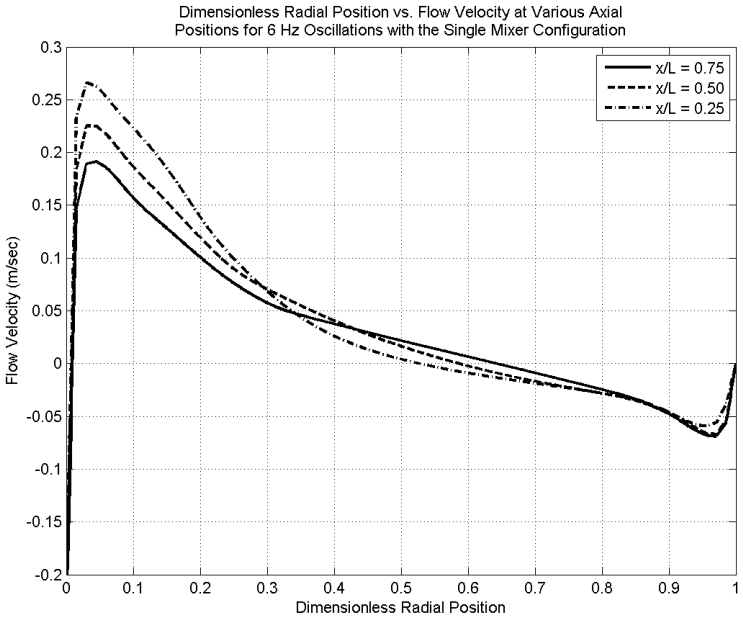
Dimensionless Radial Position vs. Flow Velocity at Various Axial Positions for 6 Hz Oscillations with the Single Mixer Configuration
x/L = 0.75
x/L = 0.50
x/L = 0.25
Flow Velocity (m/sec)
Dimensionless Radial Position
0.3
0.25
0.2
0.15
0.1
0.05
0
-0.05
-0.1
-0.15
-0.2
0
0.1
0.2
0.3
0.4
0.5
0.6
0.7
0.8
0.9
1

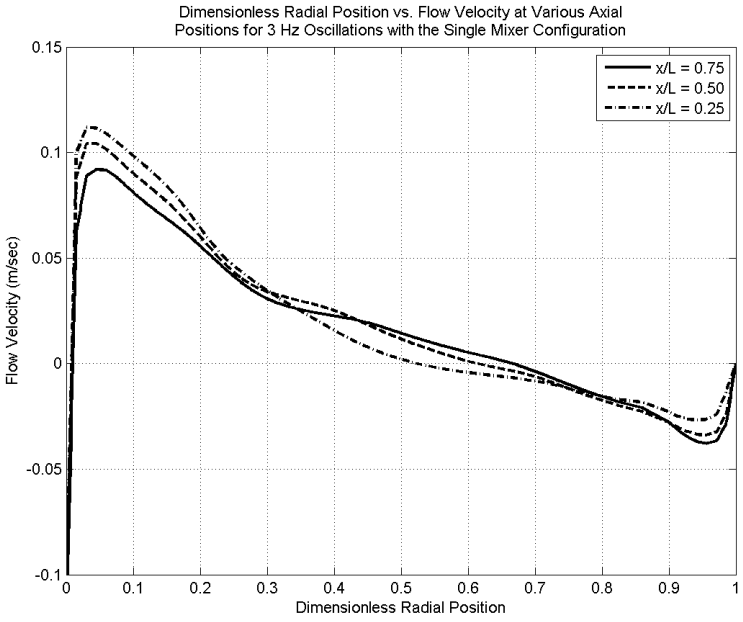
Dimensionless Radial Position vs. Flow Velocity at Various Axial Positions for 3 Hz Oscillations with the Single Mixer Configuration
x/L = 0.75
x/L = 0.50
x/L = 0.25
Flow Velocity (m/sec)
Dimensionless Radial Position
0.15
0.1
0.05
0
-0.05
-0.1
0
0.1
0.2
0.3
0.4
0.5
0.6
0.7
0.8
0.9
1

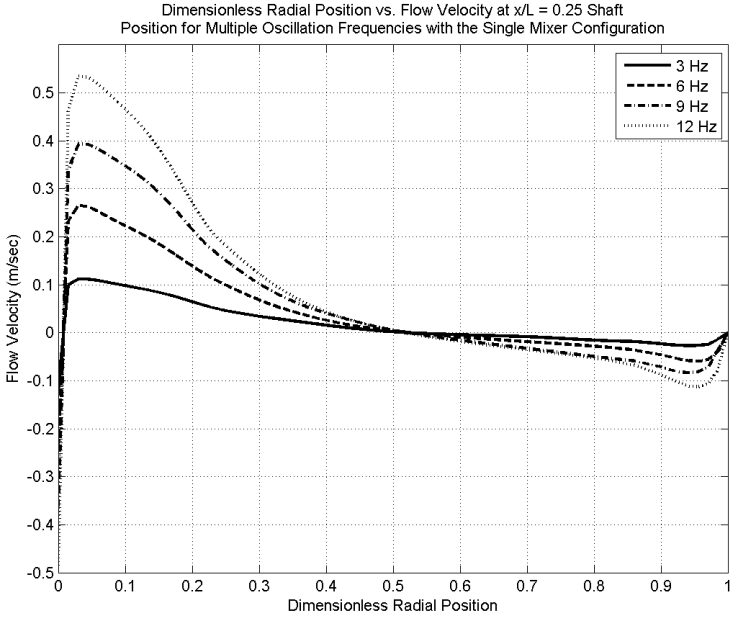
Dimensionless Radial Position vs. Flow Velocity at x/L = 0.25 Shaft
Position for Multiple Oscillation Frequencies with the Single Mixer Configuration
3 Hz
6 Hz
9 Hz
12 Hz
Flow Velocity (m/sec)
Dimensionless Radial Position

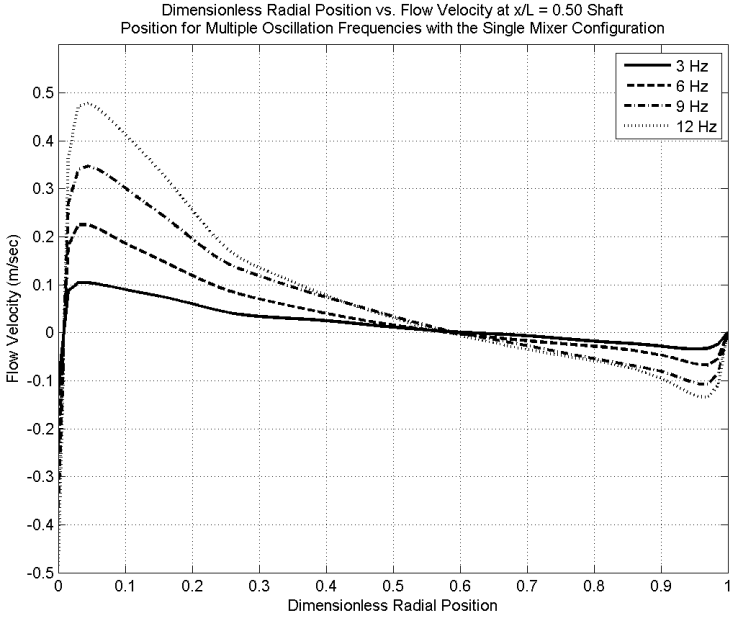
Dimensionless Radial Position vs. Flow Velocity at x/L = 0.50 Shaft
Position for Multiple Oscillation Frequencies with the Single Mixer Configuration
3 Hz
6 Hz
9 Hz
12 Hz
Flow Velocity (m/sec)
Dimensionless Radial Position

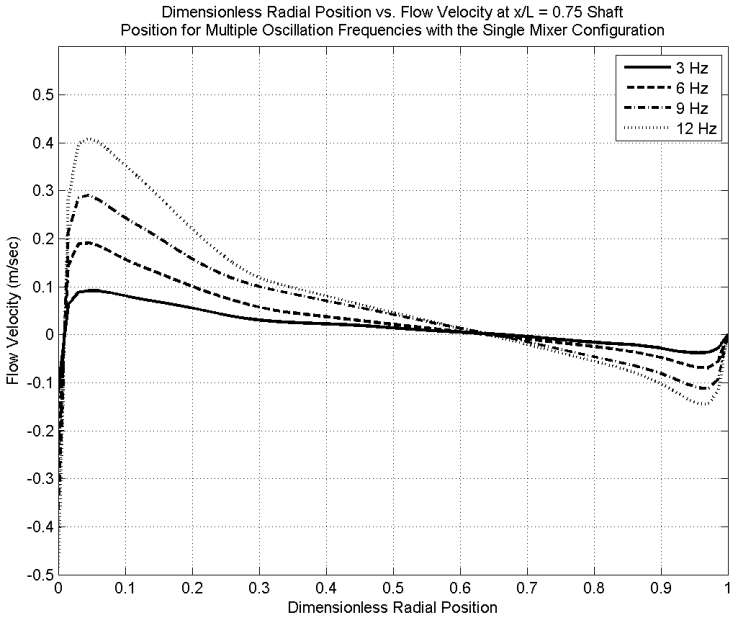
Dimensionless Radial Position vs. Flow Velocity at x/L = 0.75 Shaft
Position for Multiple Oscillation Frequencies with the Single Mixer Configuration
3 Hz
6 Hz
9 Hz
12 Hz
Flow Velocity (m/sec)
Dimensionless Radial Position
0.5
0.4
0.3
0.2
0.1
0
-0.1
-0.2
-0.3
-0.4
-0.5
0
0.1
0.2
0.3
0.4
0.5
0.6
0.7
0.8
0.9
1

Velocity Profiles – Dual Mixer Axisymmetric

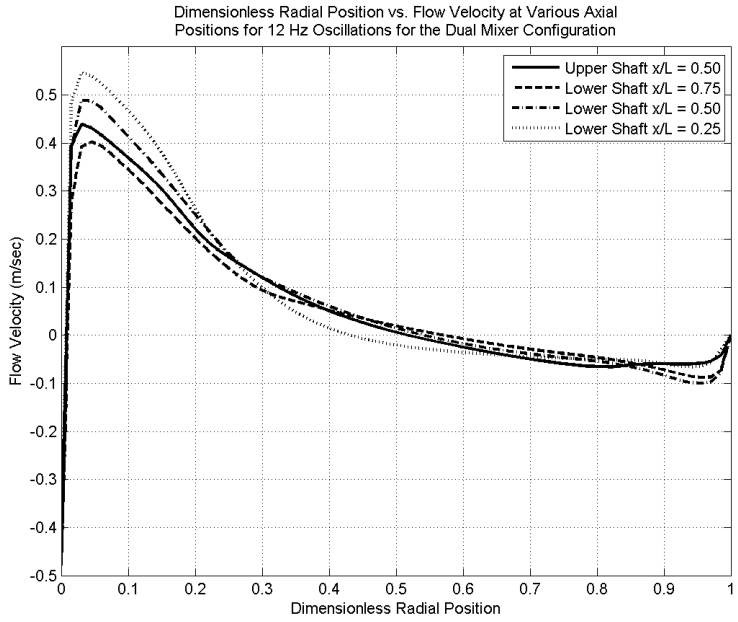

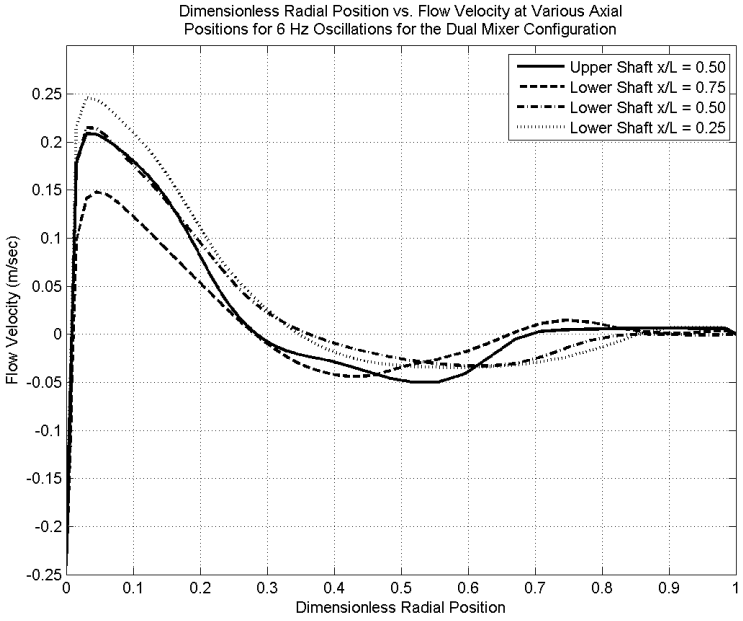

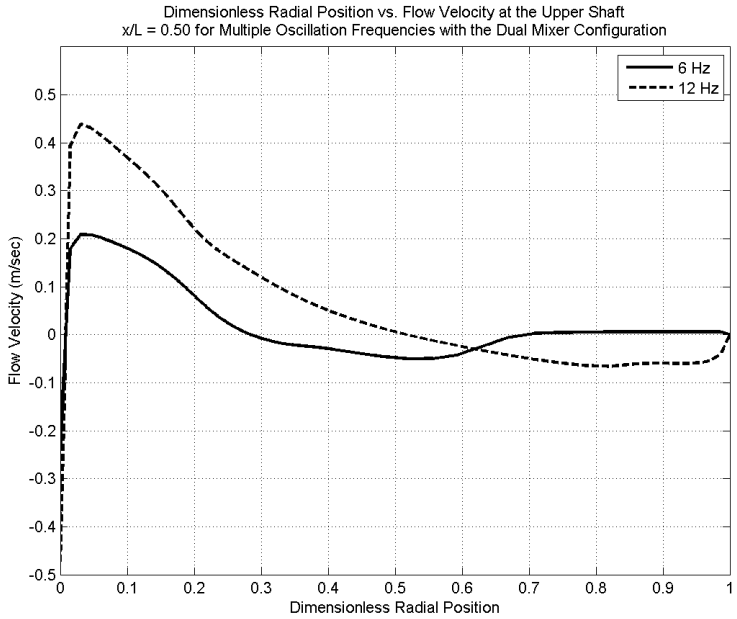
Dimensionless Radial Position vs. Flow Velocity at the Upper Shaft
x/L = 0.50 for Multiple Oscillation Frequencies with the Dual Mixer Configuration
6 Hz
12 Hz
Flow Velocity (m/sec)
Dimensionless Radial Position

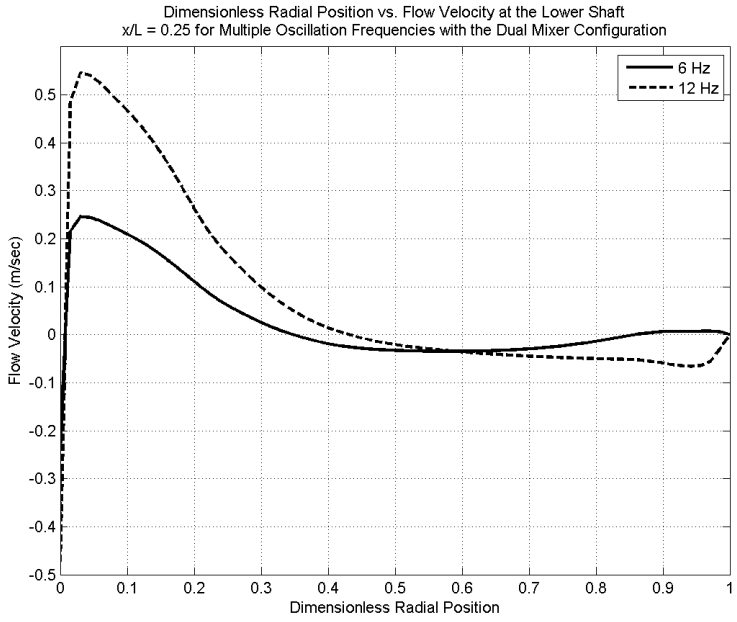
Dimensionless Radial Position vs. Flow Velocity at the Lower Shaft
x/L = 0.25 for Multiple Oscillation Frequencies with the Dual Mixer Configuration
6 Hz
12 Hz
Flow Velocity (m/sec)
Dimensionless Radial Position

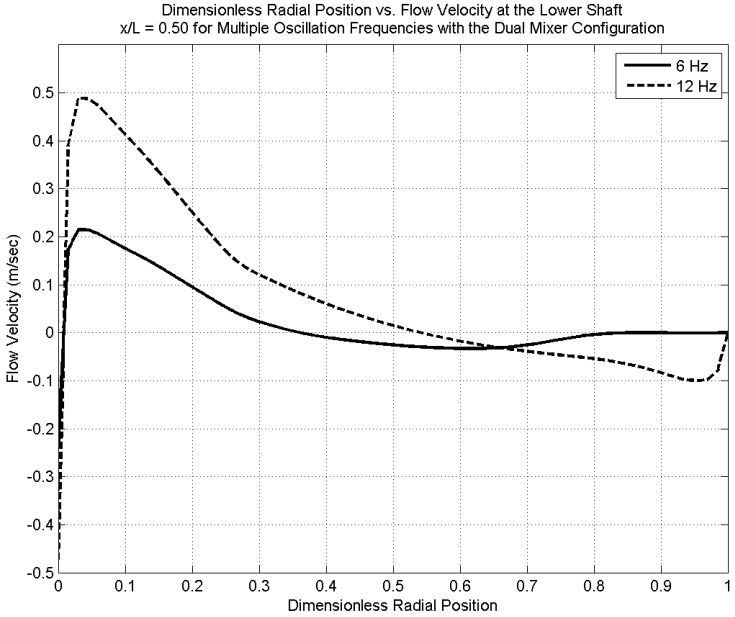
Dimensionless Radial Position vs. Flow Velocity at the Lower Shaft
x/L = 0.50 for Multiple Oscillation Frequencies with the Dual Mixer Configuration
6 Hz
12 Hz
Flow Velocity (m/sec)
Dimensionless Radial Position

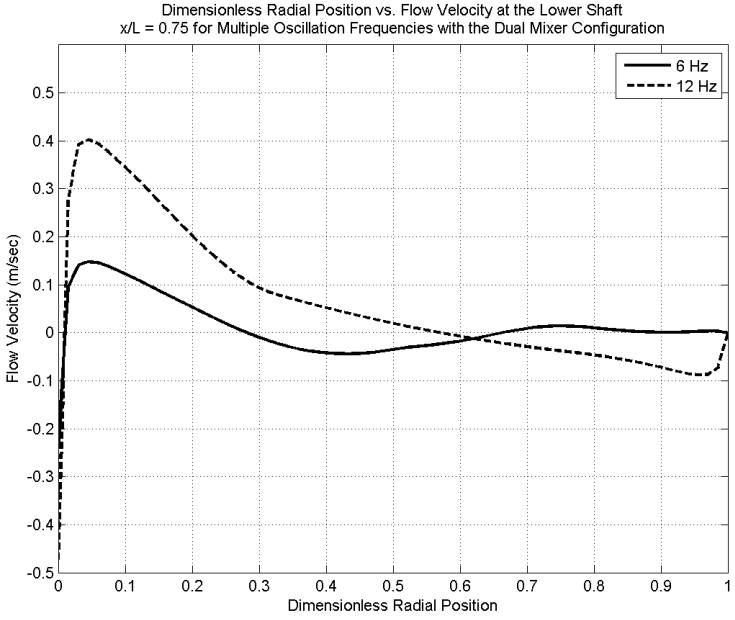
Dimensionless Radial Position vs. Flow Velocity at the Lower Shaft
x/L = 0.75 for Multiple Oscillation Frequencies with the Dual Mixer Configuration
6 Hz
12 Hz
Flow Velocity (m/sec)
Dimensionless Radial Position

Velocity Profiles – 3D 60 Degree Periodic

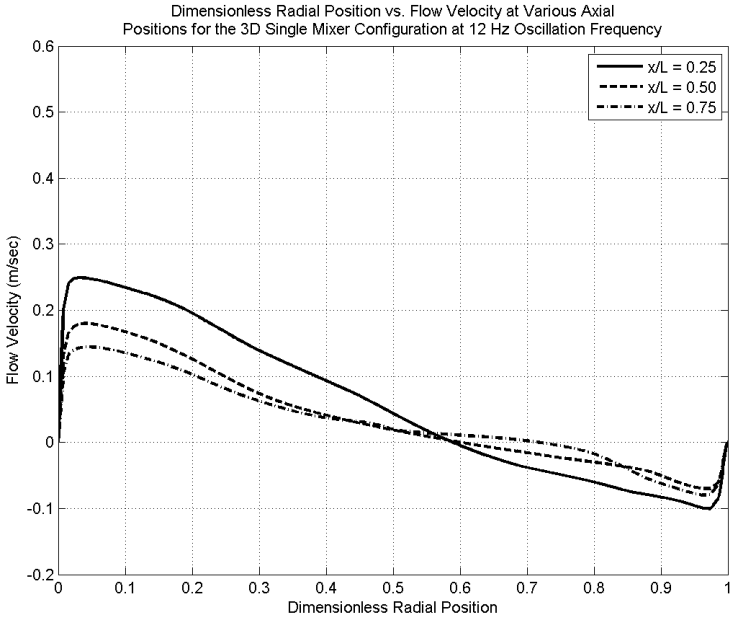

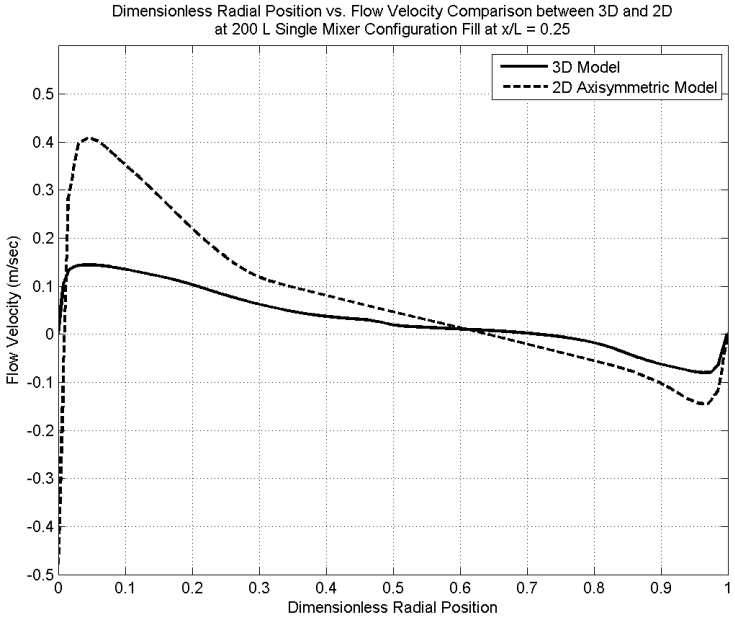

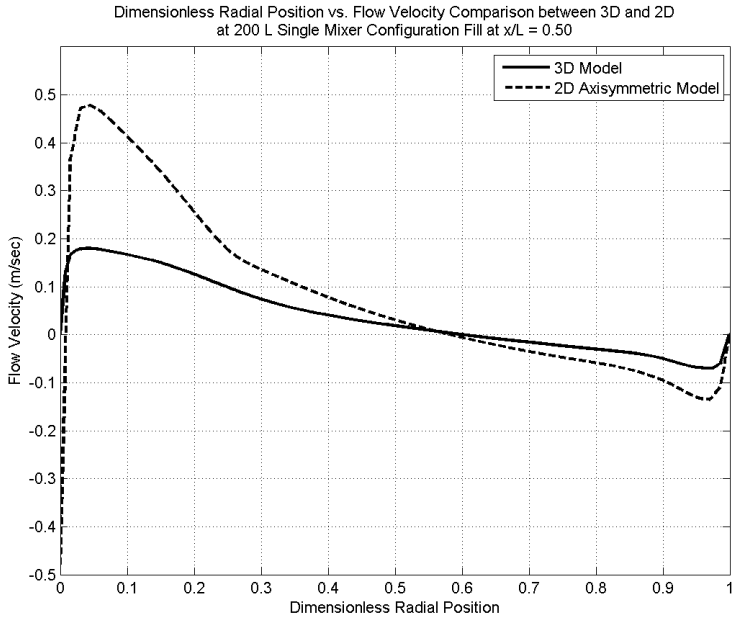
Dimensionless Radial Position vs. Flow Velocity Comparison between 3D and 2D
at 200 L Single Mixer Configuration Fill at x/L = 0.50
3D Model
2D Axisymmetric Model
Flow Velocity (m/sec)
Dimensionless Radial Position
0.5
0.4
0.3
0.2
0.1
0
-0.1
-0.2
-0.3
-0.4
-0.5
0
0.1
0.2
0.3
0.4
0.5
0.6
0.7
0.8
0.9
1

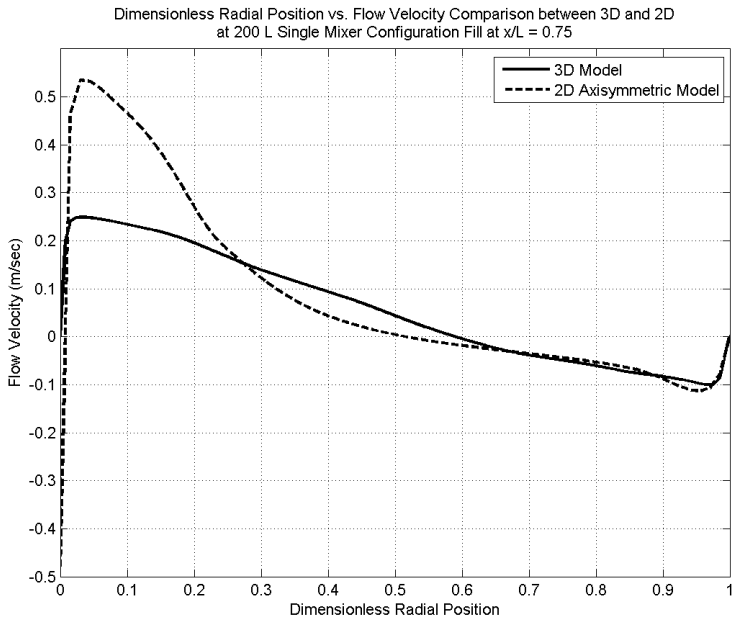
Dimensionless Radial Position vs. Flow Velocity Comparison between 3D and 2D
at 200 L Single Mixer Configuration Fill at x/L = 0.75
3D Model
2D Axisymmetric Model
Flow Velocity (m/sec)
Dimensionless Radial Position
0.5
0.4
0.3
0.2
0.1
0
-0.1
-0.2
-0.3
-0.4
-0.5
0
0.1
0.2
0.3
0.4
0.5
0.6
0.7
0.8
0.9
1

Shear Profiles

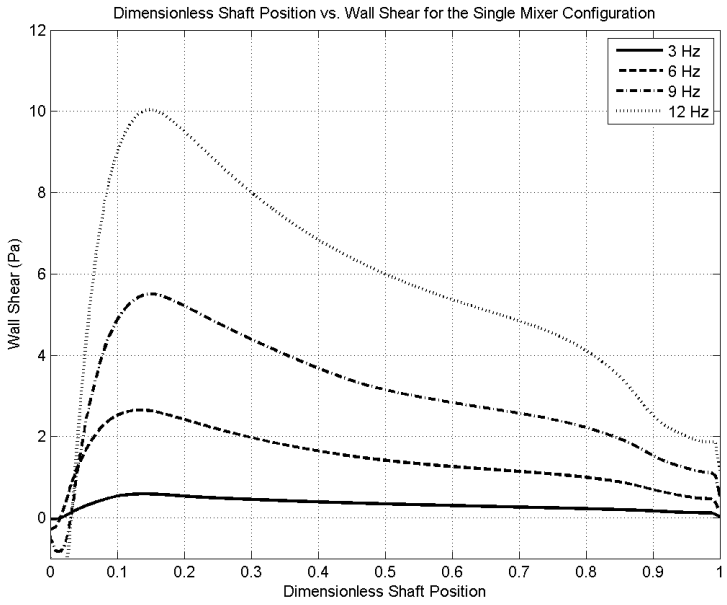

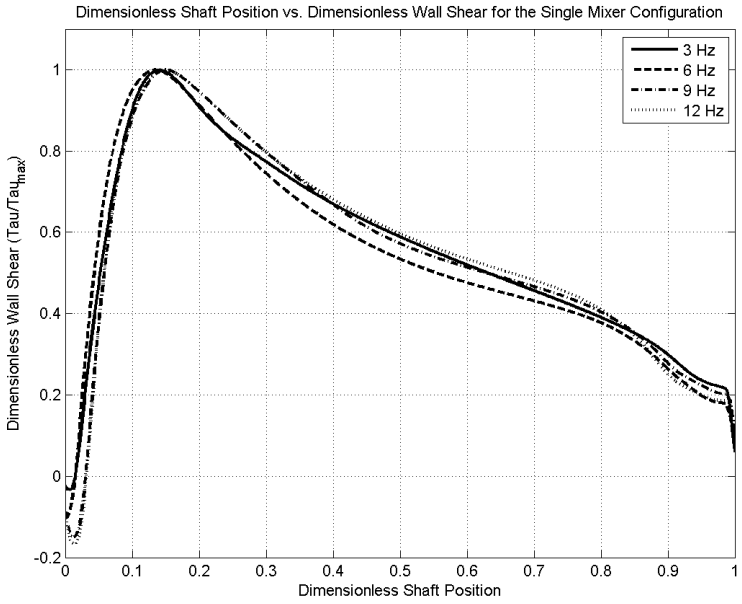

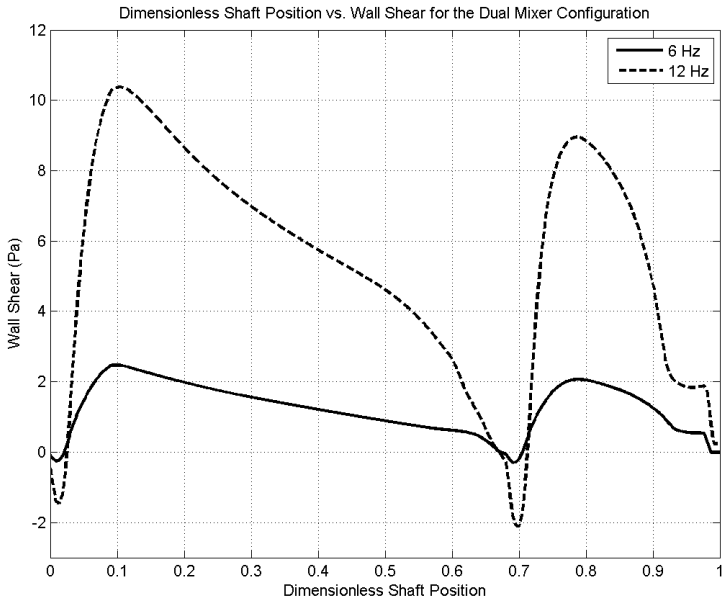
Dimensionless Shaft Position vs. Wall Shear for the Dual Mixer Configuration
6 Hz
12 Hz
Wall Shear (Pa)
Dimensionless Shaft Position
12
10
8
6
4
2
0
-2
0
0.1
0.2
0.3
0.4
0.5
0.6
0.7
0.8
0.9
1

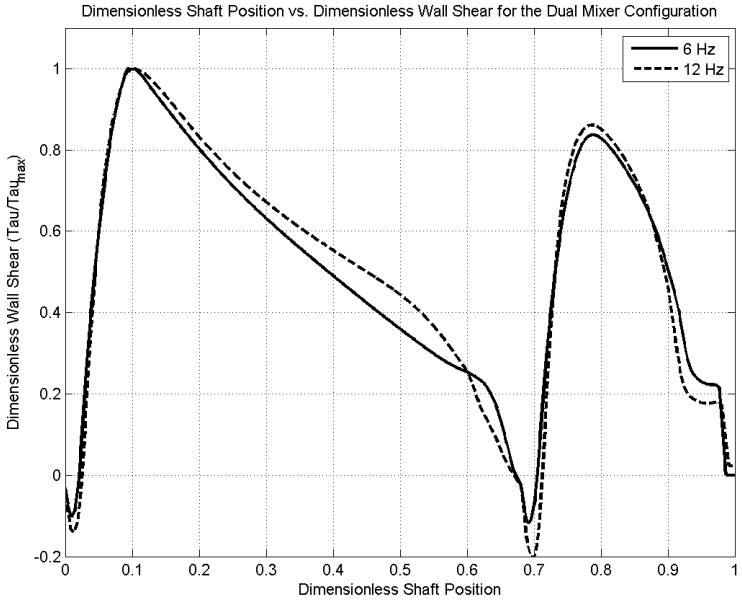
Dimensionless Shaft Position vs. Dimensionless Wall Shear for the Dual Mixer Configuration
6 Hz
12 Hz
Dimensionless Wall Shear (Tau/Tau$_{max}$)
Dimensionless Shaft Position
1
0.8
0.6
0.4
0.2
0
-0.2
0
0.1
0.2
0.3
0.4
0.5
0.6
0.7
0.8
0.9
1

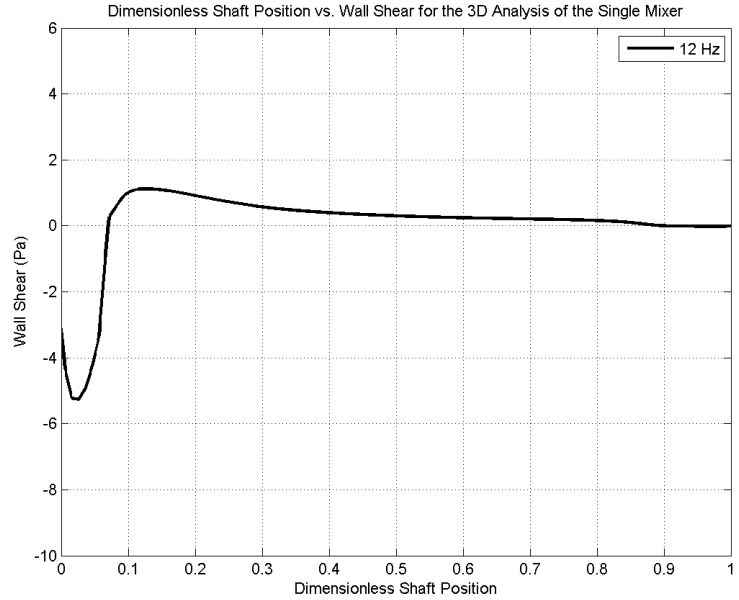
Dimensionless Shaft Position vs. Wall Shear for the 3D Analysis of the Single Mixer
12 Hz
Wall Shear (Pa)
Dimensionless Shaft Position
6
4
2
0
-2
-4
-6
-8
-10
0
0.1
0.2
0.3
0.4
0.5
0.6
0.7
0.8
0.9
1

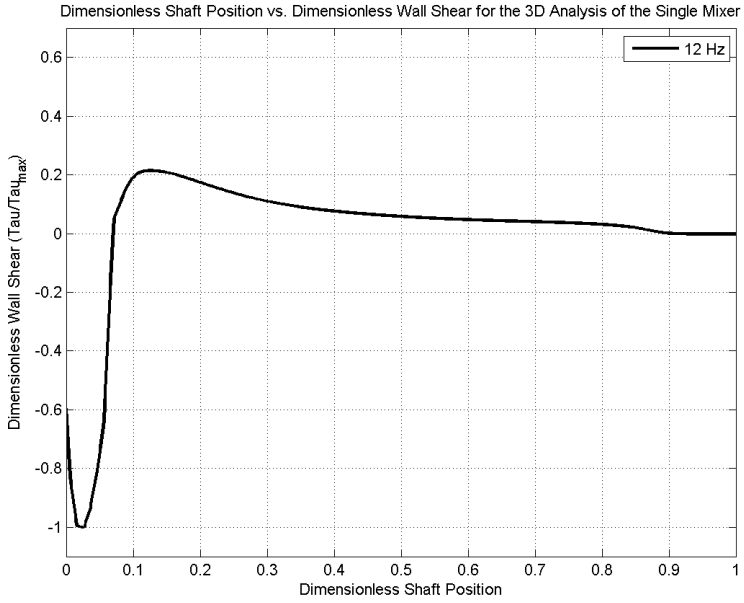
Dimensionless Shaft Position vs. Dimensionless Wall Shear for the 3D Analysis of the Single Mixer
12 Hz
Dimensionless Wall Shear (Tau/Tau$_{max}$)
Dimensionless Shaft Position
0.6
0.4
0.2
0
-0.2
-0.4
-0.6
-0.8
-1
0
0.1
0.2
0.3
0.4
0.5
0.6
0.7
0.8
0.9
1

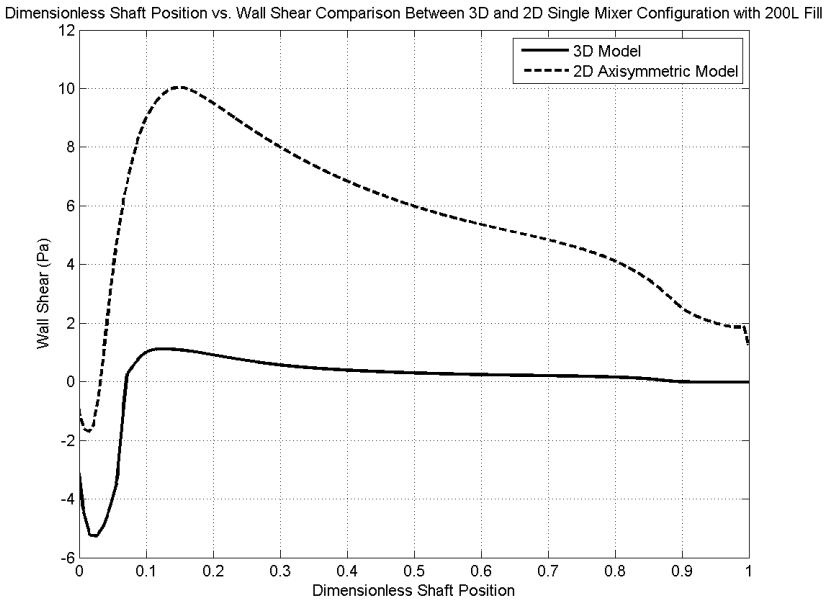
Dimensionless Shaft Position vs. Wall Shear Comparison Between 3D and 2D Single Mixer Configuration with 200L Fill
3D Model
2D Axisymmetric Model
Wall Shear (Pa)
Dimensionless Shaft Position
12
10
8
6
4
2
0
-2
-4
-6
0
0.1
0.2
0.3
0.4
0.5
0.6
0.7
0.8
0.9
1

APPENDIX C – ANALYSIS AND CFD CODE

Velocity and Shear Output Calculation

```
%% Velocity Profile Analysis
% Program used to compare the velocity and shear profiles at equivalent
% locations and different mixer speeds for the two mixer configurations and
% the single 3D case.

clc
clear

%% Import Data
freq = [3 6 9 12];

for i = 1:4
    % Import Velocity Rake Data from the CFD Output data and Organize into
    % data sets based on mesh type for further analysis.  i determines the
    % 4 cases that were tested on the single mixer case (3, 6, 9, 12 Hz)
    vel_string = ['Velocity_Rakes_' int2str(freq(i)) '_Hz_shear.csv'];
    vel_rakes(1:1000,1:2,i) = dlmread(vel_string,',',[5 0 1004 1]);
    vel_rakes(1:1000,3,i) = dlmread(vel_string,',',[1012 1 2011 1]);
    vel_rakes(1:1000,4,i) = dlmread(vel_string,',',[2019 1 3018 1]);
    vel_rakes(:,2:4,i) = -vel_rakes(:,2:4,i);

    % Imports the two dual mixer cases (6 and 12 Hz) for analysis
    if i == 2 || i == 4
        vel_string_DM = ['Velocity_Rakes_' int2str(freq(i)) '_DM_shear.csv'];
        vel_rakes_DM(1:1000,1:2,i) = dlmread(vel_string_DM,',',[5 0 1004 1]);
        vel_rakes_DM(1:1000,3,i) = dlmread(vel_string_DM,',',[1012 1 2011 1]);
        vel_rakes_DM(1:1000,4,i) = dlmread(vel_string_DM,',',[2019 1 3018 1]);
        vel_rakes_DM(1:1000,5,i) = dlmread(vel_string_DM,',',[3026 1 4025 1]);
        vel_rakes_DM(:,2:5,i) = -vel_rakes_DM(:,2:5,i);
    end

    % Imports the 12 Hz 3D case that was run
    if i == 4
         vel_string_3D = ['Velocity_Rakes_' int2str(freq(i)) '_Hz_3D.csv'];
        vel_rakes_3D(1:1000,1:2) = dlmread(vel_string_3D,',',[5 0 1004 1]);
        vel_rakes_3D(1:1000,3) = dlmread(vel_string_3D,',',[1012 1 2011 1]);
        vel_rakes_3D(1:1000,4) = dlmread(vel_string_3D,',',[2019 1 3018 1]);
        vel_rakes_3D(:,2:4) = -vel_rakes_3D(:,2:4);
    end

    % Import Shaft Shear Data from CFD Output Data and organize into data
    % sets based on mesh type
    shear_string = ['Wall_Shear_Curve_' int2str(freq(i)) '_Hz_shear.csv'];
    shear_string_DM = ['Wall_Shear_Curve_' int2str(freq(i)) '_DM_shear.csv'];
    shear_string_3D = ['Wall_Shear_Curve_' int2str(freq(i)) '_Hz_3D.csv'];

    % Imports the two dual mixer cases (6 and 12 Hz) for analysis
    if i == 2 || i == 4
        shear_DM(1:988,1:2,i) = dlmread(shear_string_DM,',',[5 0 992 1]);
        shear_DM(:,2,i) = -shear_DM(:,2,i);
        max_shear_DM(i) = max(shear_DM(:,2,i));
    end

    % Imports the 3D mesh case at 12 Hz
    if i == 4
        shear_3D(1:1000,1:2) = dlmread(shear_string_3D,',',[5 0 1004 1]);
        shear_3D(:,2) = -shear_3D(:,2);
```

```
        max_shear_3D = -min(shear_3D(:,2));
    end

    % Imports the single mixer shear stress data
    shear(1:1000,1:2,i) = dlmread(shear_string,',',[5 0 1004 1]);

    % Inverts the shear data to orient positive shear in the vertical
    % direction as on the diagrams
    shear(:,2,i) = -shear(:,2,i);

    % Determine the single mixer maximum shear for normalization
    max_shear(i) = max(shear(:,2,i));
end

% Sets the line style for all following plots
fig_style = {'k-' 'k--' 'k-.' 'k:'};

%% Plot Shear Data for comparison - Single Mixer
% Determine the maximum and minimum x-locations for normalizaiton of x
% position along the shaft.  Also determines the length of the submerged
% portion of the shaft based on the min max data
min_shear_pos = min(shear(:,1,1));
max_shear_pos = max(shear(:,1,1));
shaft_length = max_shear_pos-min_shear_pos;

% Plot the wall shear acting on the shaft in both units of N/m^2 and
% dimensionless shear
for i = 1:4
    % Wall Shear vs. Dimensionless Position
    figure(1)
    plot(1-(shear(:,1,i)-min_shear_pos)/shaft_length,shear(:,2,i),...
        fig_style{i},'LineWidth',2),hold on,...
        legend('3 Hz','6 Hz','9 Hz','12 Hz'),axis([0 1 -1 12]),...
        xlabel('Dimensionless Shaft Position'),...
        ylabel('Wall Shear (Pa)'),...
        title('Dimensionless Shaft Position vs. Wall Shear'),grid on;
    % Dimensionless wall shear vs dimensionless position
    figure(2)
    plot(1-(shear(:,1,i)-min_shear_pos)/shaft_length,...
        shear(:,2,i)/max_shear(i),fig_style{i},'LineWidth',2),hold on,...
        legend('3 Hz','6 Hz','9 Hz','12 Hz'),axis([0 1 -.2 1.1]),...
        xlabel('Dimensionless Shaft Position'),...
        ylabel('Dimensionless Wall Shear (Tau/Tau_{max})'),...
        title('Dimensionless Shaft Position vs. Dimensionless Wall Shear'),...
        grid on;
end

%% Plot Velocity Rakes for comparison - Single Mixer
% Determine the minimum and maximum radial position extending from the
% shaft outward to the tank as well as the corresponding length
min_vel_pos = min(vel_rakes(:,1,1));
max_vel_pos = max(vel_rakes(:,1,1));
radial_length = max_vel_pos - min_vel_pos;

% Velocity plots - total of 7 plots
for i = 1:4
    for j = 1:3
        % Plot axial velocity at 3 locations along the shaft for all four
        % oscillation speeds tested
        figure(2+i)
        plot((vel_rakes(:,1,i)-min_vel_pos)/radial_length,...
            vel_rakes(:,j+1,i),fig_style{j},'LineWidth',2),hold on,...
            xlabel('Dimensionless Radial Position'),...
```

```
            ylabel('Flow Velocity (m/sec)'),...
            legend('x/L = 0.75','x/L = 0.50','x/L = 0.25'),...
            axis([0 1 -.0-.1*i .0+i*.15])

        % Plot axial velocity for each oscillation speed at each axial
        % location
        figure(6+j)
        plot((vel_rakes(:,1,i)-min_vel_pos)/radial_length,vel_rakes(:,j+1,i)...
            ,fig_style{i},'LineWidth',2),hold on,...
            xlabel('Dimensionless Radial Position'),...
            ylabel('Flow Velocity (m/sec)'),...
            legend('3 Hz','6 Hz','9 Hz','12 Hz'),...
            axis([0 1 -.5 .6]),grid on
    end
end

%% Dual Mixer Shear Plots - Follows same methods as above in single mixer
% case
min_shear_pos_DM = min(shear_DM(:,1,2));
max_shear_pos_DM = max(shear_DM(:,1,2));
shaft_length_DM = max_shear_pos_DM-min_shear_pos_DM;

for i = 1:2
    figure(10)
    plot(1-(shear_DM(:,1,i*2)-min_shear_pos_DM)/shaft_length_DM,...
        shear_DM(:,2,2*i),fig_style{i},'LineWidth',2),hold on,...
        legend('6 Hz','12 Hz'),axis([0 1 -3 12]),...
        xlabel('Dimensionless Shaft Position'),...
        ylabel('Wall Shear (Pa)'),...
        title('Dimensionless Shaft Position vs. Wall Shear'),grid on;
    figure(11)
    plot(1-(shear_DM(:,1,i*2)-min_shear_pos_DM)/shaft_length_DM,...
        shear_DM(:,2,2*i)/max_shear_DM(i*2),fig_style{i},'LineWidth',2),...
        hold on,legend('6 Hz','12 Hz'),axis([0 1 -0.2 1.1]),...
        xlabel('Dimensionless Shaft Position'),...
        ylabel('Dimensionless Wall Shear (Tau/Tau_{max})'),...
        title('Dimensionless Shaft Position vs. Dimensionless Wall Shear'),...
        grid on;
end

%% Dual Mixer Velocity Plots
min_vel_pos_DM = min(vel_rakes_DM(:,1,2));
max_vel_pos_DM = max(vel_rakes_DM(:,1,2));
radial_length_DM = max_vel_pos_DM - min_vel_pos_DM;

for i = 1:2
    for j = 1:4
        figure(11+i)
        plot((vel_rakes_DM(:,1,i*2)-min_vel_pos_DM)/radial_length_DM,...
            vel_rakes_DM(:,j+1,i*2),fig_style{j},'LineWidth',2),hold on,...
            xlabel('Dimensionless Radial Position'),...
            ylabel('Flow Velocity (m/sec)'),...
            legend('Upper Shaft x/L = 0.50','Lower Shaft x/L = 0.75',...
            'Lower Shaft x/L = 0.50','Lower Shaft x/L = 0.25'),...
            axis([0 1 -.25*i .3*i])
        figure(13+j)
        plot((vel_rakes_DM(:,1,i*2)-min_vel_pos_DM)/radial_length_DM,...
            vel_rakes_DM(:,j+1,2*i),fig_style{i},'LineWidth',2),hold on,...
            xlabel('Dimensionless Radial Position'),...
            ylabel('Flow Velocity (m/sec)'),legend('6 Hz','12 Hz'),...
            axis([0 1 -.5 .6]),grid on
    end
end
```

```
%% 3D Mixer Velocity Plots - same method as above in single mixer case
min_vel_pos_3D = min(vel_rakes_3D(:,1));
max_vel_pos_3D = max(vel_rakes_3D(:,1));
radial_length_3D = max_vel_pos_3D - min_vel_pos_3D;

figure(18)
for i = 1:3
    plot((vel_rakes_3D(:,1)-min_vel_pos_3D)/radial_length_3D,...
        vel_rakes_3D(:,5-i),fig_style{i},'LineWidth',2),hold on,...
        xlabel('Dimensionless Radial Position'),...
        ylabel('Flow Velocity (m/sec)'),...
        legend('x/L = 0.25','x/L = 0.50','x/L = 0.75'),...
        axis([0 1 -.2 .6])
end

%% 3D Mixer Shear Plots
min_shear_pos_3D = min(shear_3D(:,1));
max_shear_pos_3D = max(shear_3D(:,1));
shaft_length_3D = max_shear_pos_3D-min_shear_pos_3D;

figure(19)
plot(1-(shear_3D(:,1)-min_shear_pos_3D)/shaft_length_3D,shear_3D(:,2),...
    fig_style{1},'LineWidth',2),hold on,...
    legend('12 Hz'),axis([0 1 -10 6]),...
    xlabel('Dimensionless Shaft Position'),...
    ylabel('Wall Shear (Pa)'),...
    title('Dimensionless Shaft Position vs. Wall Shear'),grid on;
figure(20)
plot(1-(shear_3D(:,1)-min_shear_pos_3D)/shaft_length_3D,...
    shear_3D(:,2)/max_shear_3D,fig_style{1},'LineWidth',2),hold on,...
    legend('12 Hz'),axis([0 1 -1.1 0.7]),...
    xlabel('Dimensionless Shaft Position'),...
    ylabel('Dimensionless Wall Shear (Tau/Tau_{max})'),...
    title('Dimensionless Shaft Position vs. Dimensionless Wall Shear'),...
    grid on;

%% Comparison of 3D to 2D Single Mixer
figure(21)
plot(1-(shear_3D(:,1)-min_shear_pos_3D)/shaft_length_3D,shear_3D(:,2),...
    fig_style{1},'LineWidth',2),hold on
plot(1-(shear(:,1,4)-min_shear_pos)/shaft_length,shear(:,2,4),...
    fig_style{2},'LineWidth',2),legend('3D Model','2D Axisymmetric Model'),...
    axis([0 1 -6 12]),xlabel('Dimensionless Shaft Position'),...
    ylabel('Wall Shear (Pa)'),...
    title('Dimensionless Shaft Position vs. Wall Shear Comparison Between 3D
and 2D Single Mixer Configuration with 200L Fill'),...
    grid on;
for i = 1:3
    figure(i+21)
    plot((vel_rakes_3D(:,1)-min_vel_pos_3D)/radial_length_3D,...
        vel_rakes_3D(:,i+1),fig_style{1},'LineWidth',2),hold on,...
        xlabel('Dimensionless Radial Position'),...
        ylabel('Flow Velocity (m/sec)'),...
        axis([0 1 -.5 .6])
    plot((vel_rakes(:,1,1)-min_vel_pos)/radial_length,vel_rakes(:,i+1,4),...
        fig_style{2},'LineWidth',2),hold on,...
        legend('3D Model','2D Axisymmetric Model')
end

%% Figure Titles for loop produced plots
figure(3)
```

```
title('Dimensionless Radial Position vs. Flow Velocity at Various Axial
Positions for 3 Hz Oscillations');
figure(4)
title('Dimensionless Radial Position vs. Flow Velocity at Various Axial
Positions for 6 Hz Oscillations');
figure(5)
title('Dimensionless Radial Position vs. Flow Velocity at Various Axial
Positions for 9 Hz Oscillations');
figure(6)
title('Dimensionless Radial Position vs. Flow Velocity at Various Axial
Positions for 12 Hz Oscillations');
figure(7)
title('Dimensionless Radial Position vs. Flow Velocity at x/L = 0.75 Shaft
Position for Multiple Oscillation Frequencies');
figure(8)
title('Dimensionless Radial Position vs. Flow Velocity at x/L = 0.50 Shaft
Position for Multiple Oscillation Frequencies');
figure(9)
title('Dimensionless Radial Position vs. Flow Velocity at x/L = 0.25 Shaft
Position for Multiple Oscillation Frequencies');
figure(12)
title('Dimensionless Radial Position vs. Flow Velocity at Various Axial
Positions for 6 Hz Oscillations');
figure(13)
title('Dimensionless Radial Position vs. Flow Velocity at Various Axial
Positions for 12 Hz Oscillations');
figure(14)
title('Dimensionless Radial Position vs. Flow Velocity at the Upper Shaft x/L =
0.50 for Multiple Oscillation Frequencies');
figure(15)
title('Dimensionless Radial Position vs. Flow Velocity at the Lower Shaft x/L =
0.75 for Multiple Oscillation Frequencies');
figure(16)
title('Dimensionless Radial Position vs. Flow Velocity at the Lower Shaft x/L =
0.50 for Multiple Oscillation Frequencies');
figure(17)
title('Dimensionless Radial Position vs. Flow Velocity at the Lower Shaft x/L =
0.25 for Multiple Oscillation Frequencies');
figure(18)
title('Dimensionless Radial Position vs. Flow Velocity at Various Axial
Positions for 12 Hz Oscillations');
figure(22)
title('Dimensionless Radial Position vs. Flow Velocity Comparison at 200 L
Single Mixer Configuration Fill at x/L = 0.25');
figure(23)
title('Dimensionless Radial Position vs. Flow Velocity Comparison at 200 L
Single Mixer Configuration Fill at x/L = 0.50');
figure(24)
title('Dimensionless Radial Position vs. Flow Velocity Comparison at 200 L
Single Mixer Configuration Fill at x/L = 0.75');

%% Print Plots to file for presentation and reports
% Sets the names of all the plots file names
file_strings = {'SM_Shear_vs_Speed'
                'SM_Dim_Shear_vs_Speed'
                'SM_3_Hz_Velocity'
                'SM_6_Hz_Velocity'
                'SM_9_Hz_Velocity'
                'SM_12_Hz_Velocity'
                'SM_xL_75_Velocity'
                'SM_xL_50_Velocity'
                'SM_xL_25_Velocity'
                'DM_Shear_vs_Speed'
```

```
                'DM_Dim_Shear_vs_Speed'
                'DM_6_Hz_Velocity'
                'DM_12_Hz_Velocity'
                'DM_xL_150_Velocity'
                'DM_xL_275_Velocity'
                'DM_xL_250_Velocity'
                'DM_xL_225_Velocity'
                '3D_12_Hz_Velocity'
                '3D_12_Hz_Shear'
                '3D_12_Hz_Dim_Shear'
                '3D_2D_Comparison_Shear'
                '3D_2D_Comparison_xL_75'
                '3D_2D_Comparison_xL_50'
                '3D_2D_Comparison_xL_25'};

% Prints the plot to file
for i = 1:24
    print(i,file_strings{i},'-dpng')
end
```

Mass Momentum Analysis Code

```
%% Mass Momentum Analysis for Saltus Mixer Head
% Compares the momentum acting on the mixer head based on the two
% dimensional axisymmetric area projection as seen in the CFD analysis
clc
clear

% Constants - Provided
r_t =   0.1397;         % Tank radius (m)
r_mo =  0.1397;         % Mixer head outer radius (m)
r_j2o = 0.1045;         % Mixer Jet 2 outer radius (m)
r_j2i = 0.0943;         % Mixer Jet 2 inner radius (m)
r_j1o = 0.0548;         % Mixer Jet 1 outer radius (m)
r_j1i = 0.0446;         % Mixer Jet 1 inner radius (m)
rho =   999;            % Fluid Density (kg/m^3)

amp = 0.013;            % Mixer movement amplitude (m)

% Constants - Calculated
A_tank = pi()*r_t^2;                    % Tank internal area - yz plane (m^2)
A_mixer_s = pi()*r_mo^2;                % Solid mixer area - yz plane (m^2)
A_jet_2 = pi()*((r_j2o^2)-(r_j2i^2));   % Jet 2 Area - yz plane (m^2)
A_jet_1 = pi()*((r_j1o^2)-(r_j1i^2));   % Jet 1 Area - yz plane (m^2)
A_mixer_a = A_mixer_s-A_jet_2-A_jet_1;  % Actual mixer area - yz plane (m^2)

f_pp = zeros(2,4);                      % Initializes the peak to peak force
array

% Case 1 - Fluid momentum applying on mixer head y-projection only

Mixer_freq = [3 6 9 12];                % Analyzed mixer frequencies

% Offsets the P1 term from the hand calculation
Calculation_offset = [-0.4 .155 .27 .37];

% Set the line settings for the plots
set(0,'defaultAxesColorOrder',[0 0 0],'defaultAxesLineStyleOrder',...
    '- | -- | -. | :');

% Calculate for the four oscillation frequencies
for i = 1:4
    % Break the oscillation period into 1000 pieces
    period = [0:.001:1];
    % Determine the maximum head velocity - used for relative flow velocity
    V_head_max(i) = (amp/2)*Mixer_freq(i)*2*pi;
    % Determine the head velocity over the span of a period
    Mixer_vel(:,i) = V_head_max(i)*sin(2*pi*Mixer_freq(i)*period-pi/1.4);
    % Maximum relative flow velocity acting on the mixer head
    Mixer_vel_max(:,i) = Mixer_vel(:,i)+V_head_max(i);

    % Set the outlet area for case 1
    A_a = A_mixer_s-A_mixer_a;
    % Determine the maximum velocity leaving the jet
    v_jet(:,i) = Mixer_vel(:,i)*A_mixer_s/A_a;

    % Ambient pressure below the mixer head - Assume 0 Gauge Pressure -
    % Will be replaced by the offset term later
    P1 = 0;

    % Determine the force acting on the mixer head as derived in the hand
    % calculation
```

```
    F_a(:,i) = A_mixer_s*(P1+rho*A_mixer_s*Mixer_vel_max(:,i).^2)-...
        A_a*(P1+(rho*(Mixer_vel_max(:,i).^2)/2)*(1+(A_mixer_s/A_a)^2));
    % Determine the average pressure acting on the mixer head
    P_mix_a(:,i) = F_a(:,i)/(A_mixer_a);

    % Plot an individual figure for each oscillation frequency
    figure(i)
    % Sets the span for one complete cycle plus 50% for each oscillation
    % frequency
    span = length(period)/Mixer_freq(i)*1.5;
    % Determines the maximum and minimum calculated force for plot scaling
    fmax = max(F_a(:,i));
    fmin = min(F_a(:,i));
    % Determine the peak to peak amplitude of applied force
    f_pp(1,i) = (fmax-fmin);
    % Plots the applied force as calculated and offsets as necessary to
    % overlap with CFD produced data
    plot(period([1:span]),F_a([1:span],i)+f_pp(1,i)*Calculation_offset(i),...
        'LineWidth',2),hold on
end

%% Import CFD Data - Import data and assign to an array
force_3 = dlmread('Force_Curve_3_Hz.csv',',',[5 0 405 1]);
force_6 = dlmread('Force_Curve_6_Hz.csv',',',[5 0 205 1]);
force_9 = dlmread('Force_Curve_9_Hz.csv',',',[5 0 204 1]);
force_12 = dlmread('Force_Curve_12_Hz.csv',',',[5 0 105 1]);

%% Process imported Data
% Determine the peak to peak force applied to the mixer head as calculated
% by the CFD solver
f_pp(2,4) = max(force_12(:,2))-min(force_12(:,2));
f_pp(2,3) = max(force_9(:,2))-min(force_9(:,2));
f_pp(2,2) = max(force_6(:,2))-min(force_6(:,2));
f_pp(2,1) = max(force_3(:,2))-min(force_3(:,2));

%% Add CFD data to previous plots for comparison
figure(4)
plot([0:.001:.1],force_12(:,2),'k--'),xlabel('Time (s)'),...
    ylabel('Applied Force (N)'),...
    title('Applied Surface Force Acting on the Bottom Surface of the Mixer
Plate Over Time at 12 Hz Oscillaton Speed'),...
    legend('Hand Calculated Data','CFD Calculated Data')
figure(3)
plot([0:.001:.199],force_9(:,2),'k--'),xlabel('Time (s)'),...
    ylabel('Applied Force (N)'),...
    title('Applied Surface Force Acting on the Bottom Surface of the Mixer
Plate Over Time at 9 Hz Oscillaton Speed'),...
    legend('Hand Calculated Data','CFD Calculated Data')
figure(2)
plot([0:.001:.2],force_6(:,2),'k--'),xlabel('Time (s)'),...
    ylabel('Applied Force (N)'),...
    title('Applied Surface Force Acting on the Bottom Surface of the Mixer
Plate Over Time at 6 Hz Oscillaton Speed'),...
    legend('Hand Calculated Data','CFD Calculated Data')
figure(1)
plot([0:.001:.4],force_3(:,2),'k--'),xlabel('Time (s)'),...
    ylabel('Applied Force (N)'),...
    title('Applied Surface Force Acting on the Bottom Surface of the Mixer
Plate Over Time at 3 Hz Oscillaton Speed'),...
    legend('Hand Calculated Data','CFD Calculated Data')

%% Overlay all the hand calculated data for magnitude comparison
figure(5)
```

```
plot(period(1:length(period)/3),F_a(1:length(period)/3,1),...
    period(1:length(period)/3),F_a(1:length(period)/3,2),...
    period(1:length(period)/3),F_a(1:length(period)/3,3),...
    period(1:length(period)/3),F_a(1:length(period)/3,4),...
    'LineWidth',2),title('Mixer Head Reaction Force vs Time'),...
    xlabel('Time (sec)'),ylabel('Reaction Force (N)'),...
    legend('3 Hz','6 Hz','9 Hz','12 Hz')

%% Print individual plots to a PNG data file for presentation
print(1,'3_Hz_Mixer_Force','-dpng')
print(2,'6_Hz_Mixer_Force','-dpng')
print(3,'9_Hz_Mixer_Force','-dpng')
print(4,'12_Hz_Mixer_Force','-dpng')
```

Area Comparison

```
%% Area Analysis of 3D and 2D Mixer for comparison
clear
clc

%% Constant Initialization
% Radius of the jets (in)
R = 0.2;
% Radial location of the jets (in)
c = [1.1 1.8 2.2 2.9 3.3 3.8 4.0 4.4 4.8 5.0];
% Number of Jets in each radial location
n = [6 6 6 12 6 6 12 6 12 12];

% Sets the radial positions where area is contributed to the total for
% every jet location
for i = 1:length(n)
    e(i,:) = [c(i)-R:0.001:c(i)+R];
end

%% Solve for Area - 2D Mixer Head
% Initialize the area vs position array
area2D = zeros(5.5/.001,2);
% Calculate over the radial length of the mixer head
for i = 1:5.5/.001
    % Current radial position
    area2D(i,1) = i/1000;

    % Integrate over the area of the first jet if the current position is
    % within this range
    if i*.001 >= 0.0446/.0254 && i*.001 <= 0.0548/.0254
        area2D(i,2) = pi*((i*0.001)^2-(0.0446/.0254)^2);

    % Integrate over the area of the second jet if the current position is
    % within this range
    elseif i*.001 >= 0.0943/.0254 && i*.001 <= 0.1045/.0254
        area2D(i,2) = pi*((i*0.001)^2-(0.0943/.0254)^2) + ...
            pi*((.0548/.0254)^2-(.0446/.0254)^2);
    end

    % Maintain area quantities for positions between jets
    if i*.001 > .0548/.0254 && i*.001 < 0.0943/.0254
        area2D(i,2) = area2D(i-1,2);
    elseif i*.001 > .1045/.0254
        area2D(i,2) = area2D(i-1,2);
    end
end

%% Initialize Symbols
syms x y f

%% Establish Equation and Integrate
% Equation of a single jet centered x = c(i) based on x^2 + y^2 = r^2 or
% rewritten as y = sqrt(r^2-x^2).  This produces only a hemisphere, so the
% value must be doubled to account for the full circle
y(1:10) = 2*sqrt(R^2-(x-c(1:10)).^2);
% Integration of each equation individually
f = int(y);

%% Solve For Area - 3D Mixer Head
% initialize the area array
area = zeros(5.5/.001,2);
```

```
% Integrate the combined areas of the jets along the radial position
for i = 1:5.5/.001
    % Write the current radial position into the array
    area(i,1) = i/1000;
    % Integrate the area
    for j = 1:length(n)
        % If the radial position is within range of the jet location, add
        % appropriate area as determined from the integration above
        if i*.001 >= (c(j)-R) && i*.001 <= (c(j)+R)
            area(i,2) = area(i,2) + n(j)*(double(subs(f(j),i*.001))+pi/50);
        end
        % If the radial position is beyond the jet, then maintain the
        % current area from the previous position
        if i*.001 > (c(j)+R)
            area(i,2) = area(i,2) + n(j)*(double(subs(f(j),c(j)+R))+pi/50);
        end
    end
end

%% Plot the data for presentation
figure(1),plot(area(:,1)/5.5,area(:,2)*.0254^2,'k-','LineWidth',2),hold on
figure(1),plot(area2D(:,1)/5.5,area2D(:,2)*.0254^2,'k--','LineWidth',2),...
    xlabel('Dimensionless Radial Position on Mixer Head (m/m)'),...
    ylabel('Total Flow Area (m^2)'),...
    title('Accumulated Flow Area vs. Radial Position'),...
    axes([0 1 0 0.01])
```

Mixing Homogenization Calculation

```
% Mixing Calculator for CFD data from Saltus Analysis
% This script will run and automatically pull data,
% calculate mixing percentage, and chart results as necessary
% A secondary task featured on some versions will also plot the mixer head
% velocity, position and applied force

% Clear any workspace variables and screen output
clc
clear

% User settable input data
t_total = input('Enter the number of time steps to analyze: ');
del_t = input('Enter the time step size (sec): ');
tank_vol = input('Enter Tank Volume (L): ');
bins = input('Enter the total bins in Histogram data: ');
tol = input('Input tolerance level (%): ');

%%  Data Import Section
% First import data from CFD-Post csv output data
% Zero the raw data matrix
data_raw = zeros(bins+2,t_total);

% Import the concentration labels data from the intial time file
data_raw(2:(bins+1),1) = dlmread('Histogram_t_mix_0.csv',',',[5 0 bins+4 0]);

% Add the 100% value to the end, which is missing from the csv data
data_raw(bins+2,1) = 1;

% Import the remaining data using a loop, with each time step being a new
% column
for i = 0:t_total
    % Add the time step value to the first row
    data_raw(1,i+2) = i*del_t;
    % Specify the csv file name based on time step
    file_string = ['Histogram_t_mix_' int2str(i*del_t) '.csv'];
    % Retrieve the data from the specified csv file
    data_raw(2:(bins+1),i+2) = dlmread(file_string,',',[5 1 bins+4 1]);
end

% Import the velocity, position, and force curves from the cfd output data
velocity = dlmread('Velocity_Curve.csv',',',[5 0 105 1]);
position = dlmread('Position_Curve.csv',',',[5 0 105 1]);
force = dlmread('Force_Curve.csv',',',[5 0 105 1]);

%% Data Format Section
% Homogenization data is then formatted to represent usuable data

% Determine the size of the raw data set
[dr_x,dr_y] = size(data_raw);
% Create a new array for formatted data
data_formatted = data_raw;
% Adjust the histogram magnitudes to represent volume in L.  Since the data
% is extracted from 2D axisymmetric models, the raw data needs to be
% multiplied by the axisymmetric wedge ratio.  Fluent uses a 7.5 degree
% wedge to represent the flow, i.e. 360/7.5 is the ratio to produce a fully
% revolved result.
data_formatted(2:dr_x, 2:dr_y) = data_raw(2:dr_x,2:dr_y)*(360/7.5);

%% Determine the mixing quality section
```

```
% Calculate the amount of water in the tank by taking a sum of all the
% liquid from the initial time step
Vol_h2o = sum(data_formatted(2:dr_x,2));
% The air volume is then calculated by subtracting the liquid volume from
% the user specified tank volume
Vol_air = tank_vol-Vol_h2o*1000;

% An initial volume of liquid A and B are calculated from the inital time
% by multiplying each concentration percentage by the corresponding volume
Vol_A = sum(data_formatted(2:dr_x,2)'*data_formatted(2:dr_x,1));
Vol_B = sum(data_formatted(2:dr_x,2)'*(1-data_formatted(2:dr_x,1)));

% The volume of each fluid is then used to determine the perfect average
% ratio for full homogenization
Ratio_final = Vol_B/(Vol_A+Vol_B);

% The row position in the formatted data set is then determined for the
% perfect mixture
Ratio_pos = round(Ratio_final*bins);

% Upper and lower bounds to perfect mixture position are then determined
% using the user specified tolerance
Upper_bnd = Ratio_pos+1+round(tol*bins/100);
Lower_bnd = Ratio_pos+1-round(tol*bins/100);

% The mixture quality array is then initialized using the time step data
% from the formatted data array
Mixture_qual(1:(dr_y-1),1) = data_formatted(1,2:dr_y)';

% A flag is set for interpolating the final homogenization time when 95% of
% the fluid falls within the tolerance
flag = 0;

% Mixture quality calculation loop starts here with the first column after
% t = 0 and works its way through the end
for i = 2:dr_y
    % Mixture quality is determined by summing the fluid that falls within
    % the tolerance band and dividing out by the total fluid volume
    Mixture_qual(i-1,2) = sum(data_formatted(Lower_bnd:Upper_bnd,i))/Vol_h2o;
    % Once 95% of the volume falls between the tolerance band and the flag
    % is still zero, the time at which 95% is achieved is interpolated by
    % using the current and previous mixing quality time step.  The flag is
    % then set to 1 to prevent overwriting at following time steps
    if Mixture_qual(i-1,2) >= 0.95 & flag == 0
        mix_time = (0.95-Mixture_qual(i-2,2))/(Mixture_qual(i-1,2)...
            -Mixture_qual(i-2,2))*(Mixture_qual(i-1,1)-...
            Mixture_qual(i-2,1))+Mixture_qual(i-2,1);
        flag = 1;
    end
end

%% Compute maxima and minima of position, velocity and force from the input
%% data
v_max = max(velocity(:,2));
v_min = min(velocity(:,2));

p_max = max(position(:,2));
p_min = min(position(:,2));
p_ave = (p_max+p_min)/2;

f_max = max(force(:,2));
f_min = min(force(:,2));
```

```
%% Print Results on the screen for intant results

disp('')
disp(Mixture_qual)

%% Plot and Save Results
% First the mixture quality is plotted and saved
figure(1)
plot(Mixture_qual(:,1),Mixture_qual(:,2)*100),xlabel('Time Step (sec)'),...
    ylabel('Mixture Quantity (%)'),...
    title('Mixture Quantity Within Specified Tolerance vs Time');

print -f1 'Mixture Quality vs Time' -dpng

% Second the mixer head position and velocity are plotted and saved
figure(2)
[ax1, p21, p22] = plotyy(position(:,1),position(:,2)-
p_ave,velocity(:,1),velocity(:,2)),...
    ylabel(ax1(1),'Position (m)'),ylabel(ax1(2),'Velocity
(m/sec)'),xlabel('Time (s)'),,...
    title('Mixer Position and Velocity with Respect to Time');

print -f2 'Velocity vs Time' -dpng

% Third the mixer head velocity and applied force are plotted
figure(3)
[ax2, p31, p32] = plotyy(velocity(:,1),velocity(:,2),force(:,1),force(:,2)),...
    xlabel('Time (s)'),ylabel(ax2(1),'Velocity (m/sec)'),ylabel(ax2(2),'Force
(N)'),...
    title('Mixer Velocity and Head Force with Respect to Time');

print -f3 'Force vs Time' -dpng

%% Print Data to file for later reference

% open file
fid = fopen('Data_Out.txt','w');

% write input data
fprintf(fid,'Analysis Settings\n');
fprintf(fid,'---------------- \n');
fprintf(fid,'Time steps analyzed:         %3i\n',t_total);
fprintf(fid,'Time step size (sec):        %3i\n',del_t);
fprintf(fid,'Tank Volume (L):             %3i\n',tank_vol);
fprintf(fid,'Number of Histogram bins:  %5i\n',bins);
fprintf(fid,'Mixture tolerance (+-%%):     %3.1f \n\n\n',tol);

fprintf(fid,'Calculated Data \n');
fprintf(fid,'---------------- \n');
fprintf(fid,'Air Volume (L):                          %3i\n',round(Vol_air));
fprintf(fid,'Liquid Volume (L):
%3i\n',round(Vol_h2o*1000));
fprintf(fid,'Liquid A Starting Volume (L):          %3i\n',round(Vol_A*1000));
fprintf(fid,'Liquid B Starting Volume (L):          %3i\n',round(Vol_B*1000));
fprintf(fid,'Maximum Head Velocity (m/sec):         %1.3f\n',v_max);
fprintf(fid,'Minimum Head Velocity (m/sec):         %1.3f\n',v_min);
fprintf(fid,'Maximum Head Force Encountered (N):    %1.3f\n',f_max);
fprintf(fid,'Minimum Head Force Encoutnered (N):    %1.3f\n',f_min);
if flag == 1
    fprintf(fid,'Time for 95%% volume to achieve \n');
    fprintf(fid,'mixing tolerance (sec):          %3.0f \n\n\n',mix_time);
else
```

```
    fprintf(fid,'Mixing Incomplete\n\n\n');
end

% Prints Mixture Data
fprintf(fid,'Analysis Data\n');
fprintf(fid,'---------------- \n\n');
fprintf(fid,'    Time      Mixture Quality\n');
fprintf(fid,'    -------------------------\n');
for i = 1:(dr_y-1)
    fprintf(fid,'    %3i           %3i%% \n',...
        Mixture_qual(i,1),round(Mixture_qual(i,2)*100));
end

% close file and check for write errors
[st] = fclose('all');

if st ~=0
    disp('Error data could not be written to output file')
    pause
end
```

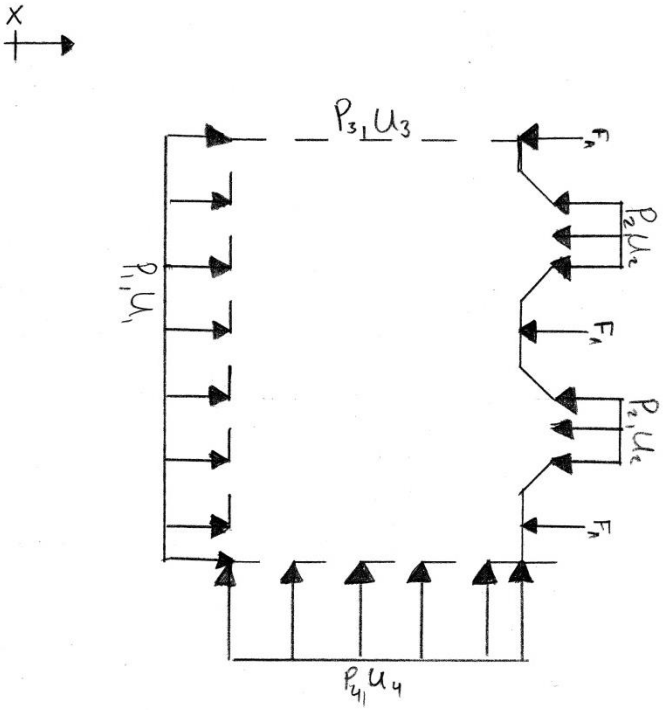

CASE #1

ASSUME

INVISCID FLOW
$\dot{m}_3 = \dot{m}_4 = 0$
STEADY FLOW

$\rho_1 = \rho_2 = \rho_3 = \rho_4$
NEGLECT CHANGES IN ELEVATION

$$A_1P_1 - A_2P_2 - F_A = \dot{m}om_{x_{out}} - \dot{m}om_{x_{IN}}$$

$$= \dot{m}_{out}U_2 - \dot{m}_{IN}U_1 \qquad \dot{m}_{out} = \dot{m}_{IN} \quad \text{CONSERVATION OF MASS}$$

$$= \rho A_2 U_2^2 - \rho A_1 U_1^2 \qquad \dot{m} = \rho A U$$

$$F_A = A_1P_1 - A_2P_2 - \rho A_2U_2^2 + \rho A_1U_1^2 \quad \leftarrow (1)$$

$$\rho U_1A_1 = \rho U_2A_2$$

$$U_1A_1 = U_2A_2$$

$$U_2 = \frac{U_1A_1}{A_2} \quad \leftarrow (2)$$

$$\frac{U_1^2}{2} + g\cancel{z_1}^{0} + \frac{P_1}{\rho} = \frac{U_2^2}{2} + g\cancel{z_2}^{0} + \frac{P_2}{\rho}$$

$$P_2 = P_1 + \frac{\rho}{2}(u_1^2 - u_2^2) \quad \longleftarrow (3)$$

COMBINING (1) AND (3)

$$F_A = A_1(P_1 + \rho A_1 u_1^2) - A_2\left(P_1 + \frac{\rho}{2}(u_1^2 - u_2^2) + \rho u_2^2\right)$$

$$F_A = A_1(P_1 + \rho A_1 u_1^2) - A_2\left(P_1 + \frac{\rho}{2}(u_1^2 + u_2^2)\right)$$

COMBINING (1) AND (2)

$$F_A = A_1(P_1 + \rho A_1 u_1^2) - A_2\left(P_1 + \frac{\rho}{2}\left(u_1^2 + \frac{u_1^2 A_1^2}{A_2^2}\right)\right)$$

$$F_A = A_1(P_1 + \rho A_1 u_1^2) - A_2\left(P_1 + \frac{\rho u_1^2}{2}\left(1 + \left(\frac{A_1}{A_2}\right)^2\right)\right)$$

$$F_A = P_1(A_1 - A_2) + \rho u_1^2\left(A_1^2 - \frac{A_2}{2}\left(1 + \frac{A_1^2}{A_2^2}\right)\right)$$

$$F_A = P_1(A_1 - A_2) + \rho u_1^2\left(A_1^2 - \frac{1}{2}\left(A_2 + \frac{A_1^2}{A_2}\right)\right)$$

$$F_A = P_1(A_1 - A_2) + \rho u_1^2\left(A_1^2\left(1 - \frac{1}{2A_2}\right) - \frac{A_2}{2}\right)$$

APPENDIX E – CFD MODEL CONFIGURATION

Single Mixer Configuration

General	
Version	2D, Double Precision
Space Model	Axisymmetric
Velocity Formulation	Absolute
Time Model	Steady

Models			
Multiphase - Volume of Fluid	Model	Volume of Fluid	
	Number of Eulerian Phases	2	
	Volume Fraction Parameters	Scheme	Explicit
		Volume Fraction Cutoff	1.00E-16
		Courant Number	0.25
Species - Species Transport	Species Transport	Phase	Phase Material
	Phase Properties	phase-1	air
		phase-2	mixture
Viscous - Transition k-kl-omega (3 eqn)	Model Constants	Cmu	0.99
		C-lambda	2.495
		CR	0.12
		ANAT	200
		ATS	200
		CNAT,crit	1250
		CTS,crit	1000
		CRNAT	0.02
		Anu	6.75
		CINT	0.75
		Cw1	0.44
		Cw3	0.3
		Calph-teta	0.035
		Ctual	4360
		TKE Prandtl Number	1
		SDR Prandtl Number	1.17
		Turbulent Schmidt Number	0.7

Materials			
Mixture			
mixture-template	Density (kg/m3)	volume-weighted-mixing-law	
	Viscosity (kg/m-s)	constant	0.001003
	Mass Diffusivity (m2/s)	constant-dilute-appx	2.88E-05
	Material Type	mixture	
	Fluent Mixture Materials	mixture-template	
Fluid			
air	Density (kg/m3)	constant	1.225
	Viscosity (kg/m-s)	constant	1.7894E-05
	Molecular Weight (kg/kgmol)	constant	28.966
	Material Type	fluid	
	Fluent Fluid Materials	air	
water-liquid	Density (kg/m3)	constant	998.2
	Viscosity (kg/m-s)	constant	0.001003
	Molecular Weight (kg/kgmol)	constant	18.0152
	Chemical Formula	h2o<l>	
	Material Type	fluid	
	Fluent Fluid Materials	water-liquid (h2o<l>)	

Cell Zone Conditions	
cap_region	Mixture
general_flow_region	Mixture
lower_region	Mixture
mixer_1_region	Mixture
mixer_jet_1	Mixture
trouble_region	Mixture

Boundary Conditions	
Axis	Axis
	Axis:007
	Axis:008
Interior	int_bottom_cap_bnd
	int_bottom_mixer_lower_flow_bnd
	int_cap_region
	int_general_flow_region
	int_interface_region
	int_lower_region
	int_mixer1_region_bnd
	int_mixer_1_region
	int_mixer_1_region:066
	int_mixer_axial_flow_bnd
	int_mixer_axial_flow_bnd:020
	int_mixer_axial_flow_bnd:021
	int_mixer_axial_flow_bnd:022
	int_mixer_axial_flow_bnd:023
	int_mixer_axial_flow_bnd:024
	int_mixer_bnd_1
	int_mixer_bnd_high_1
	int_mixer_jet_1
	int_shaft_bnd
	int_shaft_bnd:013
	int_shaft_bnd:014
	int_top_mixer1_region_bnd
	int_top_region_bnd
	int_trouble_region
	int_wall_bnd
	int_wall_bnd:015
	int_wall_bnd:016
	int_wall_bnd:017
	int_wall_bnd:018
	int_wall_bnd:019

Boundary Conditions	
Wall	mixer
No Slip	mixer:009
	mixer:010
	mixer:010:025
	mixer:010:025:063
	mixer:010:028
	mixer:010:060
	mixer:011
	mixer:012
	top_bnd
	wall
	wall:002
	wall:003
	wall:004
	wall:005
	wall:006

Dynamic Mesh	All Rigid Body Motion Uses UDF File	
Layering	Height Based	
	Split Factor	0.4
	Collapse Factor	0.2
Dynamic Mesh Zones	int_bottom_mixer_flow_bnd - Rigid Body	
	int_bottom_mixer_lower_flow_bnd - Rigid Body	
	int_general_flow_region - Rigid Body	
	int_interface_region - Rigid Body	
	int_mixer_1_region - Rigid Body	0.004 Element Size
	int_mixer_1_region:066 - Rigid Body	
	int_mixer_bnd_1 - Rigid Body	0.004 Element Size
	int_mixer_bnd_high_1 - Rigid Body	
	int_top_mixer1_region_bnd - Rigid Body	
	int_top_region_bnd - Rigid Body	
	mixer - Rigid Body	
	mixer:009 - Rigid Body	
	mixer:010 - Rigid Body	
	mixer:010:025 - Rigid Body	
	mixer:010:028 - Rigid Body	0.004 Element Size
	mixer:010:060 - Rigid Body	0.004 Element Size
	mixer:012 - Rigid Body	0.004 Element Size
	mixer_jet_1 - Rigid Body	
	top_bnd - Stationary	0.004 Element Size

Reference Values		
	Area (m2)	1
	Density (kg/m3)	1.225
	Enthalpy (j/kg)	0
	Length (m)	1
	Pressure (pascal)	0
	Temperature (k)	288.16
	Velocity (m/s)	1
	Viscosity (kg/m-s)	1.7894E-05
	Ratio of Specific Heats	1.4
Reference Zone	interface_region	

Solution			
Solution Methods	Pressure-Velocity Coupling	Scheme	SIMPLE
	Spatial Discretization	Gradient	Lease Squares Cell Based
		Pressure (pascal)	PRESTO!
		Momentum	Second Order Upwind
		Voume Fraction	CICSAM
		Turbulent Kinetic Energy	Second Order Upwind
		Laminar Kinetic Energy	Second Order Upwind
		Specific Dissipation Rate	Second Order Upwind
		phase-2 h2o <l>-new	Second Order Upwind
	Transient Formulation	First Order Implicit	

Solution Controls		
Under-Relaxation Factors	Pressure	0.3
	Density	1
	Body Forces	1
	Momentum	0.7
	Turbulent Kinetic Energy	0.8
	Laminar Kinetic Energy	0.8
	Specific Dissipation Rate	0.8
	Turbulent Viscosity	1
	phase-2 h2o<l>-new	1

Monitors					
Equation	continuity	Monitor Check	Convergence	Absolute Criteria	1.00E-06
Residual	x-velocity	Monitor Check	Convergence	Absolute Criteria	1.00E-06
	y-velocity	Monitor Check	Convergence	Absolute Criteria	1.00E-06
	kl	Monitor Check	Convergence	Absolute Criteria	1.00E-06
	kt	Monitor Check	Convergence	Absolute Criteria	1.00E-06
	omega	Monitor Check	Convergence	Absolute Criteria	1.00E-06
	h2o<l>-new-phase	Monitor Check	Convergence	Absolute Criteria	1.00E-06
Residual Values	Scale				
Convergence Criterion	absolute				

Solution Initialization		
Initialization Methods	Standard Initialization	
Reference Frame	Relative to Cell Zone	
Initial Values	Gauge Pressure (pascal)	0
	Axial Velocity (m/s)	0
	Radial Velocity (m/s)	0
	Turbulent Kinetic Energy (m2/s2)	1
	Laminar Kinetic Energy (m2/s2)	1.00E-06
	Specific Dissipation Rate (1/s)	1.00E-06
	phase-2 Volume Fraction	0
	phase-2 h2o<l>-new	1

Run Calculation	
Time Stepping Method	Fixed
Time Step Size (s)	0.001
Number of Time Steps	100
Max Iterations/Time Step	50
Reporting Interval	10
Profile Update Interval	1

Dual Mixer Configuration

General	
Version	2D, Double Precision
Space Model	Axisymmetric
Velocity Formulation	Absolute
Time Model	Steady

Models			
Multiphase - Volume of Fluid	Model	Volume of Fluid	
	Number of Eulerian Phases	2	
	Volume Fraction Parameters	Scheme	Explicit
		Volume Fraction Cutoff	1.00E-16
		Courant Number	0.25
Species - Species Transport	Species Transport	Phase	Phase Material
	Phase Properties	phase-1	air
		phase-2	mixture
Viscous - Transition k-kl-omega (3 eqn)	Model Constants	Cmu	0.99
		C-lambda	2.495
		CR	0.12
		ANAT	200
		ATS	200
		CNAT,crit	1250
		CTS,crit	1000
		CRNAT	0.02
		Anu	6.75
		CINT	0.75
		Cw1	0.44
		Cw3	0.3
		Calph-teta	0.035
		Ctual	4360
		TKE Prandtl Number	1
		SDR Prandtl Number	1.17
		Turbulent Schmidt Number	0.7

Materials			
Mixture			
mixture-template	Density (kg/m3)	volume-weighted-mixing-law	
	Viscosity (kg/m-s)	constant	0.001003
	Mass Diffusivity (m2/s)	constant-dilute-appx	2.88E-05
	Material Type	mixture	
	Fluent Mixture Materials	mixture-template	
Fluid			
air	Density (kg/m3)	constant	1.225
	Viscosity (kg/m-s)	constant	1.7894E-05
	Molecular Weight (kg/kgmol)	constant	28.966
	Material Type	fluid	
	Fluent Fluid Materials	air	
water-liquid	Density (kg/m3)	constant	998.2
	Viscosity (kg/m-s)	constant	0.001003
	Molecular Weight (kg/kgmol)	constant	18.0152
	Chemical Formula	h2o<l>	
	Material Type	fluid	
	Fluent Fluid Materials	water-liquid (h2o<l>)	

Cell Zone Conditions	
cap_region	Mixture
general_flow_region	Mixture
lower_region	Mixture
mixer_1_region	Mixture
mixer_jet_1	Mixture
mixer_jet_2	Mixture
mixer_region	Mixture
trouble_region	Mixture
upper_general_flow	Mixture

Boundary Conditions	
Axis	Axis
	Axis:008
Interior	int_bottom_cap_bnd
	int_bottom_mixer_flow_bnd
	int_bottom_mixer_lower_flow_bnd
	int_cap_region
	int_general_flow_region
	int_interface_region
	int_mixer_1_region
	int_mixer_1_region:059
	int_mixer_axial_flow_bnd
	int_mixer_axial_flow_bnd:026
	int_mixer_axial_flow_bnd:027
	int_mixer_axial_flow_bnd:028
	int_mixer_axial_flow_bnd:029
	int_mixer_axial_flow_bnd:030
	int_mixer_axial_flow_bnd:031
	int_mixer_bnd_1
	int_mixer_bnd_2
	int_mixer_bnd_high_1
	int_mixer_bnd_high_2
	int_mixer_jet_1
	int_mixer_jet_2
	int_mixer_region
	int_mixer_region:034
	int_shaft_bnd
	int_shaft_bnd:016
	int_shaft_bnd:017
	int_shaft_bnd:018
	int_shaft_bnd:019
	int_top_mixer1_region_bnd
	int_top_mixer_flow_bnd

Boundary Conditions	
Interior	int_trouble_region
	int_upper_general_flow
	int_wall_bnd
	int_wall_bnd:020
	int_wall_bnd:021
	int_wall_bnd:022
	int_wall_bnd:023
	int_wall_bnd:024
	int_wall_bnd:025
Wall	mixer
No Slip	mixer:009
	mixer:009:062
	mixer:009:065
	mixer:009:068
	mixer:009:071
	mixer:009:077
	mixer:009:080
	mixer:009:086
	mixer:009:089
	mixer:010
	mixer:011
	mixer:011:092
	mixer:011:097
	mixer:011:103
	mixer:011:106
	mixer:012
	mixer:013
	mixer:014
	mixer:015
	top_bnd
	wall
	wall:002

	int_top_mixer_flow_bnd:109			wall:003
	int_top_mixer_lower_region_bnd			wall:004
	int_top_mixer_region_bnd			wall:005

Dynamic Mesh	All Rigid Body Motion Uses UDF File	
Layering	Height Based	
	Split Factor	0.4
	Collapse Factor	0.2
Dynamic Mesh Zones	int_bottom_mixer_flow_bnd - Rigid Body	
	int_bottom_mixer_lower_flow_bnd - Rigid Body	
	int_gernal_flow_region - Rigid Body	
	int_interface_region - Rigid Body	
	int_mixer_1_region - Rigid Body	0.004 Element Size
	int_mixer_1_region:059 - Rigid Body	
	int_mixer_bnd_1 - Rigid Body	0.004 Element Size
	int_mixer_bnd_2 - Rigid Body	
	int_mixer_bnd_high_1 - Rigid Body	
	int_mixer_bnd_high_2 - Rigid Body	
	int_mixer_region - Rigid Body	
	int_mixer_region:034 - Rigid Body	
	int_top_mixer1_region_bnd - Rigid Body	
	int_top_mixer_flow_bnd - Rigid Body	
	int_top_mixer_flow_bnd:109 - Rigid Body	
	int_top_mixer_lower_region_bnd - Rigid Body	
	int_top_mixer_region_bnd - Rigid Body	
	int_top_region_bnd - Rigid Body	
	intt_upper_general_flow - Rigid Body	
	mixer - Rigid Body	
	mixer:009 - Rigid Body	
	mixer:009:065 - Rigid Body	
	mixer:009:068 - Rigid Body	
	mixer:009:071 - Rigid Body	
	mixer:009:077 - Rigid Body	
	mixer:009:080 - Rigid Body	
	mixer:009:086 - Rigid Body	
	mixer:009:089 - Rigid Body	
	mixer:010 - Rigid Body	
	mixer:011 - Rigid Body	

	mixer:011:092 - Rigid Body	
	mixer:011:097 - Rigid Body	0.004 Element Size
	mixer:011:103 - Rigid Body	0.004 Element Size
	mixer:012 - Rigid Body	
	mixer:015 - Rigid Body	0.004 Element Size
	mixer_jet_1 - Rigid Body	
	mixer_jet_2 - Rigid Body	
	top_bnd - Stationary	0.004 Element Size

Reference Values		
	Area (m2)	1
	Density (kg/m3)	1.225
	Enthalpy (j/kg)	0
	Length (m)	1
	Pressure (pascal)	0
	Temperature (k)	288.16
	Velocity (m/s)	1
	Viscosity (kg/m-s)	1.7894E-05
	Ratio of Specific Heats	1.4
Reference Zone	interface_region	

Solution			
Solution Methods	Pressure-Velocity Coupling	Scheme	SIMPLE
	Spatial Discretization	Gradient	Lease Squares Cell Based
		Pressure (pascal)	PRESTO!
		Momentum	Second Order Upwind
		Voume Fraction	CICSAM
		Turbulent Kinetic Energy	Second Order Upwind
		Laminar Kinetic Energy	Second Order Upwind
		Specific Dissipation Rate	Second Order Upwind
		phase-2 h2o <l>-new	Second Order Upwind
	Transient Formulation	First Order Implicit	

Solution Controls		
Under-Relaxation Factors	Pressure	0.3
	Density	1
	Body Forces	1
	Momentum	0.7
	Turbulent Kinetic Energy	0.8
	Laminar Kinetic Energy	0.8
	Specific Dissipation Rate	0.8
	Turbulent Viscosity	1
	phase-2 h2o<l>-new	1

Monitors					
Equation	continuity	Monitor Check	Convergence	Absolute Criteria	1.00E-06
Residual	x-velocity	Monitor Check	Convergence	Absolute Criteria	1.00E-06
	y-velocity	Monitor Check	Convergence	Absolute Criteria	1.00E-06
	kl	Monitor Check	Convergence	Absolute Criteria	1.00E-06
	kt	Monitor Check	Convergence	Absolute Criteria	1.00E-06
	omega	Monitor Check	Convergence	Absolute Criteria	1.00E-06
	h2o<l>-new-phase	Monitor Check	Convergence	Absolute Criteria	1.00E-06
Residual Values	Scale				
Convergence Criterion	absolute				

Solution Initialization		
Initialization Methods	Standard Initialization	
Reference Frame	Relative to Cell Zone	
Initial Values	Gauge Pressure (pascal)	0
	Axial Velocity (m/s)	0
	Radial Velocity (m/s)	0
	Turbulent Kinetic Energy (m2/s2)	1
	Laminar Kinetic Energy (m2/s2)	1.00E-06
	Specific Dissipation Rate (1/s)	1.00E-06
	phase-2 Volume Fraction	0
	phase-2 h2o<l>-new	1

Run Calculation	
Time Stepping Method	Fixed
Time Step Size (s)	0.001
Number of Time Steps	100
Max Iterations/Time Step	50
Reporting Interval	10
Profile Update Interval	1

Single Mixer Configuration – 3D

General	
Version	3D, Double Precision
Space Model	Axisymmetric
Velocity Formulation	Absolute
Time Model	Steady

Models			
Multiphase - Volume of Fluid	Model	Volume of Fluid	
	Number of Eulerian Phases	2	
	Volume Fraction Parameters	Scheme	Explicit
		Volume Fraction Cutoff	1.00E-16
		Courant Number	0.25
Species - Species Transport	Species Transport	Phase	Phase Material
	Phase Properties	phase-1	air
		phase-2	mixture
Viscous - Transition k-kl-omega (3 eqn)	Model Constants	Cmu	0.99
		C-lambda	2.495
		CR	0.12
		ANAT	200
		ATS	200
		CNAT,crit	1250
		CTS,crit	1000
		CRNAT	0.02
		Anu	6.75
		CINT	0.75
		Cw1	0.44
		Cw3	0.3
		Calph-teta	0.035
		Ctual	4360
		TKE Prandtl Number	1
		SDR Prandtl Number	1.17
		Turbulent Schmidt Number	0.7

Materials			
Mixture			
mixture-template	Density (kg/m3)	volume-weighted-mixing-law	
	Viscosity (kg/m-s)	constant	0.001003
	Mass Diffusivity (m2/s)	constant-dilute-appx	2.88E-05
	Material Type	mixture	
	Fluent Mixture Materials	mixture-template	
Fluid			
air	Density (kg/m3)	constant	1.225
	Viscosity (kg/m-s)	constant	1.7894E-05
	Molecular Weight (kg/kgmol)	constant	28.966
	Material Type	fluid	
	Fluent Fluid Materials	air	
water-liquid	Density (kg/m3)	constant	998.2
	Viscosity (kg/m-s)	constant	0.001003
	Molecular Weight (kg/kgmol)	constant	18.0152
	Chemical Formula	h2o<l>	
	Material Type	fluid	
	Fluent Fluid Materials	water-liquid (h2o<l>)	

Cell Zone Conditions	
flow_block	mixture

Boundary Conditions	
Axis	frontsurface
	frontsurface002
Interior	int_flow_block
	int_flow_block:006
	int_flow_block:007
	int_flow_block:008
Wall	part_1
No Slip	shaft
	shaft:005
	tank_surface
	tank_surface:004
Zero Shear	top_surface

Dynamic Mesh	All Rigid Body Motion Uses UDF File	
Layering	Height Based	
	Split Factor	0.4
	Collapse Factor	0.2
Dynamic Mesh Zones	frontsurface:002 - Rigid Body	
	int_flow_block:006 - Rigid Body	
	int_flow_block:007 - Rigid Body	0.004 Element Size
	int_flow_block:008 - Rigid Body	0.004 Element Size
	shaft:005 - Rigid Body	
	tank_surface:004 - Rigid Body	

Reference Values		
	Area (m2)	1
	Density (kg/m3)	1.225
	Enthalpy (j/kg)	0
	Length (m)	1
	Pressure (pascal)	0
	Temperature (k)	288.16
	Velocity (m/s)	1
	Viscosity (kg/m-s)	1.7894E-05
	Ratio of Specific Heats	1.4
Reference Zone	interface_region	

Solution			
Solution Methods	Pressure-Velocity Coupling	Scheme	coupled
	Spatial Discretization	Gradient	Lease Squares Cell Based
		Pressure (pascal)	PRESTO!
		Momentum	Second Order Upwind
		Turbulent Kinetic Energy	First Order Upwind
		Laminar Kinetic Energy	Second Order Upwind
		Specific Dissipation Rate	Second Order Upwind
		h2o <l>-new	First Order Upwind
		energy	First Order Upwind
	Transient Formulation	First Order Implicit	

Solution Controls		
Explicit Relaxation Factors	Momentum	0.25
	Pressure	0.25
Under-Relaxation Factors	Density	0.7
	Body Forces	0.7
	Turbulent Kinetic Energy	0.6
	Laminar Kinetic Energy	0.6
	Specific Dissipation Rate	0.6
	Turbulent Viscosity	0.4
	h2o<l>-new	1
	Energy	0.8
	Discrete Phase Sources	0.5

Monitors					
Equation	continuity	Monitor Check	Convergence	Absolute Criteria	1.00E-06
Residual	x-velocity	Monitor Check	Convergence	Absolute Criteria	1.00E-06
	y-velocity	Monitor Check	Convergence	Absolute Criteria	1.00E-06
	z-velocity	Monitor Check	Convergence	Absolute Criteria	1.00E-06
	energy	Monitor Check	Convergence	Absolute Criteria	1.00E-06
	kl	Monitor Check	Convergence	Absolute Criteria	1.00E-06
	kt	Monitor Check	Convergence	Absolute Criteria	1.00E-06
	omega	Monitor Check	Convergence	Absolute Criteria	1.00E-06
Residual Values	Scale				
Convergence Criterion	absolute				

Solution Initialization		
Initialization Methods	Standard Initialization	
Reference Frame	Relative to Cell Zone	
Initial Values	Gauge Pressure (pascal)	0
	X Velocity (m/s)	0
	Y Velocity (m/s)	0
	Z Velocity (m/s)	0
	Turbulent Kinetic Energy (m2/s2)	1.00E-05
	Laminar Kinetic Energy (m2/s2)	1.00E-06
	Specific Dissipation Rate (1/s)	1.00E-06

Run Calculation	
Time Stepping Method	Fixed
Time Step Size (s)	0.005
Number of Time Steps	100
Max Iterations/Time Step	50
Reporting Interval	10
Profile Update Interval	1